MATHEMATICAL MODELING AND ANALYSIS OF LEPTOSPIROSIS WITH OPTIMAL CONTROL

Abebe Girma Regassa

A Ph.D Dissertation Submitted to the Department of Applied Mathematics, College of Applied Natural Science

Presented in Partial Fulfillment of the Requirement for the Degree of Doctor of Philosophy in Applied Mathematics

School of Graduate Studies
Adama Science and Technology University

December, 2025
Adama, Ethiopia

MATHEMATICAL MODELING AND ANALYSIS OF LEPTOSPIROSIS WITH OPTIMAL CONTROL

Abebe Girma Regassa
Supervisor: Dr. Legesse Lemecha Obsu
Co-Supervisor: Dr. Abdissa Shiferaw Melese

A Ph.D Dissertation Submitted to the Department of Applied Mathematics, College of Applied Natural Science

Presented in Partial Fulfillment of the Requirement for the Degree of Doctor of Philosophy in Applied Mathematics

School of Graduate Studies
Adama Science and Technology University

December, 2025
Adama, Ethiopia

APPROVAL PAGE

We hereby certify that the recommendations and suggestions made by the board of examiners are appropriately incorporated into the final version of the dissertation entitled "**Mathematical Modeling and Analysis of Leptospirosis with Optimal Control**" by **Abebe Girma Regassa**.

Supervisor	Signature	Date
Co-Supervisor	Signature	Date

We, the undersigned, members of the Board of Examiners of the dissertation open defense by **Abebe Girma Regassa** have read and evaluated the dissertation entitled "**Mathematical Modeling and Analysis of Leptospirosis with Optimal Control**" and examined the candidate during open defense. This is, therefore, to certify that the dissertation is accepted for partial fulfillment of the requirement of the degree of Doctor of Philosophy in Applied Mathematics.

Chairperson	Signature	Date
External Examiner 1	Signature	Date
External Examiner 2	Signature	Date
Internal Examiner 1	Signature	Date
Internal Examiner 2	Signature	Date

Finally, approval and acceptance of the dissertation is contingent upon submission of its final copy to the Office of Postgraduate Studies (OPGS) through the candidate's Department Graduate Council (DGC) and College Graduate Committee (CGC).

Department Head	Signature	Date
College Dean	Signature	Date
Office of Postgraduate Studies, Dean	Signature	Date

DECLARATION

I hereby declare that this Dissertation entitled "**Mathematical Modeling and Analysis of Leptospirosis with Optimal Control**" is my original work. That is, it has not been submitted for the award of any academic degree, diploma or certificate in any other university. All sources of materials used for this dissertation have been duly acknowledged through appropriate citations.

Name	Signature	Date

RECOMMENDATION OF SUPERVISORS

We, the supervisors of this dissertation, hereby certify that we have read and revised the dissertation entitled "**Mathematical Modeling and Analysis of Leptospirosis with Optimal Control**" prepared under our guidance by **Abebe Girma Regassa** submitted in partial fulfillment of the requirements for the degree of Doctor of Philosophy in Applied Mathematics. Therefore, we recommend the submission of the dissertation to the department for further review and defense.

Supervisor	Signature	Date
Co-Supervisor	Signature	Date

ACKNOWLEDGMENTS

First and foremost, I would like to thank the Almighty God and his mother, St. Mary, for strengthening me to reach here. Next, I am extremely grateful to my supervisor, Dr. Legesse Lemecha, for his priceless inspiration, guidance, support, and assistance and for providing me valuable advice to be familiar with the scientific research world. Also, my gratitude goes to my co-supervisor, Dr. Abdissa Shiferaw, for all the support, guidance, and assistance and for reviewing my articles during publications. I also thank Adama Science and Technology University for its financial support and providing an excellent environment for study and research throughout my education. Last, but not least, I would like to express my heartfelt gratitude to my family and friends, particularly my wife, Mrs. Enisha Fana, and my kids, Yordanos, Hawetan, Milki, and Kena, for their love, prayers, moral support, incredible understanding, and encouragement to successfully complete my study.

TABLE OF CONTENTS

List of Tables

List of Figures

ABBREVIATIONS AND ACRONYMS

ACER	Average cost-effectiveness Ratio
CFD	Caputo Fractional Derivative
CDC	Center for Disease Control
FODE	Fractional Order Differential Equation
ICER	Incremental Cost-effectiveness Ratio
IVP	Initial Value Problem
LFE	*Leptospira*-Free Equilibrium
LPE	*Leptospira*-Persistent Equilibrium
ODE	Ordinary Differential Equation
PMP	Pontryagin Maximum Principle
SA	Susceptible-Asymptomatic Infected
SEIR	Susceptible-Exposed-Infected-Recovered
SIRV	Susceptible-Infected-Recovered-Vaccinated
WHO	World Health Organization

ABSTRACT

Leptospirosis is an emerging zoonotic disease with high health and economic damage that is caused by Leptospiara bacteria. In this dissertation, we developed a deterministic mathematical model that describes the dynamics of leptospirosis transmission in cattle herds, rats, and humans using both integer and non-integer systems of differential equations. The study examined the role of asymptomatic cattle and rats in the transmission of animal and human leptospirosis. For this, we formulated three models: cattle-environment, cattle-rat-environment, and cattle-human-environment models based on the epidemiological behavior of the Leptospira pathogen. For each model, we proved the well-posedness and also found the basic/effective reproduction numbers using the next-generation matrix approach. Analytically, we have shown the stability of Leptospira-free and Leptospira-persistent equilibrium points for the threshold value less than unity and greater than unity. Sensitivity analysis is also done to identify the most sensitive parameters in the proposed models. Accordingly, the contact rate between cattle, the contact rate between cattle and humans, the vaccination rate of cattle, the recovery rate of cattle, the recovery rate of humans, the rat mortality rate, and the environmental Leptospira decay rate are the most sensitive parameters. Furthermore, the first model is extended to an optimal control problem to optimally manage the spread of disease and determine the cost-efficient strategy. Numerical simulations have been conducted for each model using the Python language (odeint solver, scipy.optimize.fSolve, and GEKKO optimization packages). Accordingly, lowering the rate of contact with asymptomatic infected cattle, promoting the rate of recovery for both asymptomatic infected cattle and humans, increasing the rate of vaccination among susceptible cattle, raising the rate of rat mortality, and maximizing the rate of Leptospira decay could all contribute to a significant drop in the prevalence of the disease. Findings of this dissertation underscore the remarkable importance of targeted interventions, such as maximizing prevention efforts, enhancing regular vaccination of cattle, pre-diagnosis treatment of cattle and humans using proper antibiotics, and implementing environmental sanitation programs, which are very useful to manage leptospirosis. In addition, the consideration of different fractional orders in the last model provides valuable insights into the model's behavior, highlighting its variability and sensitivity to changes in the ordering.

KEYWORDS: Mathematical model; Leptospirosis; Asymptomatic cattle; Optimal control; Cost-effectiveness analysis; Stability analysis; Fractional-order model.

CHAPTER 1

INTRODUCTION

This chapter offers crucial background information on leptospirosis diseases by describing its important epidemiological aspects. The chapter then clearly defines the research problem, outlines the objectives of the study, and underscores its significance. Finally, it provides a brief overview of the dissertation's structure, guiding through the subsequent chapters.

1.1 Background of the Study

Zoonotic diseases are infectious diseases that are transmitted from non-human animals to humans (WHO, 2020). They are caused by bacteria, viruses, fungi, parasites, and prions through direct or indirect contacts, vector-borne transmission, or contaminated food (CDC, 2025). These diseases have the potential to affect the society either by threatening the animals' health, which results in illness and loss of productivity, or by infecting the people around them (Pieracci et al., 2016). According to Salyer et al. (2017), over 60% of infectious diseases that currently have been identified are zoonotic, and over 75% of newly discovered diseases have their origins in domestic or wild animals. Over two billion people worldwide are affected by zoonotic diseases annually, which result in approximately two million fatalities and billions of USD in economic damages (Gruber, 2021). During the past decade, the world has experienced a number of zoonotic public health problems, such as the COVID-19 pandemic, Ebola, Monkey-pox, and Middle East respiratory syndrome (MERS) (Sun et al., 2024).

East Africa, particularly Ethiopia, is a region with many endemic and emerging zoonoses, posing a significant public health concern and having a substantial economic burden on local livelihoods (Nyokabi et al., 2023). Poor access to human and livestock health services contributed towards the widespread transmission of zoonotic pathogens in the region (Alemu et al., 2023). Ethiopia is home to Africa's largest livestock population and the second-largest human population on the continent. Approximately 80% of Ethiopians rely on agriculture and have direct contact with animals, creating a high risk for zoonotic disease transmission (Pieracci et al., 2016). Consequently, the country is vulnerable to animal-related diseases because many people rely on livestock farming, which can lead to serious economic and health problems (Nyokabi et al., 2023).

1.1.1 The Leptospirosis Disease

Leptospirosis is an emerging zoonotic disease caused by a pathogenic bacteria that belong to the genus *Leptospira* (Desa et al., 2021). The disease was first described by Adolf Weil in 1886 and named Weil's disease but later identified as *Leptospires* by Stimson in 1907. Leptospirosis in cattle was first reported in Russia in 1940, as cited by Adler (2014). More than 250 *Leptospira* serovars have been identified so far, and serovar *Hardjo* is among the most common pathogenic serovars that affect cattle (Pyskun et al., 2019). The reproduction of *Leptospira* typically takes place in the renal tubules of infected mammals (Oguntolu et al., 2024; Thibeaux et al., 2018). Subsequently, these bacteria are expelled into the environment through urine, posing a risk of infecting other organisms. The average incubation period is one week or two weeks, with a range spanning from two days to thirty days (Aslan et al., 2021; Bierque et al., 2020; Desa et al., 2021).

The symptoms of leptospirosis infection can range in intensity from mild illness to life-threatening complications (Rajapakse et al., 2025). Common clinical manifestations of leptospirosis in cattle include abortions, infertility, stillbirths, weak calves, and sudden drop in milk in lactating cows (Lilenbaum & Martins, 2014). Infected calves experience an acute, more severe form of the disease, which is often fatal (Fraga et al., 2015; Paixão et al., 2025). However, infections can often remain asymptomatic in most cattle, shedding the pathogen in their urine and continuously contaminating the environment (van den Brink et al., 2023). Fever, headaches, and red eyes are typical human symptoms. Severe cases may result in meningitis, kidney or liver failure, and jaundice (yellowing of the skin and eyes)(MedicalNews, 2025).

Leptospirosis is a neglected infectious disease due to socioeconomic and geographical factors. It is one of the main public health problems in tropical and subtropical regions, where high temperatures and humid weather encourage the growth of the pathogens (Karpagam & Ganesh, 2020; Khairullah et al., 2024). Approximately one million cases of leptospirosis occur globally each year, resulting in 60,000 human deaths (Rajapakse et al., 2025; Thibeaux et al., 2018). In Sub-Saharan African countries, it is one of the leading causes of reproductive disorders in livestock production (De Vries et al., 2014). Globally, animal seroprevalence is up to 46%, while in Sub-Saharan Africa, estimates for cattle reach as high as 30.1% (Selim et al., 2024).

Leptospirosis is a potential veterinary and public health concern in Ethiopia, with studies showing high seroprevalence in cattle, around 70.7%, and in humans, with one pilot study in Wonji finding 47.46% seropositivity among febrile patients (Yimer et al., 2004). This is due to Ethiopia's climate, high livestock densities, and frequent human–animal contact, which creates favorable conditions for the emergence and transmission of leptospirosis (Robi et al., 2024). According to Pieracci et al. (2016), leptospirosis is among the top five zoonotic diseases in

Ethiopia, and it is also the main reason for abortion in livestock, next to brucellosis. Despite this risk, several gaps persist: limited awareness of the disease among farmers, poor sanitation and biosecurity practices, and a scarcity of reliable, up-to-date data on the prevalence of leptospirosis in both animals and humans across the country. Moreover, the asymptomatic nature of the disease poses a core challenge for control of leptospirosis, as asymptomatic carriers silently disseminate the disease in a herd prior to farmers' knowledge (van den Brink et al., 2023). Together with other reproductive diseases, it reduces the reproductive stock of livestock and creates significant obstacles in increasing the cattle population, sustaining the local demand for meat and dairy products, and export competitiveness of the nation (Orjuela et al., 2022).

1.1.2 The Transmission Cycle

Transmission of leptospirosis requires continuous circulation of the pathogen between the reservoirs (known as maintenance hosts) and the environment, as shown in Figure 1.1. Maintenance hosts (such as rats, dogs and cattle) are chronically infected but usually asymptomatic carriers that shed *leptospira* through their urine, maintaining the life cycle of the bacteria (Rojas et al., 2010). Accidental hosts (including humans) become infected by contact with contaminated urine or environments, often developing severe, acute, and sometimes fatal forms (Rajapakse et al., 2025). Rats are well-known maintenance hosts of *Leptospira* infection in humans and animals, but domestic and wild mammals may also act as maintenance or accidental hosts (Boey et al., 2019; Denipitiya et al., 2017).

The transmission routes of leptospirosis are direct contact with infected animals and indirect contact with soil or water contaminated with the urine of reservoir hosts (Mughini-Gras et al., 2014). Direct transmission may include exposure to urine from infected animals through mucous membranes (such as the eye, mouth, or nose) and any cut on the body. In addition, vertical transmissions (through placental fluid or suckling) are also important alternative direct routes for *Leptospira* (Nogueira et al., 2020; Otaka et al., 2012). On the other hand, indirect transmission through contaminated soil and water contributes significantly to the spread of *Leptospira* infections (Samrot et al., 2021). Humans become infected by direct contact with urine of infected animal or indirect contact with contaminated soil, or bodily fluids of animals, or by drinking contaminated water. The usual human exposure occurs during or very shortly after flood events. This is in line with the mathematical study by Chadsuthi et al. (2021), which predicted that flooding would be a major contributor to disease transmission. Leptospirosis outbreak is commonly related to flood, and the extent to which infection is transmitted depends on factors such as precipitation, humidity, temperature, and contact rate with reservoir hosts (Davignon et al., 2023).

The arrows in Figure 1.1 clearly depict that susceptible humans become infected by direct contact with infected cattle or infected rats or by indirect contact with water and soil contaminated by animal urine (Samrot et al., 2021). In addition, susceptible cattle become infected by direct contact with infected cattle themselves or infected rats or by indirect contact with water and soil (Aslan et al., 2021). Moreover, susceptible rats become infected by direct contact with infected rats themselves or by indirect contact with water and soil (Holt et al., 2006). This complex interspecies and environmental transmission of leptospirosis emphasizes the need for mathematical tools to analyze its dynamics and anticipate management strategies.

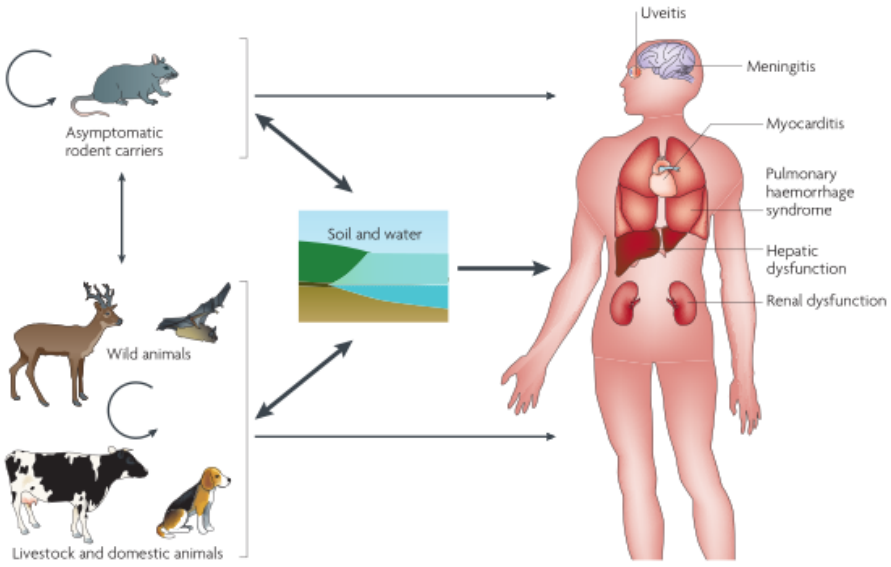

Figure 1.1: Leptospirosis transmission cycle [Figure credit Ko et al. (2009)].

1.1.3 The Control Strategies

Leptospirosis causes significant economic losses globally by reducing human productivity, damaging breeding stock of livestock, and increasing treatment costs, particularly in developing countries. Thus, it is crucial to apply control strategies to safeguard people at higher risk (such as farmers, veterinarians, and sewer workers) and enhance livestock productivity. The diversity of pathogenic *Leptospira* serovars in animal hosts creates serious challenges to the prevention and control of leptospirosis (Orjuela et al., 2022). However, a scheduled vaccination program for animals, excellent rodent control, an extra environmental sanitation program, and limiting access to contaminated water are some of the effective prevention and control strategies for the disease (Pimenta et al., 2019).

In cattle, a combination of vaccination and biosecurity measures, such as avoiding co-grazing

or mixing with other animal species, such as pigs, and avoiding introducing new animals to a herd without first conducting medical screening and vaccination, may be used to prevent leptospirosis (CDC, 2025). Vaccines for cattle leptospirosis are available to protect against different serovars like *Pomona* and *Hardjo*. They are useful to reduce the occurrence of infection, duration, and intensity of urinary shedding (Aslan et al., 2021; Fraga et al., 2015). However, the vaccines are imperfect, are mostly serovar-specific, and have a short duration of protection (Fraga et al., 2015). According to authors in Esteves et al. (2022), commercially available leptospirosis vaccines provide 84% effective protection against clinical illness and 88% efficiency against asymptomatic status. There is currently no widely available vaccine for human leptospirosis in the standard market because of the diverse group of serovars and dependency of the effectiveness of a vaccine on its ability to protect against the prevalent strains in a given region.

Furthermore, most leptospirosis cases of infected cattle and humans can be treated with appropriate antibiotics. The aim of treatment is to prevent irreparable damage to the kidneys and liver and also eliminate shedding of *Leptospira* to the environment (Aymée et al., 2024). Human leptospirosis is treated with antibiotics, which should be started as early as possible to prevent severe illness. Mild cases can be treated with oral medications like doxycycline, while severe cases require intravenous (IV) antibiotics, such as penicillin or ceftriaxone (Murray & Hospenthal, 2004). In cattle, the recommended treatment is early antibiotic treatment based on the combination of penicillin and streptomycin or streptomycin–tetracycline combinations, which can effectively reduce recovery periods and minimize sequelae (Hartskeerl et al., 2011).

Although the above control strategies are known, their relative effectiveness and cost- effectiveness in an integrated multi-host system are poorly quantified by scholars. For example, it is unknown whether vaccination of cattle or controlling rodents provides a better return on investment to reduce human cases. Hence, it is crucial to prioritize effectively and ethically applying mathematical tools.

1.1.4 Mathematical Modeling in Infectious Disease Dynamics

A deeper comprehension of the dynamics of infectious diseases has been made possible by mathematical modeling (Grassly & Fraser, 2008). The dynamics of an infectious disease under many scenarios can be understood and predicted by policymakers using mathematical modeling and analysis (Sweileh, 2022). Compartmental models have been widely used for predicting the course of epidemics, from estimating the basic reproduction number to guiding intervention policies (Siegenfeld et al., 2022). The study of Kermack & McKendrick (1927) is the first deterministic compartmental epidemic modeling.

In this regard, some researchers have developed a mathematical model that demonstrates

how leptospirosis spreads among humans and animals (Alalhareth et al., 2023; Aslan et al., 2021; Chadsuthi et al., 2022; Engida et al., 2023; Farman et al., 2023; Holt et al., 2006; Okosun et al., 2016). The first breakthrough deterministic compartmental leptospirosis model was published by Holt et al. (2006). They proposed a *SI* model for African rodents incorporating free-environmental *Leptospira* load as a separate compartment. Their model considered direct rat-to-rat and indirect environment-to-rat transmission. Okosun et al. (2016) also developed a leptospirosis model with optimal control for a combined human and livestock population. In this study, authors impose prevention and treatment control for humans and also vaccination and treatment for animals, ignoring preventive measures for animals. They have analyzed the cost-effectiveness of the controls in different scenarios.

Another study by Aslan et al. (2021) designed an *SIR* model that includes a free-environmental *Leptospira* load to investigate the propagation of leptospirosis in cattle ranches. This study considered the age structure and vaccination of newly recruited cattle. Although multiple serovars can exist in a herd, this work focused only on infection with a single serovar, and hence reinfection is ignored. In paper Chadsuthi et al. (2022), an SEIRS stochastic compartmental model was designed for leptospirosis transmission in cattle herds. It is a model that combines infection kinetics (progression of infection) and antibody kinetics (sero-conversion) with time delay to assess the disease status and the implementation of strategies for controlling the associated risks. Furthermore, in Engida et al. (2022), an SEIR-SIR compartmental model was used in human and rat populations incorporating free-living *Leptospira*.

Although existing studies provide valuable insights into the transmission dynamics of leptospirosis, most have concentrated on single-host scenarios (Aslan et al., 2021; Chadsuthi et al., 2022; Holt et al., 2006) or human-to-rodent transmission (Alalhareth et al., 2023; Engida et al., 2022; Farman et al., 2023; Okosun et al., 2016). For instance, the model proposed by Aslan et al. (2021) incorporated vaccination of newly recruited cattle and environmental *Leptospira* concentration, but it did not distinguish between symptomatic and asymptomatic infections. Similarly, two-species (human–rat) models (Alalhareth et al., 2023; Engida et al., 2022; Farman et al., 2023) overlooked the role of cattle as well as the contribution of asymptomatic infections to human transmission. To address these gaps, our study develops a unified leptospirosis transmission model that captures cattle–rat–human–environment interactions.

In addition, optimal control theory is a useful tool to identify the most effective mitigation strategy to minimize the number of infections while efficiently balancing the controls applied to the models with various cost scenarios (Igoe et al., 2023; Sharomi & Malik, 2017). In this optimization approach, control variables vary with time, allowing dynamic minimization of both the cost of disease burden and the costs of intervention (Igoe et al., 2023). A cost-effectiveness

analysis of the intervention strategy is another benefit of modeling studies that can be particularly useful for identifying efficient strategies when resources are limited.

Engida et al. (2022) extend their work to an optimal control problem, proposing personal prevention and treatment for the human population, rodenticide for the rat population, and proper sanitation for environmentally free bacteria as control measures (Engida et al., 2023). The cost-effectiveness analysis of this work suggests that the rodenticide control-only strategy is most effective to combat the spread of disease when available resources are limited. A mathematical model developed by Oguntolu et al. (2024) is another comprehensive multi-species leptospirosis optimal control analysis. They include controls such as preventive measures, environmental sanitation, and animal vaccination. Here, they fail to include treatments for either animals or humans to enhance the recovery rate. The result of their numerical analysis indicates that the number of infected humans and the population of bacteria are not significantly affected by the vaccination-alone control method. However, the number of infected humans, infected animals, and the total population of bacteria in the environment can all be significantly decreased by combining the three time-dependent control measures.

Recently, fractional calculus has had a remarkable development in modeling biological phenomena (Caputo & Fabrizio, 2015; Chakraverty et al., 2020). Unlike integer-order models, fractional-order derivatives are better suited to capture the memory effects and long-range interactions inherent in epidemiological systems. This allows the model to more accurately simulate real-world scenarios where disease spread is influenced by past conditions and responses over time (Pongsumpun et al., 2025). Leptospirosis has unique epidemiological features, such as asymptomatic carriers, environmental persistence, multi-host transmission, and relapse behavior, that make its dynamics strongly dependent on past states. This makes fractional-order modeling a particularly promising approach to study transmission dynamics of leptospirosis compared to integer-order models. Thus our study uses this approach to analyze the model formulated in cattle-human-environment interface.

1.2 Statement of the Problem

Leptospirosis is a worldwide disease, particularly common in tropical and subtropical areas, with an estimated 1 million cases and 58,900 deaths annually in humans (Rajapakse et al., 2025). In countries like Ethiopia, where livestock and human populations are large and mixed farming practices are common, leptospirosis poses both economic and public health threats (Sohm et al., 2023). Leptospirosis receives less emphasis as a global health priority due to challenges in its asymptomatic nature and the fact that it affects marginalized populations.

Current veterinary studies of leptospirosis have shown that asymptomatic infections can

silently spread within herds, reducing productivity and exposing farmers, abattoir operators, and veterinarians to risk (Davignon et al., 2023; Monti et al., 2023). However, the role of asymptomatic cattle has not been addressed in existing mathematical models, despite the fact that the recovery time and levels of *Leptospira* shedding of asymptomatic carriers differ significantly from the symptomatic cattle. Likewise, although vaccination of susceptible cattle in endemic areas is highly recommended both for existing herds and newly recruited animals (Aymée et al., 2024; Wilson-Welder et al., 2020), mathematical models on leptospirosis dynamics rarely incorporate vaccinated compartments. In addition, the current modeling landscape lacks a unified approach that simultaneously incorporates the primary reservoir host (cattle), human populations, and environmental contamination. This critical knowledge gap hinders the design of effective, evidence-based control strategies for leptospirosis at the human–cattle–environment interface. Furthermore, leptospirosis has unique epidemiological features, such as asymptomatic carriers, environmental persistence, multi-host transmission, and relapse behavior, that make its dynamics strongly dependent on past states.

Therefore, in the first part of this study, we formulate and analyze a comprehensive mathematical model of leptospirosis within cattle by modifying the SEIR model (Chadsuthi et al., 2022) to asymptotic infected, vaccinated, and environmental free *Leptospira* compartments. Then, we extended this model to include a well-known reservoir host (rat), human beings, and free-living *Leptospira* pathogens to analyze the interspecies transmission dynamics of leptospirosis. Furthermore, our study addresses the fractional-order model analysis to capture the unique features of leptospirosis, particularly in cattle-human interfaces.

1.3 Objective of the Study

1.3.1 General Objective

The general objective of this study is to develop and analyze a mathematical model that describes the transmission dynamics of leptospirosis to assess interspecies risk and design optimal control strategies for effective disease prevention and management.

1.3.2 Specific Objectives

The specific objectives of the proposed research are to:

1. formulate a deterministic compartmental model for leptospirosis that integrates symptomatic, asymptomatic, and vaccinated cattle classes,
2. extend the proposed model into an optimal control problem and recommend the cost-effective control strategy that reduces the burden of leptospirosis in cattle and humans.

3. construct a mathematical model that captures the transmission dynamics of leptospirosis within a system of cattle, rat reservoirs, and the surrounding environment,

4. formulate and analyze fractional-order mathematical model that characterizes the role of cattle in the transmission dynamics of human leptospirosis.

1.4 Significance of the Study

This study provides a basic understanding of how to use mathematical modeling in describing the transmission dynamics of leptospirosis with optimal control in both integral and fractional order derivatives. Thus the models proposed in our study are significant for the following reasons:

1. helps to understand the interspecies dynamical property of leptospirosis,

2. to suggest an appropriate intervention method,

3. serve as a reference for scholars and policymakers working in the area,

4. it will add knowledge to the existing literature on leptospirosis, and

5. motivate other researchers to extend and study the transmission dynamics of leptospirosis.

1.5 Delimitation of the Study

This study focuses on mathematical modeling of leptospirosis transmission, with particular emphasis on the role of cattle as the primary host, separating infectious cattle into symptomatic and asymptomatic groups to capture differences in recovery time. In addition, the model includes rat populations, human populations, and environmental contamination pathways. Other animal reservoir hosts (such as dogs) and spatial heterogeneity of transmission are not considered in our model formulation. Furthermore, the study is limited to a theoretical and simulation-based framework; it does not involve the collection of primary epidemiological data but instead relies on published parameter estimates.

1.6 The Organization of the Dissertation

There are seven chapters in this dissertation. Our study's introduction, which covers several essential biological background topics, the statement of the problem, and the objective and significance of the study, is presented in chapter 1. A brief discussion of important and previous related literature is covered in chapter 2. chapter 3 presents the method utilized to conduct

this dissertation. In chapter 4, a system of nonlinear ordinary differential equations is used to build a deterministic mathematical model for the transmission dynamics of leptospirosis. Using three time-dependent controls, the developed model is further extended into an optimal control problem. chapter 5 proposes and analyzes a new mathematical model for the dynamics of leptospirosis in cattle and rats. In chapter 6, the fractional order extension of the proposed leptospirosis model is formulated by incorporating human population. chapter 7 concludes the dissertation with suggestions.

CHAPTER 2

LITERATURE REVIEW

2.1 Introduction

Mathematical models are essential tools for better understanding of the dynamics of infectious disease since its inception as a discipline more than a century ago (Grassly & Fraser, 2008). Mathematical analysis and modeling allow policymakers to understand and predict the dynamics of an infectious disease under several scenarios (Sweileh, 2022). The use of mathematical models in epidemiology started as early as 1760 by Bernoulli & Chapelle (2023) who were working on the epidemiology of Smallpox in England.

The modern mathematical modeling started with Ross in his book published in 1911 in which he investigated the dynamics of malaria transmission (Ross, 1911). Then after, Kermack & McKendrick (1927) founded the deterministic compartmental epidemic modeling suggesting that the probability of infection of a susceptible individual is analogous to the number of his contacts with infected individuals and the rate at which susceptible individuals become infected is given by kSI where S and I represent population densities of susceptible and infected people, respectively while k is a constant. They have shown that, an infectious disease can spread in a susceptible population only if the so-called basic reproduction number is above a threshold value.

The field developed throughout the course of the 20th century to incorporate increasingly intricate models that took into consideration variables such as diverse populations, latent periods, and birth and death rates. The advent of computers in the mid-20th century allowed researchers to simulate more complex models, such as malaria and HIV. Epidemic modeling has emerged as a vital tool for public health planning in the twenty-first century, particularly during disease outbreaks such as SARS, Ebola, COVID-19, and Mpox. Models now include comprehensive population dynamics, vaccination plans, and treatments due to advancements in data availability, computing power, and understanding of disease biology. In order to effectively inform public health interventions, real-time prediction, and data-driven approaches are becoming increasingly important in epidemic modeling (Kretzschmar & Wallinga, 2009; Mata & Dourado, 2021).

2.2 Leptospirosis Model

In recent years many scholars in the area of mathematics studied the transmission dynamics of leptospirosis both in human being and animal population. In this regards the study of Caley & Ramsey (2001) is the earliest mathematical model for leptospirosis. In this study the researchers estimate leptospirosis transmission rate (force of infection) from sampled data and find effect of fertility control in Possums. Their result suggests that fertility control by tubal ligation of females possibly increases the disease transmission parameter, resulting in an increase of the basic reproduction number.

The next impressive Mathematical model in the area of leptospirosis is the study by Holt et al. (2006). They proposed a susceptible-infected compartmental model for transmission of leptospirosis in African rodents with age structure of juvenile, sub-adult and adult. In this model the direct transmission from mother to an offspring (called vertical transmission) was considered in addition to contact within animal. It also includes the indirect transmission from free environmental bacterial load with saturation term which limits the effect of *Leptospira* value in the environment becoming large. Their model suggests that rodent removal methods, such as trapping, will be more effective in reducing leptospirosis risk. Many researchers thereafter use this model as a benchmark, despite its focus on a single species.

Khan et al. (2014) formulate a model that considers both the population of human and animal (rat) but fails to include the contribution of environmental *Leptospira* load to the spread of the disease. They also extend their own work to study the dynamic behavior of leptospirosis with a saturated incidence rate (Khan et al., 2016). Their result shows that the population of infected humans and vectors decreases, as well as the population of susceptible humans increases, with the increase of proposed controls. Gallego & Simoy (2021) investigated a SIR-SI model and conducted an analytical examination of the system's characteristics in order to comprehend the dynamics of leptospirosis in humans and rodents. In this article, rodent population presents a logistic growth unlike previous papers. According to their findings, the basic reproduction number depends on rodents infection rate, birth rate and environmental carrying capacity, the infection may continue if the environment is conducive to the expansion of the rodent population. This work did not include environmental free *Leptospira* as a separate compartment. Engida et al. (2022) developed and examined a deterministic mathematical model for transmission dynamics of leptospirosis described by nonlinear ordinary differential equations with eight state variables in human, rodent and bacterial populations. They demonstrated a detailed qualitative and quantitative analysis to show more insight into the spread of disease. The sensitivity of different parameters was analyzed and numerical simulations were incorporated to support their theoretical findings. The article did not include cattle which are well-known maintenance hosts that

affect humans. Baca-Carrasco et al. (2015); Bhalraj & Azmi (2019) also formulate a similar leptospirosis model of the combined population of human and rodents with environmental-free bacteria under consideration.

Studies by Babylon et al. (2018), Aslan et al. (2021), and Chadsuthi et al. (2022) can be pointed out as a good reference point for a study focusing on livestock leptospirosis. Babylon et al. (2018) also formulate an SI model with environmental *Leptospira* concentration to investigate the transmission cycle of leptospirosis in lambs. Since the authors assumed a short-term stay of lambs on a farm, they did not consider recovery and reinfection in this model. According to the results of this study, increasing *Leptospira* decay rate on the farm to decrease infection in livestock could decrease the incidence of disease in humans. Aslan et al. (2021) also developed a mathematical model to analyze the spread of leptospirosis and to find a control method to eradicate the disease in a cattle ranch. They designed an SIR model with each compartment subdivided into two age groups, namely juvenile and adult. The model includes free environmental *Leptospira* load and vertical transmission. It incorporates vaccination of newly recruited cattle in the form of impulse actions as a control measure to prevent the propagation of leptospirosis in the ranch. This article fails to consider asymptomatic infectious cattle separately and vaccination of susceptible cattle. Moreover, the authors assumed a single serovar with no reinfection, despite the possible existence of multiple serovars in a herd. In the work of Chadsuthi et al. (2022), an SEIR stochastic compartmental model was designed for leptospirosis in cattle herds considering the dynamics of sero-conversion of the *Leptospira* pathogen, and their results described the general framework of the combination of infection and antibody dynamics. Here, the role of vaccination and free environmental *Leptospira* was not addressed.

Recently, Artiono et al. (2024) aimed to create a mathematical model of leptospirosis involving interactions between multiple species. This study takes into account the interactions between humans, animal hosts, animal vectors, and free-living *Leptospira* at a time, despite the focus of the majority of studies on the human-rodent interface. The authors ignored direct transmission from animal vectors to animal hosts, although it has a significant contribution in addition to indirect transmission from the environment.

2.3 Leptospirosis Model with Optimal Control

Optimal control theory helps us to identify the most effective methods for managing infectious diseases and to look into the effects of applied controls (Igoe et al., 2023). The approach is useful in recommending the best mitigation plan to reduce the number of affected population during a disease while effectively managing control applied to the models with different cost scenarios (Bussell et al., 2019; Sharomi & Malik, 2017). Unlike other optimization techniques that

assume control variables remain constant over time, it permits the control variables to change over time, enabling dynamic minimization of both the burden of disease and intervention costs (Igoe et al., 2023).

Authors in Okosun et al. (2016) developed a leptospirosis model for a combined human and livestock population. They have also extended the model to an optimal control problem by introducing prevention and treatment control for humans and also vaccination and treatment for animals. They did not include environmental *Leptospira* concentration and the asymptomatic infected animal compartment. They have analyzed the cost-effectiveness of the controls in different scenarios. The model suggests that policymakers may adopt a strategy with vaccination and treatment of infective animals over other strategies, which include the additional cost of prevention and treatment of humans, in case of limited resources.

In article Minter et al. (2019), an optimal control problem for leptospirosis transmission in rat populations was formulated by extending a model developed by Holt et al. (2006). The authors include four control measures: rodenticide, resource reduction, carry capacity control, and *Leptospira* mortality control. Consequently, they examined the effectiveness of each control in different cases. This article did not examine the transmission of leptospirosis between species and the corresponding control strategies.

In addition, Engida et al. (2023) developed an optimal control problem and conducted cost-effectiveness analysis by extending the leptospirosis model formulated by Engida et al. (2022). In this article, the authors proposed personal prevention and treatment for the human population, rodenticide for the rat population, and proper sanitation for environmentally free bacteria as control measures. They have provided cost-effectiveness assessments and numerical simulations of various control schemes. Their cost-effectiveness analysis suggests that the rodenticide control-only strategy is most effective to combat the spread of disease when available resources are limited.

Furthermore, Oguntolu et al. (2024) developed a mathematical model for the dynamics of leptospirosis transmission in human and animal populations with optimal controls. The controls include preventive measures, environmental sanitation, and animal vaccination. Here, they fail to include treatments for either animals or humans to enhance the recovery rate. The number of infected humans and the population of bacteria are not significantly affected by the vaccination of animals as a stand-alone control method, according to the results of numerical simulations. However, the number of infected humans, infected animals, and the total population of bacteria in the environment can all be significantly decreased by combining the three time-dependent control measures.

2.4 Leptospirosis Model with Fractional Order

Unlike traditional integer-order models, fractional-order models incorporate memory and hereditary properties that provide a more realistic representation of disease spread and often yield a better fit to observed outbreak data (Farman et al., 2023). The dynamics of leptospirosis are heavily influenced by previous status due to its distinct epidemiological characteristics, which include asymptomatic carriers, environmental persistence, multi-host transmission, and relapse behavior. Therefore fractional-order is suitable for studying the dynamics of leptospirosis transmission.

In this regard, Alalhareth et al. (2023) and Farman et al. (2023) are among the recent studies that focuses on leptospirosis in fractional order differential equation. Alalhareth et al. (2023) studied the Leptospirosis model, which is described by a nonlinear fractional-order differential equation that accounts for environmental influences. The stability of the suggested fractional order system is examined both qualitatively and quantitatively. The authors missed considering the exposed human population, although its symptoms usually start within two to fourteen days. Also, the study fails to separate asymptomatic individuals before their chronic stage because the exposed individuals can be recorded earlier as compared to infected ones.

Farman et al. (2023) use fractional-order differential equations to build and assess a compartmental mathematical model in order to investigate the effects of rodent-borne leptospirosis on the human population by extending the work of Engida et al. (2022). The model takes into account the rate of human infection brought on by contact with infected rats and the environment, as well as the existence of disease-causing agents in the surroundings. Their numerical findings offer strong proof that setting preventive and control measures together can significantly decrease the spread of human leptospirosis infection. On the other hand, Mukdasai et al. (2022) present a novel numerical method to solve fractional order leptospirosis model using the supervised neural network. They have also compared the exactness of the obtained numerical outcomes with the Adams scheme.

In general, most mathematical models of leptospirosis focus primarily on human–rodent interactions, neglecting the role of livestock such as cattle, which are important maintenance hosts. Many existing models also omit key transmission pathways, including direct animal-to-animal contact, asymptomatic infections, and reinfection dynamics. Furthermore, environmental *Leptospira* persistence, vaccination effects, and cross-species interactions are often excluded, limiting the ability of current models to capture the complex multi-host nature of leptospirosis transmission. Therefore, this study contributes to the literature by addressing these gaps.

CHAPTER 3

RESEARCH METHODOLOGY

This chapter provides a complete summary of the research design. It outlines the theoretical models, data collection methods, analysis techniques, and mathematical procedures used to attain the general and specific objectives. It serves as a foundation for understanding the research methodology and the derivation of findings.

3.1 Mathematical Procedure

To achieve the objective of this study, we first developed and analyzed mathematical models that describe the transmission dynamics of leptospirosis in cattle, rats, and humans using the system of nonlinear ordinary differential equations. We separated the entire cattle herd into six compartments for the first model, incorporating environmentally free pathogens. Then, the basic model properties, such as positivity and boundedness of solutions, are analyzed, and the region of invariance where the model is biologically and mathematically well-posed is established. We then determined the basic/effective reproduction number and the stability analysis of the model equilibria. The sensitivity analysis of the model parameters and different numerical simulations are performed to support the analytical results. Further, we extended the proposed model, including an optimal control strategy and cost-effectiveness analysis to minimize the disease burden and related costs. For the proposed extended leptospirosis model, we have analyzed the existence and characterization of the optimal control problem using Pontryagin's Minimum Principle.

Secondly, we proposed a mathematical model that describes the dynamics of leptospirosis in cattle and reservoir hosts (rats). To examine the role of rats, we take into account the direct contact within cattle and with rats as well as the indirect transmission via the environmental free-living *Leptospira*. Fundamental characteristics of the model solution are examined, along with the stability analysis of equilibria points. Numerical simulations are also conducted to support analytical results.

Lastly, we formulated a system of nonlinear fractional-order differential equations for two species (cattle and human) together with the environmental free-*Leptospira* pathogen to examine the role of cattle in the transmission of human leptospirosis. The proposed fractional order system is analyzed qualitatively as well as quantitatively to identify its stable position. Local stability of the system is verified, and global stability is checked using Lyapunov functions. The

existence, boundedness, and positivity of the system are also checked.

3.2 Method of Analysis

Our models are analyzed both qualitatively and quantitatively using appropriate methods.

3.2.1 Qualitative Analysis

The proposed leptospirosis mathematical models are analyzed using different mathematical tools, theories, and theorems that are suitable for the system of ordinary differential equations. The basic properties of the model, such as biological feasibility and mathematical well-posedness, are illustrated by showing non-negativity and boundedness of the solutions. The local and global stability is shown by the Castillo-Chavez and Song theorem, and Descartes' Rule of Signs is used to show the existence of the equilibria. Furthermore, the fixed point theorem, Laplace transform, and inverse Laplace transform are used to provide the qualitative analysis of the fractional order derivative model. The Pontryagin minimum principle is applied to the optimal control problem to investigate the necessary condition of optimal control.

3.2.2 Numerical Analysis

In our research, we have used parameter values from previously published journals in the area of our study and conducted the analysis using numerical methods and algorithms set in the PYTHON language (odeint solver, scipy.optimize.fSolve, and GEKKO optimization packages). Further, we used the generalized Adams-Bashforth-Moulton predictor-evaluator-corrector-evaluator (PECE) algorithm for the simulation of the fractional-order derivative model.

CHAPTER 4

MATHEMATICAL MODELING AND ANALYSIS OF LEPTOSPIROSIS DYNAMICS IN CATTLE HERD WITH OPTIMAL CONTROL

This chapter investigates a mathematical model for leptospirosis transmission dynamics with an optimal control analysis. First, we develop and analyze a mathematical model for leptospirosis transmission dynamics. The basic properties of the model and stability of the model equilibria are studied. Then we extend the model to an optimal control problem by considering some control strategies. Further, the numerical simulations of both models with and without optimal control are performed.

4.1 Model Formulation

In order to study the dynamics of leptospirosis transmission in cattle, we presented a nonlinear deterministic model in this section. The SEIR model (Aslan et al., 2021; Chadsuthi et al., 2022; Okosun et al., 2016) was modified to include the vaccinated population and the asymptomatic infected population as separate compartments. $N(t) = S(t)+E(t)+I(t)+A(t)+R(t)+V(t)$ represents the total population of cattle, where $S(t)$ represents susceptible cattle, $E(t)$ represents exposed cattle, $I(t)$ represents symptomatic infected cattle, $A(t)$ represents asymptomatic infected cattle, $R(t)$ represents recovered cattle, $V(t)$ represents vaccinated cattle, and $L(t)$ represents free-living *Leptospira* in the environment. The vaccinated class receives a portion $\rho\Lambda$ of the recruitment (Aymée et al., 2024), whereas the susceptible class, receives the remaining $(1-\rho)\Lambda$, where $\rho \in [0,1]$.

The force of infection, denoted by λ, is given by $\lambda = \frac{\beta_L L}{K+L} + \beta_A A + \beta_I I$, where the nonlinear term $\frac{\beta_L L}{K+L}$ is a saturation term that limits the effect of transmission to cattle as *Leptospira* concentration in the environment becomes large (Holt et al., 2006). Vaccinated cattle are infected at a reduced force of infection given by $(1-r)\lambda$, where r is the efficiency of vaccination. Both asymptomatic and symptomatic infected cattle shed *Leptospira* into the environment at rates of ω_A and ω_I, respectively. The rate at which recovered cattle lose their natural immunity is denoted as γ, and μ is the natural death rate of the cattle. $\frac{1}{\alpha}$ is the incubation period, and ν indicates the portion of exposed cattle that shows symptoms. δ and σ are the recovery rates of symptomatic and asymptomatic infected cattle, respectively. The descriptions of other parameters used in the model are summarized in Table 4.1. The following are the governing assumptions of the proposed model:

(i) There is no age structure.

(ii) Symptomatic infected cattle include pregnant and lactating cattle, calves, and weak cattle due to co-infection, while the rest of the cattle population are considered asymptomatic cattle (Fraga et al., 2015; Robi et al., 2024).

(iii) Direct transmission from asymptomatic and symptomatic infected cattle occurred at rates of β_A and β_I, respectively, while indirect transmission through the environment occurred at a rate of β_L.

(iv) Portion of newborns from symptomatic infected cattle acquires the disease during birth and hence is subtracted from susceptible cattle (Aslan et al., 2021; Baloba et al., 2020; Minter et al., 2019).

(v) The vaccines are imperfect and hence some portion become exposed (Esteves et al., 2022).

(vi) The immunity granted through vaccination is not lifelong (Fraga et al., 2015), and hence the cattle become susceptible.

(vii) The herd in this study includes all cattle from small holder farmers in a specific village that share the same grazing field.

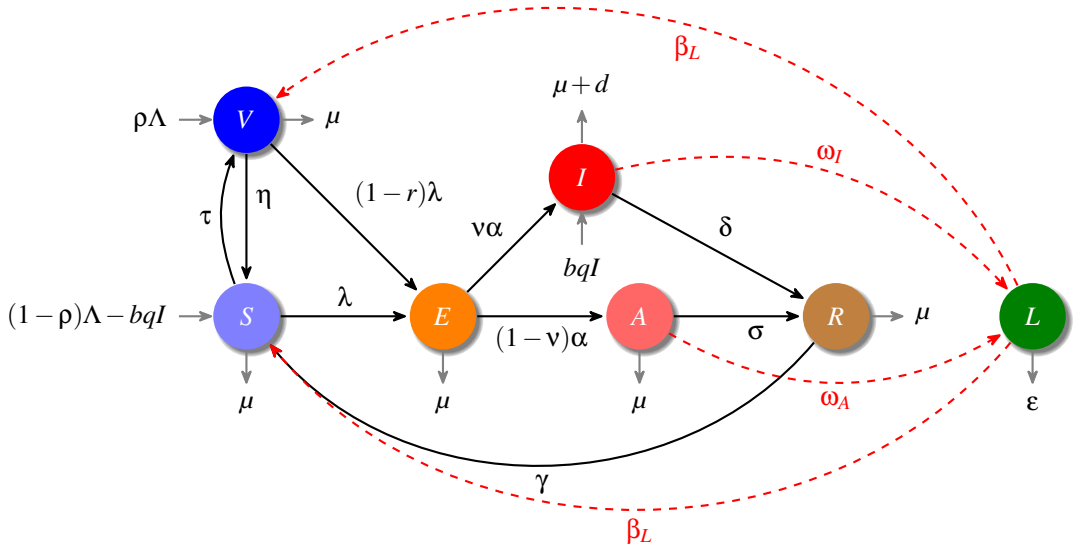

Figure 4.1: Flow diagram for leptospirosis transmission in cattle: Bold arrow shows transition from one compartment to the other and dotted arrow shows pathogen contribution.

From the flow diagram in Figure 4.1 the following differential equation system is generated to describe the transmission dynamics of leptospirosis in cattle.

$$\begin{aligned}
\frac{dS}{dt} &= (1-\rho)\Lambda - bqI - (\frac{\beta_L L}{K+L} + \beta_A A + \beta_I I)S + \gamma R + \eta V - \tau S - \mu S,\\
\frac{dE}{dt} &= (\frac{\beta_L L}{K+L} + \beta_A A + \beta_I I)(S + (1-r)V) - \alpha E - \mu E,\\
\frac{dA}{dt} &= (1-\nu)\alpha E - \sigma A - \mu A,\\
\frac{dI}{dt} &= bqI + \nu\alpha E - \delta I - \mu I - dI,\\
\frac{dR}{dt} &= \sigma A + \delta I - \gamma R - \mu R,\\
\frac{dV}{dt} &= \rho\Lambda - (1-r)(\frac{\beta_L L}{K+L} + \beta_A A + \beta_I I)V + \tau S - \eta V - \mu V,\\
\frac{dL}{dt} &= \omega_A A + \omega_I I - \varepsilon L,
\end{aligned} \tag{4.1}$$

with the initial conditions; $S(0) = S_0 > 0$, $E(0) = E_0 \geq 0$, $A(0) = A_0 \geq 0$, $I(0) = I_0 \geq 0$, $R(0) = R_0 \geq 0$, $V(0) = V_0 \geq 0$, $L(0) = L_0 \geq 0$.

4.2 Model Analysis

4.2.1 Existence and Uniqueness of Solutions

Theorem 4.2.1 (Existence and Uniqueness). Consider the initial value problem (4.1) for the leptospirosis transmission model defined by the system:

$$\frac{d\mathbf{X}}{dt} = \mathbf{F}(\mathbf{X}(t)), \quad \mathbf{X}(0) = \mathbf{X}_0,$$

where

$$\mathbf{X}(t) = \begin{pmatrix} S(t)\\ E(t)\\ A(t)\\ I(t)\\ R(t)\\ V(t)\\ L(t) \end{pmatrix}, \quad \mathbf{F}(\mathbf{X}) = \begin{pmatrix} (1-\rho)\Lambda - bqI - (\frac{\beta_L L}{K+L} + \beta_A A + \beta_I I)S + \gamma R + \eta V - \tau S - \mu S\\ (\frac{\beta_L L}{K+L} + \beta_A A + \beta_I I)(S + (1-r)V) - \alpha E - \mu E\\ (1-\nu)\alpha E - \sigma A - \mu A\\ bqI + \nu\alpha E - \delta I - \mu I - dI\\ \sigma A + \delta I - \gamma R - \mu R\\ \rho\Lambda - (1-r)(\frac{\beta_L L}{K+L} + \beta_A A + \beta_I I)V + \tau S - \eta V - \mu V\\ \omega_A A + \omega_I I - \varepsilon L \end{pmatrix},$$

with $N = S + E + A + I + R + V$, and initial conditions satisfying $\mathbf{X}_0 \in \mathbb{R}^7_+$.

Assume that all the parameters are positive constants and the initial conditions satisfy $\mathbf{X}_0 \in \Omega$, where $\Omega = \Omega_C \times \Omega_L$ is the biologically feasible region defined by:

$$\Omega_C = \left\{ (S(t), E(t), A(t), I(t), R(t), V(t)) \in \mathbb{R}^6_+;\ 0 \leq N(t) \leq \frac{\Lambda}{\mu} \right\}$$

and

$$\Omega_L = \left\{ (L(t)) \in \mathbb{R}^1_+;\ \ 0 \leq L(t) \leq \frac{\Lambda(\omega_A + \omega_I)}{\varepsilon\mu} \right\}$$

.

Then the governing model (4.1) admits a unique, nonnegative, and bounded solution $\mathbf{X}(t)$ that exists for all time $t \geq 0$ and remains in the region Ω.

Proof. We establish the result as follows. Note that the function $\mathbf{F}(\mathbf{X})$ is continuously differentiable with respect to all state variables in $\mathbb{R}^7_+$, provided $N > 0$. Since $\mathbf{F}$ and its Jacobian matrix are continuous on the closed, bounded set Ω, they satisfy a Lipschitz condition inside Ω. By the Picard-Lindelöf theorem (Coddington & Levinson, 1955; Hartman, 1964), there exists a unique local solution $\mathbf{X}(t)$ on some maximal interval of existence $[0, t_{\max})$. The derivative of the vector field $\mathbf{F}$ is also nonnegative, for each state variable, when it approaches zero. That is,

$$\left.\frac{dS}{dt}\right|_{S=0} = (1-\rho)\Lambda - bqI + \gamma R + \eta V > 0, \quad \left.\frac{dE}{dt}\right|_{E=0} = \left(\frac{\beta_L L}{K+L} + \beta_A A + \beta_I I\right)(S + (1-r)V) \geq 0,$$

and similarly for other compartments. Thus, by the invariance principle for cooperative systems (Smith, 1995), solutions starting in the nonnegative orthant $\mathbb{R}^7_+$ remain nonnegative for all $t \geq 0$.

Next, define the total cattle population $N(t) = S(t) + E(t) + A(t) + I(t) + R(t) + V(t)$. Adding the first six equations yields:

$$\frac{dN}{dt} = \Lambda - \mu N(t) - dI(t) \leq \Lambda - \mu N.$$

Applying Grönwall's inequality (Gronwall, 1919), we obtain:

$$N(t) \leq \frac{\Lambda}{\mu} + \left(N(0) - \frac{\Lambda}{\mu}\right) e^{-\mu t} \leq \max\left\{N(0), \frac{\Lambda}{\mu}\right\}.$$

For the pathogen compartment $L(t)$, we have:

$$\frac{dL}{dt} \leq (\omega_A + \omega_I)\frac{\Lambda}{\mu} - \varepsilon L,$$

which similarly implies boundedness of $L(t)$. Thus, all state variables remain uniformly bounded

on any finite time interval.

Since the right-hand side $\mathbf{F}$ is Lipschitz continuous on Ω and solutions remain bounded, by the continuation theorem for ordinary differential equations (Hirsch et al., 1974), the local solution can be extended to all $t \geq 0$. Specifically, the boundedness of solutions prevents finite-time blow-up, ensuring global existence.

From the bounds derived above, it follows directly that if $\mathbf{X}(0) \in \Omega$, then $\mathbf{X}(t) \in \Omega$ for all $t \geq 0$. Thus, Ω is positively invariant (Hale, 1969).

Therefore, by combining the Picard-Lindelöf theorem, Grönwall's inequality, and the continuation principle, we conclude that the model equations (4.1) has a unique, nonnegative, bounded solution that exists globally in time and remains within the biologically feasible region Ω. □

Remark 1. The mathematical foundation established here follows standard results in dynamical systems theory (Perko, 2013; Wiggins, 2003). The boundedness argument via Grönwall's inequality is particularly crucial, as it ensures that population variables do not grow without bound which is an important requirement for biological realism. The invariance of Ω confirms that the model respects basic demographic constraints. These features ensure that the model is both mathematically well-posed and biologically realistic.

4.2.2 *Leptospira*-free Equilibrium and Effective Reproduction Number

The *Leptospira*-free equilibrium(LFE) can be found by equating the right-hand side of Eq. (4.1) to zero by setting disease state equal to zero ($A^* = I^* = L^* = 0$). The remaining state variables result in $E^* = 0$, $R^* = 0$, $V^* = \dfrac{\Lambda(\rho\mu+\tau)}{\mu(\eta+\tau+\mu)}$ and $S^* = \dfrac{\Lambda((1-\rho)\mu+\eta)}{\mu(\eta+\tau+\mu)}$. Hence, the *Leptospira*-free equilibrium point denoted by, $\mathscr{E}^*$, is given by

$$\mathscr{E}^* = \left(\frac{\Lambda((1-\rho)\mu+\eta)}{\mu(\eta+\tau+\mu)}, 0, 0, 0, 0, \frac{\Lambda(\mu\rho+\tau)}{\mu(\eta+\tau+\mu)}, 0\right). \tag{4.2}$$

To compute the effective reproduction number we used next generation matrix approach presented in Van den Driessche & Watmough (2002) as follows. The rate of appearance of new infection and rate of transfer from one compartment to another in the infectious classes gives the following:

$$\mathscr{F} = \begin{bmatrix} (\frac{\beta_L L}{K+L} + \beta_A A + \beta_I I)(S + (1-r)V) \\ 0 \\ 0 \\ 0 \end{bmatrix}, \qquad \mathscr{V} = \begin{bmatrix} (\alpha+\mu)E \\ (\sigma+\mu)A - (1-\nu)\alpha E \\ (\delta+\mu+d-bq)I - \nu\alpha E \\ \varepsilon - \omega_A A - \omega_I I \end{bmatrix}. \tag{4.3}$$

Derivation of Eq. (4.3) with respect to disease state variables and evaluating at $\mathscr{E}^*$,

$$F = \frac{\partial \mathscr{F}_i}{\partial x_j} = \begin{bmatrix} 0 & \beta_A(S^*+(1-r)V^*) & \beta_I(S^*+(1-r)V^*) & \frac{\beta_L}{K}(S^*+(1-r)V^*) \\ 0 & 0 & 0 & 0 \\ 0 & 0 & 0 & 0 \\ 0 & 0 & 0 & 0 \end{bmatrix},$$

$$V = \frac{\partial \mathscr{V}_i}{\partial x_j} = \begin{bmatrix} (\alpha+\mu) & 0 & 0 & 0 \\ -(1-\nu)\alpha & (\sigma+\mu) & 0 & 0 \\ -\nu\alpha & 0 & (\delta+\mu+d)-bq & 0 \\ 0 & -\omega_A & -\omega_I & \varepsilon \end{bmatrix}.$$

Hence the effective reproduction number $\mathscr{R}_e$ is given by the largest spectral radius of the next generation matrix, FV^{-1}. That is

$$\mathscr{R}_e = \rho(FV^{-1}) = \mathscr{R}_A + \mathscr{R}_I + \mathscr{R}_L, \tag{4.4}$$

where,

$$\begin{aligned} \mathscr{R}_A &= \frac{\beta_A(S^*+(1-r)V^*)(1-\nu)\alpha}{(\alpha+\mu)(\sigma+\mu)}, \\ \mathscr{R}_I &= \frac{\beta_I(S^*+(1-r)V^*)\nu\alpha}{(\alpha+\mu)[(\delta+\mu+d)-bq]}, \\ \mathscr{R}_L &= \frac{\beta_L}{K}\frac{(S^*+(1-r)V^*)(\omega_A(1-\nu)\alpha[(\delta+\mu+d)-bq]+\omega_I\nu\alpha(\sigma+\mu))}{\varepsilon(\alpha+\mu)(\sigma+\mu)[(\delta+\mu+d)-bq]}, \end{aligned}$$

with $(\delta+\mu+d)-bq>0$ as $\mathscr{R}_e$ is non-negative for epidemiological sense-full model. $\mathscr{R}_A$, $\mathscr{R}_I$ and $\mathscr{R}_L$ are reproduction numbers that corresponds to transmissions from asymptomatic cattle , infected cattle and from the environment respectively. We can further subdivide $\mathscr{R}_L$ for suitability as $\mathscr{R}_L = \mathscr{R}_L^{'} + \mathscr{R}_L^{''}$, where

$$\mathscr{R}_L^{'} = \frac{\beta_L}{K}\frac{(S^*+(1-r)V^*)\omega_A(1-\nu)\alpha}{\varepsilon(\alpha+\mu)(\sigma+\mu)} \quad and \quad \mathscr{R}_L^{''} = \frac{\beta_L}{K}\frac{(S^*+(1-r)V^*)\omega_I\nu\alpha}{\varepsilon(\alpha+\mu)[(\delta+\mu+d)-bq]}$$

Remark 2. Epidemiologically, $\mathscr{R}_A$ and $\mathscr{R}_I$ shows a new infection generated by asymptomatic and symptomatic infected cattle respectively prior to their recovery. In particular $\mathscr{R}_I$ is regulated by the term $[(\delta+\mu+d)-bq]$, which implies increasing $(\delta+\mu+d)$ and/or decreasing either of b or q will decrease the effective reproduction number. Furthermore, $\mathscr{R}_L$ signifies the pace at which *Leptospira* is released into the environment by asymptomatic and symptomatic infected cattle (ω_A and ω_I). This factor amplifies the transfer rate of bacteria to susceptible and vaccinated cattle, potentially triggering disease outbreaks. However, implementing control measures that

aim to enhance the decay rate of *Leptospira* in the environment (ε) will effectively minimize the rate of new infections.

When there is no vaccination of susceptible cattle in the herd, that is, $\tau = 0$, then the effective reproduction number (4.4) reduces to the basic reproduction number, $\mathscr{R}_0$, given by

$$\mathscr{R}_0 = \frac{\Lambda[\eta+\mu(1-r\rho)]}{\mu(\eta+\mu)}\left(\frac{\beta_A(1-\nu)\alpha}{(\alpha+\mu)(\sigma+\mu)} + \frac{\beta_I\nu\alpha}{(\alpha+\mu)[(\delta+\mu+d)-bq]} + \frac{\beta_L}{K}\frac{(\omega_A(1-\nu)\alpha[(\delta+\mu+d)-bq]+\omega_I\nu\alpha(\sigma+\mu))}{\varepsilon(\alpha+\mu)(\sigma+\mu)[(\delta+\mu+d)-bq]}\right) \tag{4.5}$$

Biologically, $\mathscr{R}_0$ represents the average number of secondary cases arising from single infectious cattle in a completely susceptible population (Van den Driessche & Watmough, 2008).

Re-writing (4.4) in terms of (4.5),

$$\mathscr{R}_e = \left(\frac{(\eta+\mu)-r\rho\mu+(1-r)\tau}{(\eta+\tau+\mu)}\right)\left(\frac{(\eta+\mu)}{(\eta+\mu)-r\rho\mu}\right)\mathscr{R}_0$$

$$\mathscr{R}_e(\infty) := \lim_{\tau\to\infty}\mathscr{R}_e = \frac{(1-r)(\eta+\mu)}{[\eta+\mu(1-r\rho)]}\mathscr{R}_0.$$

Moreover, $\dfrac{\partial\mathscr{R}_e}{\partial\tau} = -r\dfrac{(1-\rho)\mu+\eta}{(\eta+\tau+\mu)^2}\dfrac{(\eta+\mu)}{[\eta+\mu(1-r\rho)]}\mathscr{R}_0 < 0$ (decreasing)

Therefore, $\dfrac{(1-r)(\eta+\mu)}{[\eta+\mu(1-r\rho)]}\mathscr{R}_0 \le \mathscr{R}_e \le \mathscr{R}_0$, and therefore $\mathscr{R}_0 < 1$ implies $\mathscr{R}_e < 1$. This shows that vaccination coverage τ plays a great role in controlling leptospirosis for $\mathscr{R}_0 < 1$. However, for $\mathscr{R}_0 > 1$, it is important to note that

$$\mathscr{R}_e(\infty) \le 1 \iff \frac{(1-r)(\eta+\mu)}{[\eta+\mu(1-r\rho)]}\mathscr{R}_0 < 1 \iff r > r^* := \frac{(\mathscr{R}_0-1)(\eta+\mu)}{(\eta+\mu)\mathscr{R}_0-\rho\mu} \tag{4.6}$$

where r^* is critical vaccine efficacy. This could indicate that even with high vaccination coverage, the disease might not be completely eradicated if vaccine efficacy r is low and $\mathscr{R}_0$ is significantly higher than unity (Diagne et al., 2021). Figure 4.2(a) suggests that even in cases where vaccine coverage τ is high, additional efforts will be required to bring $\mathscr{R}_e$ below unity. Using better biosecurity practices and giving antibiotics to the entire herd, along with vaccinations, can help control *Leptospira* outbreaks in dairy cattle herds (Mughini-Gras et al., 2014).

Also, for $\mathscr{R}_0 > 1$ the critical vaccination threshold τ^* for disease eradication can be derived by setting $\mathscr{R}_e = 1$ and it is given by

$$\tau^* = \frac{(\eta+\mu)[(\eta+\mu)\mathscr{R}_0-r\rho\mu](\mathscr{R}_0-1)}{(r-r^*)[(\eta+\mu)\mathscr{R}_0-\rho\mu]} \tag{4.7}$$

Note that $\mathscr{R}_e < 1 (> 1)$ when $\tau > (<)\tau^*$. Figure 4.2(b) shows the vaccine coverage τ as a function of $\mathscr{R}_0$, where the vaccine efficacy is 95% ($r > r^*$). The shaded region indicates the

situation when vaccine coverage τ is greater than the critical vaccination threshold τ^*.

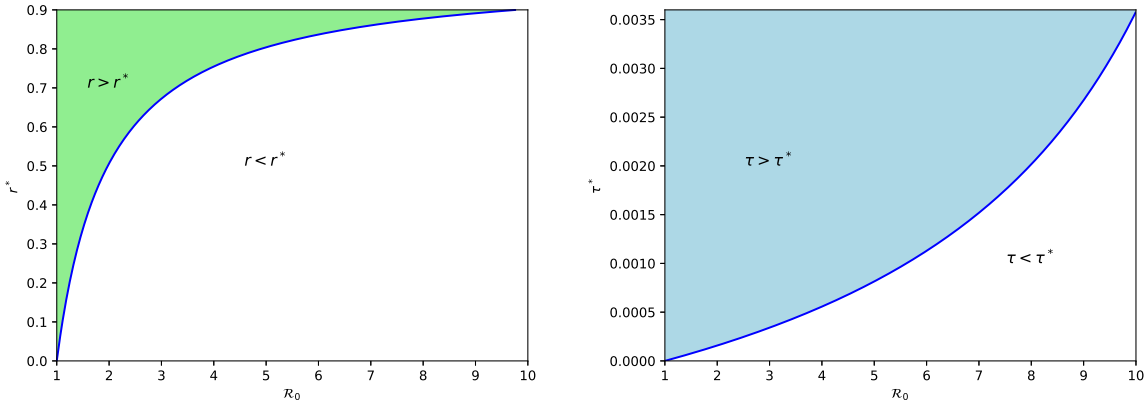

(a) (b)

Figure 4.2: (a) Critical vaccination efficacy, $r^*(\mathscr{R}_0)$ (b) Critical vaccination coverage, $\tau^*(\mathscr{R}_0)$

4.2.3 Local Stability of *Leptospira*-Free Equilibrium

Theorem 4.2.2. The *Leptospira*-free equilibrium point, $\mathscr{E}^*$, of system in Eq.(4.1) is locally asymptotically stable whenever $\mathscr{R}_e < 1$ and unstable otherwise.

Proof. Go to Appendix (A.9). □

Remark 3. The biological implication of Theorem 4.2.2 is that the flow of *Leptospira* infected cattle will not generate an outbreak of the disease and eventually extincts for $\mathscr{R}_e$ less than unity for the herd size sufficiently close to *Leptospira*-free equilibrium as time goes very large.

4.2.4 Global Stability of *Leptospira*-Free Equilibrium

In this section we will present the global stability of the *Leptospira*-free equilibrium using the method of Castillo-Chavez (2002),

Theorem 4.2.3. The *Leptospira*-free equilibrium $\mathscr{E}^*$ of the system Eq. (4.1) is globally asymptotically stable for $\mathscr{R}_e < 1$ on its feasible region.

Proof. Re-writing the model (4.1) as;

$$\begin{aligned} \frac{d\mathbf{X}}{dt} &= F(\mathbf{X},\mathbf{Y}), \\ \frac{d\mathbf{Y}}{dt} &= G(\mathbf{X},\mathbf{Y}); with, G(\mathbf{X},0) = 0, \end{aligned} \tag{4.8}$$

where, $\mathbf{X} = (S,R,V) \in \mathbb{R}^3$ denotes the uninfected compartment and $\mathbf{Y} = (E,A,I,L) \in \mathbb{R}^4$ denotes the infected compartments. Let $\mathscr{E}^* = (\mathbf{X}^*, 0)$ denotes the *Leptospira*-free equilibrium of the system (4.1). The following conditions grants the global stability of the *Leptospira*-free equilibrium according to Castillo-Chavez (2002),

H_1 : For $\dfrac{d\mathbf{X}}{dt} = F(\mathbf{X},\mathbf{Y})$, $\mathbf{X}^*$ is a globally asymptotically stable where $F(\mathbf{X}^*,0) = 0$

H_2 : $G(\mathbf{X},\mathbf{Y}) = B\mathbf{Y} - \hat{G}(\mathbf{X},\mathbf{Y})$, $\hat{G}(\mathbf{X},\mathbf{Y}) > 0$ for $(\mathbf{X},\mathbf{Y}) \in \Omega$, where $B = D_Y G(\mathbf{X}^*,0)$ is an M-matrix (the matrix with off-diagonal elements non-negative).

To show condition H_1, take a sub-model of our model (4.1)

$$\frac{d\mathbf{X}}{dt} = F(\mathbf{X},0) = \begin{bmatrix} (1-\rho)\Lambda + \gamma R + \eta V - (\tau+\mu)S \\ -(\gamma+\mu)R \\ \rho\Lambda + \tau S - (\eta+\mu)V \end{bmatrix} \tag{4.9}$$

Solving the sub-system (4.9) and taking the limit as $t \to \infty$ gives us,

$$S(t) \to \frac{\Lambda}{\mu}\left[\frac{(1-\rho)\mu+\eta}{\eta+\mu+\tau}\right], \quad R(t) \to 0, \text{ and } \quad V(t) \to \frac{\Lambda(\rho\mu+\tau)}{\mu(\eta+\tau+\mu)}$$

that is (S^*,R^*,V^*) is global attract on Ω and sub-system (4.9) is globally stable,

On the other hand to show condition H_2,

$$B = D_Y G(\mathbf{X}^*,0) = \begin{bmatrix} -(\alpha+\mu) & \beta_A(S^*+(1-r)V^*) & \beta_I(S^*+(1-r)V^*) & \frac{\beta_L(S^*+(1-r)V^*)}{K} \\ (1-\nu)\alpha & -(\sigma+\mu) & 0 & 0 \\ \nu\alpha & 0 & -[(\delta+\mu+d)-bq] & 0 \\ 0 & \omega_A & \omega_I & -\varepsilon \end{bmatrix},$$

where, $S^* = \dfrac{\Lambda}{\mu}\left[\dfrac{(1-\rho)\mu+\eta}{\eta+\mu+\tau}\right]$, $\quad V^* = \dfrac{\Lambda(\rho\mu+\tau)}{\mu(\eta+\tau+\mu)}$,

and $G(\mathbf{X},\mathbf{Y}) = \begin{bmatrix} (\frac{\beta_L L}{K+L} + \beta_A A + \beta_I I)(S+(1-r)V) - \alpha E - \mu E \\ (1-\nu)\alpha E - \sigma A - \mu A \\ bqI + \nu\alpha E - \delta I - \mu I - dI \\ \omega_A A + \omega_I I - \varepsilon L \end{bmatrix}$

Thus,

$$\hat{G}(\mathbf{X},\mathbf{Y}) = \begin{bmatrix} (S^*+(1-r)V^*)\left[(\beta_A A+\beta_I I)(1-\frac{(S+(1-r)V)}{(S^*+(1-r)V^*)}) + \frac{\beta_L L}{K}(1-\frac{(S+(1-r)V)K}{(S^*+(1-r)V^*)(K+L)})\right] \\ 0 \\ 0 \\ 0 \end{bmatrix}$$

Where $\hat{G}(\mathbf{X},\mathbf{Y}) = B\mathbf{Y} - G(\mathbf{X},\mathbf{Y})$. For $S \le S^*$ and $V \le V^*$ in the feasible region Ω, $\hat{G}(\mathbf{X},\mathbf{Y}) \ge 0$. Therefore both H_1 and H_2 conditions are satisfied and $\mathscr{E}^*$ is globally asymptotically stable for $\mathscr{R}_e < 1$. □

Remark 4. Epidemiologically Theorem 4.2.3 implies that, independent of the initial available cattle herd size *Leptospira* infected cattle will not lead to an outbreak of the disease and it extincts in the long run for $\mathscr{R}_e$ less than unity.

4.2.5 Existence of *Leptospira*-Persistent Equilibrium

Leptospira-persistent equilibrium(LPE) can be found by setting right side of Eq. (4.1) to zero and solving for state variables. Let $\mathscr{E}^{**} = (S^{**}, E^{**}, A^{**}, I^{**}, R^{**}, V^{**}, L^{**})$ be an LPE and expressing all state variables in terms of exposed class, E^{**} gives,

$$\begin{aligned} A^{**} &= k_A E^{**}, \\ I^{**} &= k_I E^{**}, \\ R^{**} &= k_R E^{**}, \\ L^{**} &= k_L E^{**}, \\ S^{**} &= \frac{k_2((1-r)\lambda^{**} + k_6)E^* - (1-r)\rho\Lambda\lambda^*}{\lambda^{**}((1-r)\lambda^{**} + k_6 + (1-r)\tau)}, \\ V^{**} &= \frac{\rho\Lambda + \tau S^{**}}{(1-r)\lambda^{**} + k_6}, \end{aligned} \tag{4.10}$$

where,

$\lambda^{**} = \beta_A A^{**} + \beta_I I^{**} + \frac{\beta_L L^{**}}{K+L^{**}}$, $\quad k_A = \dfrac{(1-\nu)\alpha}{k_3}$, $\quad k_I = \dfrac{\nu\alpha}{k_4}$,

$k_R = \dfrac{\sigma k_A + \delta k_I}{k_5}$, $\quad k_L = \dfrac{\omega_A k_A + \omega_I k_I}{\varepsilon}$, $\quad k_1 = \tau + \mu$, $\quad k_2 = \alpha + \mu$,

$k_3 = \sigma + \mu$, $\quad k_4 = (\delta + \mu + d) - bq$, $\quad k_5 = \gamma + \mu$, $\quad k_6 = \eta + \mu$.

Substituting Eq. (4.10) in the first equation of Eq. (4.1), will give us the following characteristic equation for $E^{**} \neq 0$,

$$A_6 E^{**6} + A_5 E^{**5} + A_4 E^{**4} + A_3 E^{**3} + A_2 E^{**2} + A_1 E^{**} + A_0 = 0 : \tag{4.11}$$

where,

$A_0 = \mu k_2 k_6 (k_6 + \tau) K^3 [\mathscr{R}_e - 1] > 0$, for $\mathscr{R}_e > 1$,

$A_6 = (1-r)^2 k_L^3 (\beta_A k_A + \beta_I k_I)^3 (\gamma k_R - bq k_I - k_2) \leq -\mu (1-r)^2 k_L^3 (\beta_A k_A + \beta_I k_I)^3 < 0$.

Here, $A_6 < 0$ and $A_0 > 0$, which shows that equation Eq. (4.11) has at least one positive root for $\mathscr{R}_e > 1$ by exploiting Descartes' rule of sign (Descartes, 1937). In fact, substituting the parameter values in Table 4.1 gives us $A_6 < 0, A_5 < 0, A_4 < 0, A_3 < 0, A_2 < 0, A_1 < 0, A_0 > 0$, which shows the system has a unique LPE for $\mathscr{R}_e > 1$ since there is only one sign change for Eq. (4.11). Because of the complexity of qualitative analysis, stability of the unique *Leptospira*-persistent equilibrium will be discussed graphically in subsection 4.3.1. Moreover, the global stability of *Leptospira*-free equilibrium shows system (4.1) undergoes forward bifurcation at $\mathscr{R}_e = 1$.

4.2.6 Sensitivity Analysis

To show how changes in model parameter values affect $\mathscr{R}_e$, we figure out which model parameters are most important for disease transmission and then show in a graph how the effective reproduction number changes when the model parameters are changed. Prioritizing intervention measures based on their impact could help farmers, veterinarians, and policymakers to focus on those key interventions. Figure 4.3(a) indicates that when the cattle recovery rate σ is improved in line with better vaccination coverage τ, then $\mathscr{R}_e$ could be less than unity and the disease can be eradicated from the herd.

Figure 4.3(b) shows that improving cattle recovery through proper treatment and reducing contact rate β_A properly minimizes the spread of leptospirosis in the cattle herd. Similarly, Figure 4.3(c) depicts the impact of vaccine coverage τ and the contact rate β_A on the effective reproduction number $\mathscr{R}_e$. As expected, to reduce the value of $\mathscr{R}_e$ below unity, the contact rate must be very low, almost irrespective of the vaccine coverage. That is, despite the availability of vaccines, protective measures such as avoiding the introduction of infected animals into the herd and isolation/quarantine of newly recruited cattle until proven negative could manage the spread of leptospirosis.

We have also conducted the sensitivity analysis on the effective reproduction number, $\mathscr{R}_e$ using sensitivity index given by Definition A.5.1. Accordingly, the most sensitive parameters are the vaccine efficiency, r, recruitment rate, Λ and contact rate from asymptomatic infected cattle, β_A respectively. Also the least sensitive parameter is vertical transmission rate, q. As an example a 10% increase (or decrease) in β_A, increase (or decrease) $\mathscr{R}_e$ by 9.2% and similarly 10% increase (or decrease) in σ, decrease (or increase) $\mathscr{R}_e$ by 6.5%. The sensitivity indices of $\mathscr{R}_e$ with respect to each parameter values are summarized in Table 4.2.

Table 4.2 shows that the dynamics of leptospirosis transmission is much affected by direct transmission from asymptomatic infected cattle than other transmission route. However vertical transmission has least effect on the dynamics.

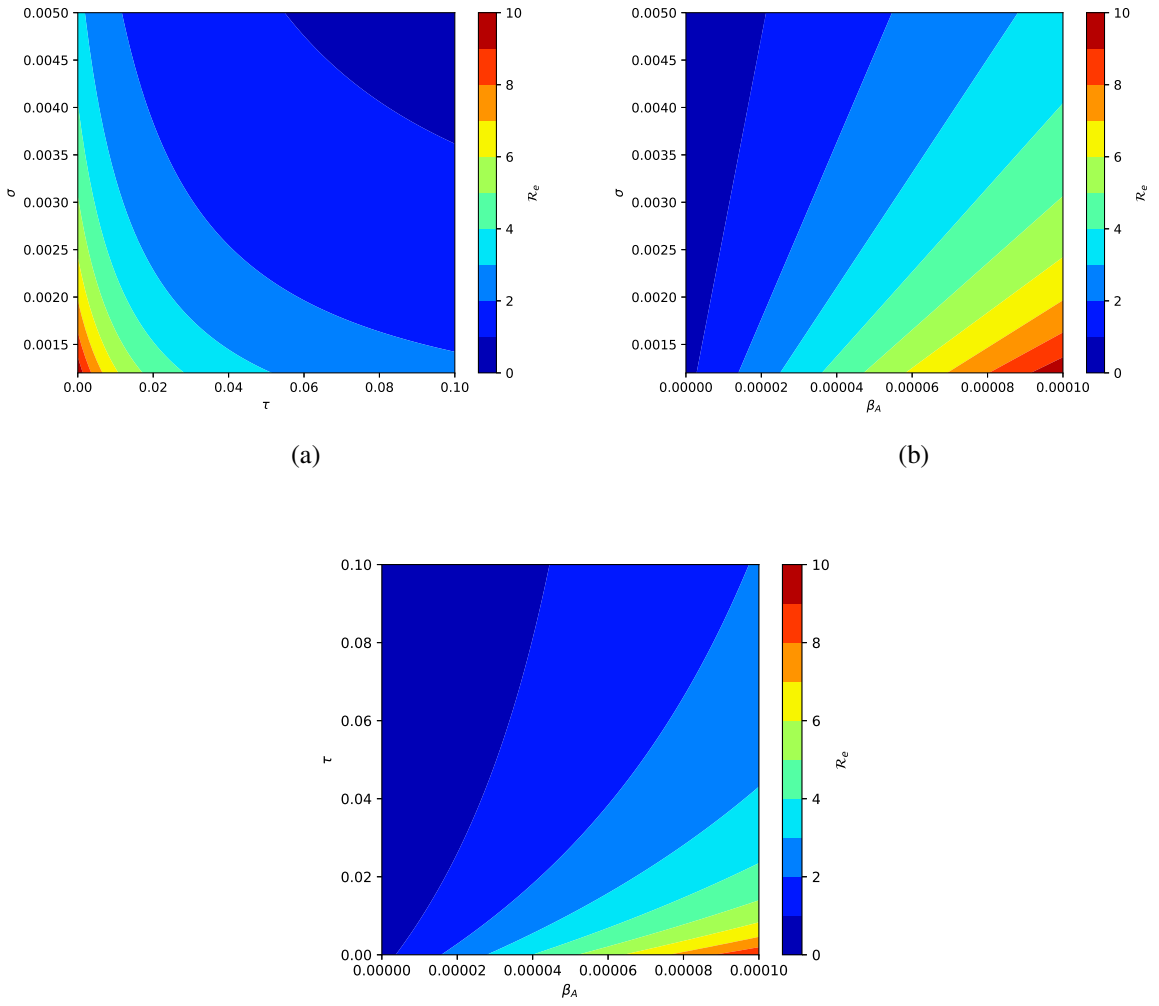

(a)

(b)

(c)

Figure 4.3: Contour plot of $\mathscr{R}_e$ (a) with respect to recovery rate σ and vaccination rate τ. (b) with respect to recovery rate σ and contact rate β_A. (c) with respect to vaccination rate τ and contact rate β_A.

4.3 Numerical Simulation and Discussion

In this section, we present a numerical simulation of model Eq.(4.1) using parameter values in Table 4.1 and odeint package in PYTHON programing language section B.1 to validate the qualitative analysis. The initial herd size is assumed as $(S_0, E_0, A_0, I_0, R_0, V_0, L_0) = (300, 60, 30, 10, 0, 100, 10)$. Because of lack of data, we were unable to perform parameter estimation. The parameters in Table 4.1 are taken from previously published articles, and others are assumed with the following justification:

Table 4.1: Parameters description and their values

Parameter	Description	Value/Unit	Source
Λ	Recruitment rate of cattle	0.15 cattle(day^{-1})	Assumed
b	birth rate of cattle	0.000685 day^{-1}	Assumed
q	Portion of symptomatic infected offspring during birth	0.2	(Minter et al., 2019)
ρ	Portion of recruited cattle that are vaccinated	0.5	[Assumed]
r	Effectiveness of vaccine	0.88	(Esteves et al., 2022; Wilson-Welder et al., 2020)
K	Density of *Leptospira* in the environment	1000 unit*	Holt et al. (2006)
β_A	Transmission coefficient of the disease from asymptomatic infected cattle to susceptible cattle	0.0001 (cattle.day)$^{-1}$	(Aslan et al., 2021; Minter et al., 2019)
β_I	Transmission coefficient of the disease from symptomatic infected cattle to susceptible cattle	0.00005 (cattle.day)$^{-1}$	Assumed
β_L	Transmission coefficient of the disease from environment to susceptible cattle	0.005 day^{-1}	Holt et al. (2006)
α	Transition rate from exposed to symptomatic and asymptomatic infected cattle	0.1 day^{-1}	(Chadsuthi et al., 2022)
ν	Portion of transition from exposed to symptomatic infected	0.2	Assumed
δ	Transition rate from symptomatic infected to recovered	0.0027 day^{-1}	(Aslan et al., 2021; Okosun et al., 2016)
σ	Transition rate from asymptomatic infected to recovered	0.00137 day^{-1}	Assumed
μ	Natural death rate	0.000685 day^{-1}	(Chadsuthi et al., 2022)
d	Disease induced death rate	0.01 day^{-1}	(Holt et al., 2006)
ε	Decay rate of *Leptospira*	0.0111 day^{-1}	(Baca-Carrasco et al., 2015)
ω_A	Shedding rate of *Leptospira* from asymptomatic infected cattle into the environment	0.014 unit.(cattle.day)$^{-1}$	(Baca-Carrasco et al., 2015)
ω_I	Shedding rate of *Leptospira* from symptomatic infected cattle into the environment	0.01 unit.(cattle.day)$^{-1}$	[Assumed]
τ	Rate of vaccination of susceptible cattle	0.05 day^{-1}	[Assumed]
γ	Rate of losing temporary immunity	0.00185 day^{-1}	(Chadsuthi et al., 2022)
η	Rate of losing vaccine immunity	0.013 day^{-1}	(Okosun et al., 2016)

*Usually a unit abundance of bacteria is defined as 10^{10}. Here K is assumed as 1000×10^{10} *Leptospira* (Aslan et al., 2021; Baca-Carrasco et al., 2015; Barragan et al., 2017).

Table 4.2: Sensitivity of the Parameters

Parameters	Value	Sensitivity index
Λ	0.15	+1
q	0.20	+0.0002
ρ	0.5	-0.0156
K	1000	-0.0578
β_A	0.0001	+0.9223
β_I	0.00005	+0.0179
β_L	0.005	+0.0598
α	0.1	+0.0068
ν	0.2	-0.2256
δ	0.0027	-0.0040
σ	0.00137	-0.6537
μ	0.000685	-1.3256
d	0.01	-0.0147
ε	0.0111	-0.0598
ω_A	0.014	+0.0582
ω_I	0.01	+0.0016
η	0.013	+0.4665
b	0.000685	-0.0002
r	0.88	-2.2855
τ	0.05	-0.4756

- β_I : In this study, we assume β_A be twice as much as β_I because in traditional farming, farmers commonly isolate and treat cattle with disease symptoms rather than sending them to the field. Also, calves, lactating, and pregnant cattle rarely go far away, and they have a lower probability of infecting others. Moreover, the amount of urine discharge per day in calves is half that of adults, which reduces the probability of contacting others. The authors in Aslan et al. (2021) took the contact rate for adult cattle as 0.0001, and we assume half of it, $\beta_I = 0.00005$.

- ν : Articles Fraga et al. (2015); Rajeev et al. (2014), emphasize that the majority of the cattle are asymptomatic of leptospirosis disease. Accordingly, we assume symptomatic infected cattle to be at most 20% (i.e ν=0.2).

- σ : In Okosun et al. (2016), authors used in their model one year for infected cattle to recover. Whereas in Mughini-Gras et al. (2014), it is documented that chronic carrier cattle excrete *Leptospira* in their urine for up to 542 days. Also in Monti et al. (2023), it is noted that the recovery can be extended up to three years for asymptomatic infected cattle. Accordingly, we assume at least two years for asymptomatic cattle to recover,

$\sigma = 0.00137$ (i.e $1/\sigma = 730$days).

- ω_I: From Baca-Carrasco et al. (2015); Barragan et al. (2017) it follows that there are $1\text{x}10^8$ leptospira bacteria per milliliter of cattle's urine. Taking a unit abundance of bacteria as 10^{10} *Leptospira*, then there are 10 units of bacteria per one liter of cattle's urine. Not all these *Leptospira* will remain on the surface of the field or grass; some will sink into the soil and not be accessible by the cattle Babylon et al. (2018). If we assume 0.01% of these *Leptospira* survive, the *Leptospira* contributing to the transmission of the disease is 0.001 units per one liter of infected cattle urine. Since a cattle produces 7 to 14 liters of urine in a day Robichaud et al. (2011), taking an average value of 10 liters will give us $\omega_I = 0.01$.

4.3.1 Stability of *Leptospira*-Free Equilibrium and *Leptospira*-persistent Equilibrium

Using the parameter values in Table 4.1 and the above initial condition, Eq. (4.4) gives the effective reproduction number, $\mathscr{R}_e \approx 2.794 > 1$. Applying numerical method for system of nonlinear equation, *scipy.optimize.fSolve* (Moruzzi & Moruzzi, 2020), if we solve model (4.1) by setting the right hand side to zero gives us a unique positive *Leptospira*-persistent equilibrium given by $\mathscr{E}^{**} = (S^{**}, E^{**}, A^{**}, I^{**}, R^{**}, V^{**}, L^{**}) \approx (16.51, 1.63, 63.45, 2.46, 36.91, 62.09, 82.25)$. Figure 4.4 (a and b) illustrates the unique *Leptospira*-persistent equilibrium is local asymptotically stable.

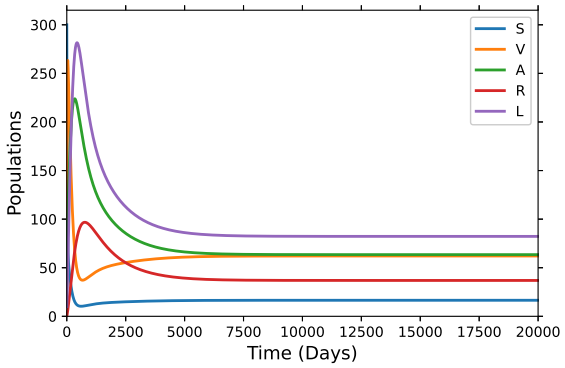

(a) As $t \to \infty$, $S \to 16.51$, $V \to 62.09$, $A \to 63.45$, $R \to 36.91$ and $L \to 82.25$

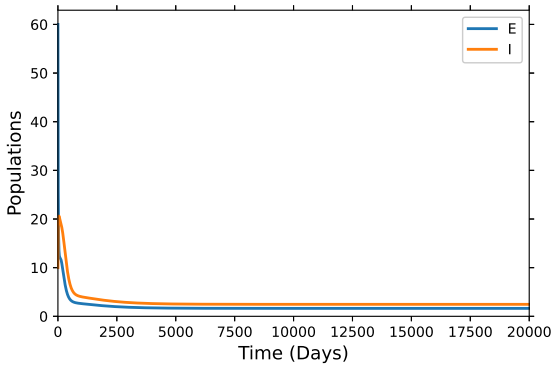

(b) As $t \to \infty$, $E \to 1.63$, $I \to 2.46$

Figure 4.4: Stability of LPE, $\mathscr{E}^{**} \approx (16.51, 1.63, 63.45, 2.46, 36.91, 62.09, 82.25)$, when $\mathscr{R}_e = 2.794 > 1$ using the baseline parameter values in the Table 4.1.

Also if we modify the parameters, $\beta_A = 0.00005$ and $\tau = 0.15$, the effective reproduction number is reduced to, $\mathscr{R}_e \approx 0.948 < 1$. Figure 4.5 (a and b) justify that the *Leptospira*-Free equi-

librium, $\mathscr{E}^* \approx (17.85, 0, 0, 0, 0, 201.13, 0)$, which is evaluated from Eq.(4.2), is locally asymptotically stable and this is also shown analytically in Theorem 4.2.2 above.

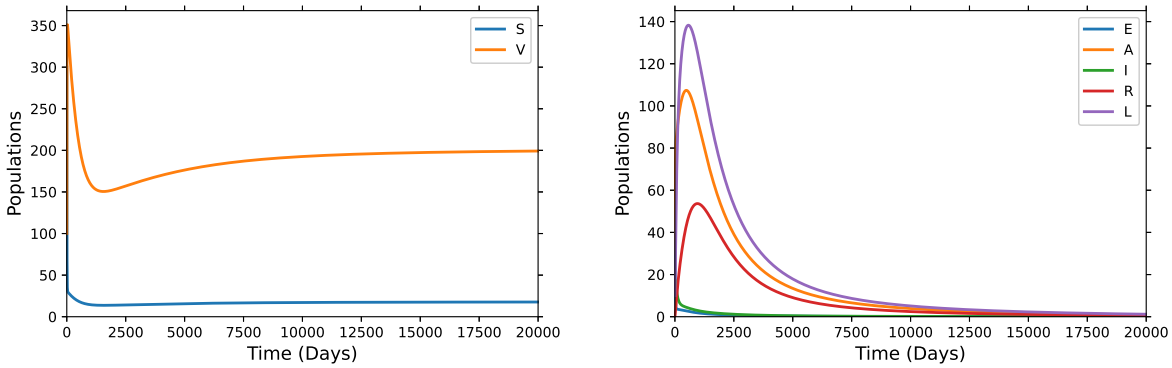

(a) As $t \to \infty$, $S \to 17.85$,$V \to 201.13$

(b) As $t \to \infty$, $E \to 0$, $A \to 0$, $I \to 0$, $R \to 0$, $L \to 0$

Figure 4.5: Stability of LFE, $\mathscr{E}^* \approx (17.85, 0, 0, 0, 0, 201.13, 0)$ for $\mathscr{R}_e = 0.948 < 1$ using $\beta_A = 0.00005, \tau = 0.15$ and the other baseline parameters as in Table 4.1

.

4.3.2 Effect of Most Sensitive Parameters

Effect of Contact Rate with Asymptomatic Cattle, β_A.

In this subsection, we demonstrate the sensitivity of the asymptomatic, symptomatic, susceptible, and vaccinated population in model Eq.(4.1) and also the bacterial load by varying the contact rate of the asymptomatic infected cattle, β_A. Accordingly, Figure 4.6(a) shows that for $\beta_A = 0.0001$ (the baseline value), the infected population (sum of asymptomatic and symptomatic) rapidly grows and approaches 250 in the first year, gradually declining to an endemic value in the next two years. However, 50% reduction in the contact rate (i.e., $\beta_A = 0.00005$) significantly controlled rapid growth, and the maximum infected population size did not exceed 150. In addition, as observed from Figure 4.6(c), the leptospiral load in the environment grows rapidly in the first year for the base-line value of the contact rate. However, a reduction in the contact rate with asymptomatic cattle, β_A by half could properly manage growth speed and maximum load in the first year due to the decrease in the size of the asymptomatic and symptomatic infected cattle. Further, the sizes of susceptible and vaccinated cattle were improved by a decrease in contact with asymptomatic infected cattle, as observed in Figure 4.6(b) and Figure 4.6(d). In all cases, as the contact rate decreased, the pick values decreased; however, the time to reach the pick values was slightly elongated (shifted to the right). These results are very similar to the findings of the article Engida et al. (2022).

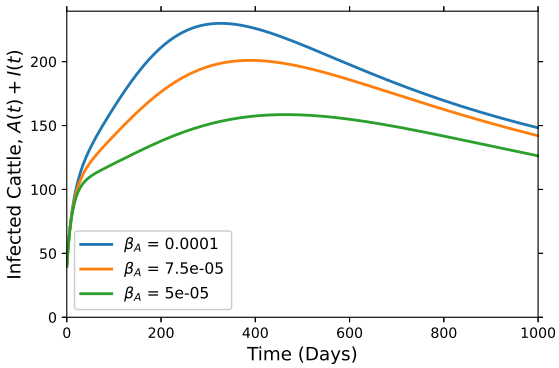

(a) Effect of β_A on Asymptomatic and Symptomatic Infected Cattle.

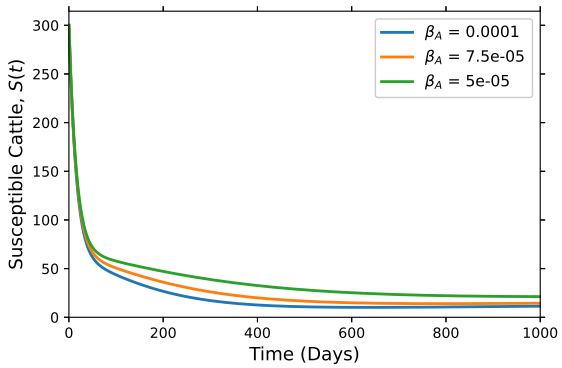

(b) Effect of β_A on Susceptible Cattle.

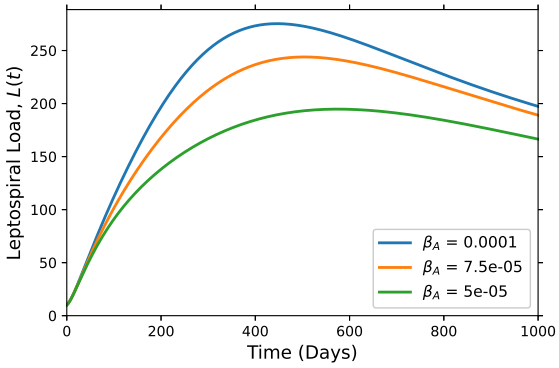

(c) Effect of β_A on *Leptospiral* Load.

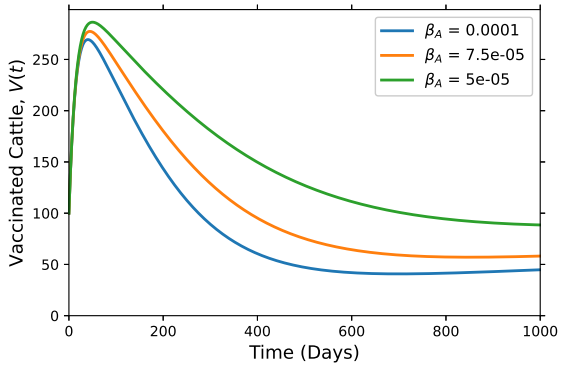

(d) Effect of β_A on Vaccinated Cattle.

Figure 4.6: Effect of contact rate with asymptomatic cattle, β_A.

Effect of Recovery Rate of Asymptomatic Cattle, σ.

Figure 4.7 illustrates the sensitivity of our model (4.1) with respect to the variation of the rate of recovery of asymptomatic infected cattle, σ. Here, an increase in the recovery rate of asymptomatic cattle, σ, results in a decrease in both the size of the infected population and the time elapsed to reach the pick size. Fig. 4.7(a) shows the size of the infected population picked in a year for the base value $\sigma = 0.00137$, but this time is reduced to a few months when the recovery rate is improved to $\sigma = 0.00537$ and the pick value is also radically minimized. Similarly, the bacterial load in the environment could be significantly reduced by increasing the recovery rate, σ as observed in Figure 4.7(c). The decrease of *Leptospira* here is clearly due to a decrease in the number of infected cattle, which contributed to environmental bacteria through shedding (Monti et al., 2023). In addition, the size of the susceptible and vaccinated

cattle increased with the recovery rate, σ, since recovered cattle had no permanent immunity and were susceptible again.

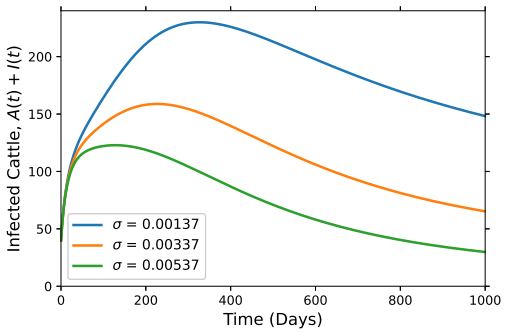

(a) Effect of σ on Asymptomatic and Symptomatic Infected Cattle.

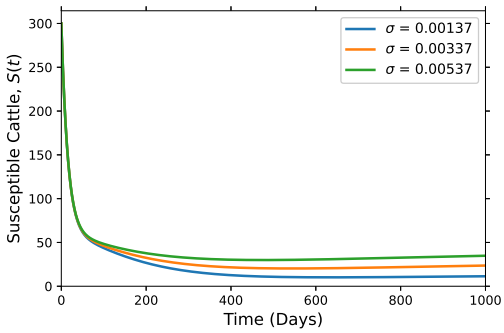

(b) Effect of σ on Susceptible Cattle.

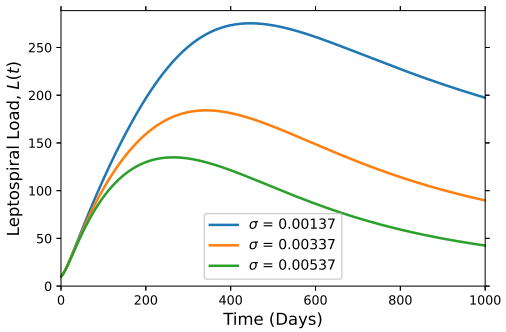

(c) Effect of σ on *Leptospiral* Load.

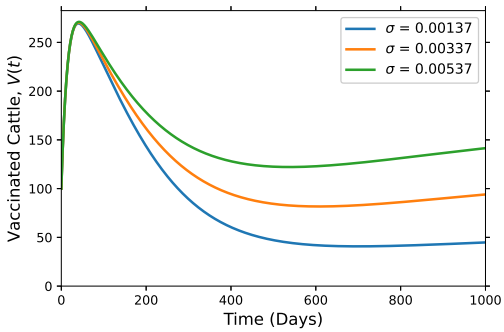

(d) Effect of σ on Vaccinated Cattle.

Figure 4.7: Effect of Recovery rate of Asymptomatic Cattle, σ.

Effect of Vaccination Rate, τ.

Figure 4.8 shows the effect of the vaccination rate of the susceptible population on our model (4.1). Similar to the above parameters, increasing the vaccination rate for susceptible cattle resulted in a significant decrease in the number of infected cattle, as shown in Figure 4.8(a). Obviously, the number of vaccinated cattle increased, as observed in Figure 4.8(d) by the increase in vaccination rate. In line with the decrease in the number of infected cattle, the environmental *Leptospira* load decreased, as shown in Figure 4.8(c). Although a small proportion of vaccinated cattle got infected because of the inefficiency of currently available vaccines, Figure 4.8 clearly shows that the overall effect of vaccination reduced the transmission of leptospirosis in the population.

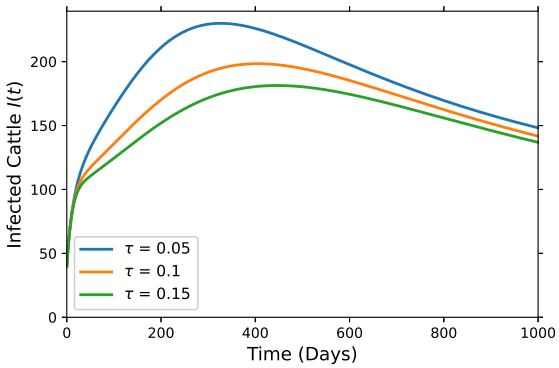

(a) Effect of τ on Asymptomatic and Symptomatic Infected Cattle.

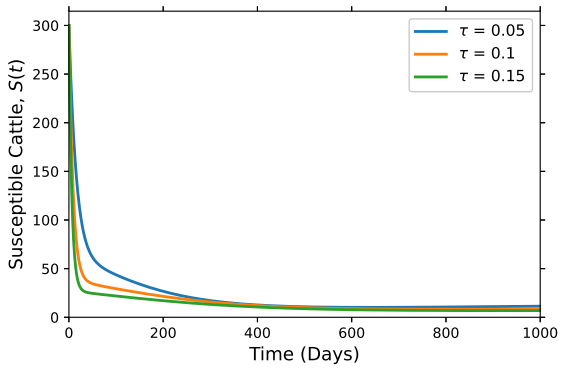

(b) Effect of τ on Susceptible Cattle.

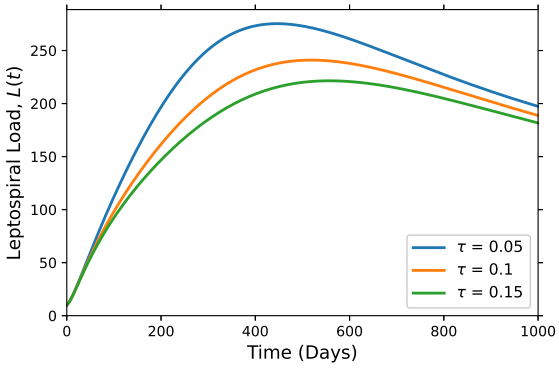

(c) Effect of τ on *Leptospiral* Load.

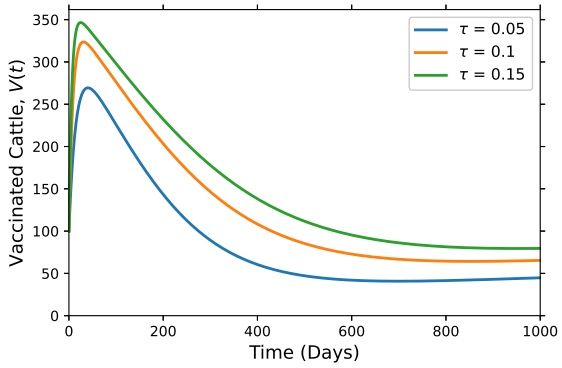

(d) Effect of τ on Vaccinated Cattle.

Figure 4.8: Effect of vaccination rate, τ.

The numerical simulations presented in Figure 4.6 - Figure 4.8 and the sensitivity analysis result in Table 4.2 show that decreasing the contact rate with asymptomatic cattle, β_A, increasing the recovery rate of asymptomatic cattle, σ, and increasing the vaccination rate of susceptible cattle, τ, can meaningfully reduce the infection status in cattle herds. These results clearly indicate that parameters related to asymptomatic cattle play a major role in leptospirosis transmission dynamics. This is because asymptomatic infected cattle have an extended recovery rate as well as continuous shedding of *Leptospira* into the environment during their infected period (Davignon et al., 2023). In line with our results, authors in Engida et al. (2022) found that the reduction of contact rate with infected cattle and with contaminated environments significantly changed the transmission dynamics. On the other hand, pre-diagnosis and treatment with appropriate antimicrobials can eliminate the asymptomatic status of cattle by improving their recovery rate (Aymée et al., 2024). Successful administration of antibiotics (such as oxytetracycline, tu-

lathromycin, and ceftiofur) resulted in effective elimination of urinary shedding *Leptospira* and its transmission within herd (Bautista et al., 2022). In addition, leptospiral vaccines provide excellent protection by preventing the shedding of *Leptospia* in urine and from reproductive tracts (Esteves et al., 2022). In support of this, authors in Aslan et al. (2021); Okosun et al. (2016) showed that effective vaccination and treatment of cattle can control transmission of leptospirosis in cattle and humans. Immunization of the herd is a notable control measure if applied regularly in addition to vaccination of newly recruited cattle before they join the herd in endemic areas (Mughini-Gras et al., 2014). Therefore, farmers, veterinarians, and policymakers should focus on regular testing of herds in endemic areas to identify and take necessary action to treat asymptomatic infected cattle and vaccinate the herd prior to higher health complications, such as kidney failure and reproductive disorder (Davignon et al., 2023; Monti et al., 2023).

4.4 Formulation of Leptospirosis Optimal Control Problem

Following the sensitivity analysis result of autonomous model (4.1) and the flow diagram Figure 4.1, we formulated an optimal control problem to identify the best management strategies of leptospirosis dynamics within cattle herds. Table 4.2 clearly shows that the reproduction number is highly influenced by the contact, recovery, and vaccination rate of cattle. Hence, targeting these sensitive parameters, we introduce three time-dependent control functions as follows (similar control functions are also used in Asamoah et al. (2021); Baloba et al. (2023); Falowo et al. (2023); Okosun et al. (2016); Wu et al. (2022); Zewdie et al. (2022)):

- $u_1(t)$ represents preventive efforts (such as isolation and separate feeding facilities) of infected cattle,
- $u_2(t)$ represents vaccination effort of susceptible cattle to improve their immunity against *Leptospira* pathogen,
- $u_3(t)$ represents treatment effort to improve the recovery rate of infected cattle.

with the following assumptions:

(i) The cattle population is homogeneous,

(ii) The application of the controls is imperfect due to the skill gap of smallholder farmers,

(iii) The effect of temperature and weather variability on the application of controls is ignored.

The corresponding mathematical model with optimal control is the system of non-linear ordinary differential equations given in (4.12)

$$\begin{aligned}
\frac{dS}{dt} &= (1-\rho)\Lambda - bqI - (1-u_1)\lambda S + \gamma R + \eta V - (\phi_1 u_2 + \mu)S,\\
\frac{dE}{dt} &= (1-u_1)\lambda[S + (1-r)V] - (\alpha+\mu)E,\\
\frac{dA}{dt} &= (1-\nu)\alpha E - (\sigma + \phi_2 u_3 + \mu)A,\\
\frac{dI}{dt} &= bqI + \nu\alpha E - (\delta + \phi_3 u_3 + \mu + d)I,\\
\frac{dR}{dt} &= (\sigma + \phi_2 u_3)A + (\delta + \phi_3 u_3)I - (\gamma+\mu)R,\\
\frac{dV}{dt} &= \rho\Lambda - (1-u_1)(1-r)\lambda V + \phi_1 u_2 S - (\eta+\mu)V,\\
\frac{dL}{dt} &= \omega_A A + \omega_I I - \varepsilon L,
\end{aligned} \tag{4.12}$$

with $S(0) = S_0 > 0$, $E(0) = E_0 \geq 0$, $A(0) = A_0 \geq 0$, $I(0) = I_0 \geq 0$, $R(0) = R_0 \geq 0$, $V(0) = V_0 \geq 0$, $L(0) = L_0 \geq 0$, and $\lambda = \left(\frac{\beta_L L}{K+L} + \beta_A A + \beta_I I\right)$.

In the control-imposed model (4.12), the parameters ϕ_1, ϕ_2, and ϕ_3 are the constant vaccination rate, asymptomatic cattle treatment rate, and symptomatic cattle treatment rate, respectively. The incidence rate of infection in susceptible and vaccinated populations is reduced by the factor $(1-u_1(t))$ due to the prevention effort. The asymptomatic and symptomatic infected populations are minimized by recovery at the rate of $\phi_2 u_3(t)$ and $\phi_3 u_3(t)$, respectively. Further, the vaccinated class is increased and the susceptible class is decreased by $\phi_1 u_2(t)$ due to vaccination effort.

4.5 Optimal Control Analysis

Our goal is to minimize the burden of leptospirosis in cattle and the costs of the three control strategies proposed above. To do this, we develop the objective functional as

$$\mathcal{J}(u_i(t)) = \int_0^T \left(W_1 A(t) + W_2 I(t) + W_3 L(t) + (0.5)\sum_{i=1}^{3} c_i u_i^2(t) \right) dt \to min \tag{4.13}$$

subjected to equation (4.12), where the coefficients W_1, W_2, and W_3 are positive weight constants of asymptomatic cattle, symptomatic cattle, and *Leptospira* concentration, respectively. The constants c_i's are weights of imposed controls, and T is the final intervention time. Here the cost of controls is taken in a quadratic form to avoid the situation of singular or bang–bang optimal control (Asamoah et al., 2017; Kifle & Lemecha Obsu, 2023).

Therefore, the aim is to minimize equation (4.13) and obtain the optimal control $u^* = (u_1^*, u_2^*, u_3^*)$ such that the corresponding state trajectories are the solution of equation (4.12) for $t \in [0, T]$. That is,

$$\mathcal{J}(u^*(t)) = \min_{\mathscr{U}}(\mathcal{J}(u(t))) \tag{4.14}$$

subject to state equation (4.12), where $\mathscr{U} = \{u(t) = (u_1(t), u_2(t), u_3(t)) : 0 \leq u_i(t) \leq u_{i\max} \leq 1, \forall t \in [0, T]\}$ is the non-empty admissible Lebesgue measurable set.

4.5.1 Existence of Optimal Controls

The existence of optimum control functions that minimize the cost function during the finite intervention period is demonstrated in this subsection. The existence of optimal control functions is ensured by the following theorem.

Theorem 4.5.1. There exists an optimal control $u^* = (u_1^*, u_2^*, u_3^*)$ with the associated solution $(S^*, E^*, A^*, I^*, R^*, V^*, L^*)$ to the model equation (4.12) that minimizes (4.14) over the admissible control set $\mathscr{U}$.

Proof. Adopting the procedures used by Asamoah et al. (2022); Engida et al. (2023); Kifle & Lemecha Obsu (2023); Lemecha Obsu & Feyissa Balcha (2020), the existence of optimal control u^* is granted if the following conditions hold,

1. The allowable control set $\mathscr{U}$ is closed and convex,
2. The system in equation (4.12) is bounded by a linear function in the state and control variables,
3. The integrand of objective functional (4.13) is convex with respect to the controls,
4. The Lagrangian is bounded below by

$$\xi_1 \|u\|^{\xi_3} - \xi_2,$$

where ξ_1,$\xi_2 > 0$ and $\xi_3 > 1$.

To show the first condition, let $u_1, u_2 \in \mathscr{U}$. That is $\|u_1\| \leq 1$ and $\|u_2\| \leq 1$. Then for any $\zeta \in [0, 1]$,

$$\|\zeta u_1 + (1-\zeta)u_2\| \leq \zeta\|u_1\| + (1-\zeta)\|u_2\| \leq 1$$

Hence, set U is closed and convex.

For the second condition, let $x = (S,E,A,I,R,V,L)$ and $u = (u_1,u_2,u_3)$. The right-hand side of equation (4.12) can be re-written as

$$f(t,x,u) = f_1(t,x) + f_2(t,x)u$$

where,

$$f_1(t,x) = \begin{bmatrix} (1-\rho)\Lambda - bqI - \lambda S + \gamma R + \eta V - \mu S \\ \lambda[S + (1-r)V] - (\alpha+\mu)E \\ (1-\nu)\alpha E - (\sigma+\mu)A \\ bqI + \nu\alpha E - (\delta+\mu+d)I \\ \sigma A + \delta I - (\gamma+\mu)R \\ \rho\Lambda - (1-r)\lambda V - (\eta+\mu)V \\ \omega_A A + \omega_I I - \varepsilon L, \end{bmatrix},$$

and

$$f_2(t,x)u = \begin{bmatrix} \lambda S & -\phi_1 S & 0 \\ -\lambda(S+(1-r)V) & 0 & 0 \\ 0 & 0 & -\phi_2 A \\ 0 & 0 & -\phi_3 I \\ 0 & 0 & \phi_2 A + \phi_3 I \\ (1-r)\lambda V & \phi_1 S & 0 \\ 0 & 0 & 0 \end{bmatrix} \begin{bmatrix} u_1 \\ u_2 \\ u_3 \end{bmatrix}.$$

This shows that the right-hand side functions of equation (4.12) depend linearly on the controls. Further, by definition, each right-hand side of the optimal control problem in equation (4.12) is continuous and bounded since it is the sum of bounded controls and the state variables (Engida et al., 2023). Hence, condition (ii) also holds.

Also to show the third condition, let $x = (S,E,A,I,R,V,L)$ and the objective functional (4.13) has the Lagrangian form defined as

$$\mathscr{L}(t,x,u) = \mathscr{L}_1(t,x) + \mathscr{L}_2(t,u)$$

where, $\mathscr{L}_1(t,x) = W_1A(t) + W_2I(t) + W_3L(t)$, and $\mathscr{L}_2(t,u) = (0.5)\sum_{i=1}^{3} c_i u_i^2(t)$. Here, $\mathscr{L}_2(t,u)$ is a finite sum of convex control functions. Thus, $\mathscr{L}(t,x,u)$ is convex with respect to variable u. Hence condition (iii) holds.

Since the Lagrangian, $\mathscr{L}(t,x,u)$,is sum of the terms $\mathscr{L}_1(t,x)$ and $\mathscr{L}_2(t,u)$, the last hypothesis

is shown as follow:

$$\mathscr{L}(t,x,u) = \mathscr{L}_1(t,x) + (0.5)\sum_{i=1}^{3} c_i u_i^2(t) \geq (0.5)\sum_{i=1}^{3} c_i u_i^2(t) \geq \xi_1 \left(\sum_{i=1}^{3} u_i^2\right)^{\frac{\xi_3}{2}} - \xi_2$$

where, $\xi_1 = \frac{1}{2}\min\{c_1, c_2, c_3\}$, $\xi_2 > 0$ and $\xi_3 = 2$. □

4.5.2 Characterization of Optimal Control Solutions

We provide optimality requirements for the optimal control problem (4.12) in this subsection. According to Pontryagin's Minimum Principle (Pontryagin, 2018), if $u^*(t) \in U$ is optimal for problem (4.14) subjected to (4.12) with fixed final time T, then there exists a non-trivial absolutely continuous mapping $\lambda : [0,T] \to \mathbb{R}^7$, $\lambda = (\lambda_1(t), \lambda_2(t), \lambda_3(t), \lambda_4(t), \lambda_5(t), \lambda_6(t), \lambda_7(t))$ called the adjoint vector, such that

1. the Hamiltonian function is defined as

$$\mathscr{H} = W_1 A(t) + W_2 I(t) + W_3 L(t) + (0.5)\sum_{i=1}^{3} c_i u_i^2(t) + \sum_{i=1}^{7} \lambda_i(t) g_i(t,u,S,E,A,I,R,V,L), \quad (4.15)$$

   where, g_i denotes the right-hand side functions in equation (4.12).

2. the control system

$$S' = \frac{\partial \mathscr{H}}{\partial \lambda_1},\ E' = \frac{\partial \mathscr{H}}{\partial \lambda_2},\ A' = \frac{\partial \mathscr{H}}{\partial \lambda_3},\ I' = \frac{\partial \mathscr{H}}{\partial \lambda_4},\ R' = \frac{\partial \mathscr{H}}{\partial \lambda_5},\ V' = \frac{\partial \mathscr{H}}{\partial \lambda_6},\ L' = \frac{\partial \mathscr{H}}{\partial \lambda_7}, \quad (4.16)$$

3. the adjoint system

$$\lambda_1' = -\frac{\partial \mathscr{H}}{\partial S},\ \lambda_2' = -\frac{\partial \mathscr{H}}{\partial E},\ \lambda_3' = -\frac{\partial \mathscr{H}}{\partial A},\ \lambda_4' = -\frac{\partial \mathscr{H}}{\partial I},\ \lambda_5' = -\frac{\partial \mathscr{H}}{\partial R},\ \lambda_6' = -\frac{\partial \mathscr{H}}{\partial V},\ \lambda_7' = -\frac{\partial \mathscr{H}}{\partial L}, \quad (4.17)$$

4. the optimality condition

$$\mathscr{H}(S^*,E^*,A^*,I^*,R^*,V^*,L^*,u^*,\lambda_i^*) = \min_{\mathscr{U}}(\mathscr{H}(S^*,E^*,A^*,I^*,R^*,V^*,L^*,u,\lambda_i^*)), \quad (4.18)$$

5. the transversality condition

$$\lambda_i(T) = 0, \quad i = 1,..,7 \quad (4.19)$$

are all holds.

The following theorem provides the necessary optimality condition.

Theorem 4.5.2. Let u^* be the optimal control to (4.12),(4.13),(4.14) and $(S^*,E^*,A^*,I^*,R^*,V^*,L^*)$ be the associated optimal solution. Then there exist $\lambda_i(t), i = 1,..,7$, called adjoint functions given by

$$\begin{aligned}
\frac{\partial\lambda_1}{\partial t} &= (1-u_1)\left[\frac{\beta_L L}{K+L}+\beta_A A+\beta_I I\right](\lambda_1-\lambda_2)+\phi_1 u_2(\lambda_1-\lambda_6)+\mu\lambda_1,\\
\frac{\partial\lambda_2}{\partial t} &= (\alpha+\mu)\lambda_2-(1-\nu)\alpha\lambda_3-\nu\alpha\lambda_4,\\
\frac{\partial\lambda_3}{\partial t} &= -W_1+(1-u_1)\beta_A S(\lambda_1-\lambda_2)+(1-u_1)(1-r)\beta_A V(\lambda_6-\lambda_2)+(\sigma+\phi_2 u_3)(\lambda_3-\lambda_5)+\mu\lambda_3-\omega_A\lambda_7,\\
\frac{\partial\lambda_4}{\partial t} &= -W_2+(1-u_1)\beta_I S(\lambda_1-\lambda_2)+(1-u_1)(1-r)\beta_I V(\lambda_6-\lambda_2)+(\delta+\phi_3 u_3)(\lambda_4-\lambda_5)-bq\lambda_4+(\mu+d)\lambda_4-\omega_I\lambda_7,\\
\frac{\partial\lambda_5}{\partial t} &= \gamma(\lambda_5-\lambda_1)+\mu\lambda_5,\\
\frac{\partial\lambda_6}{\partial t} &= (1-u_1)(1-r)\left[\frac{\beta_L L}{K+L}+\beta_A A+\beta_I I\right](\lambda_6-\lambda_2)+\eta(\lambda_6-\lambda_1)+\mu\lambda_6,\\
\frac{\partial\lambda_7}{\partial t} &= -W_3+(1-u_1)\left(\frac{\beta_L KS}{(K+L)^2}\right)(\lambda_1-\lambda_2)+(1-u_1)(1-r)\left(\frac{\beta_L KV}{(K+L)^2}\right)(\lambda_6-\lambda_2)+\varepsilon\lambda_7,
\end{aligned} \tag{4.20}$$

subjected to transversality conditions, $\lambda_i(T) = 0, i = 1,..,7$. Further, the optimal control $u^* = (u_1^*, u_2^*, u_3^*)$ is given by

$$\begin{aligned}
u_1^* &= \min\left\{\max\left\{0, \frac{\left[\frac{\beta_L L^*}{K+L^*}+\beta_A A^*+\beta_I I^*\right](S^*(\lambda_2-\lambda_1)+(1-r)V^*(\lambda_2-\lambda_6))}{c_1}\right\}, u_{1\max}\right\},\\
u_2^* &= \min\left\{\max\left\{0, \frac{\phi_1 S^*(\lambda_1-\lambda_6)}{c_2}\right\}, u_{2\max}\right\},\\
u_3^* &= \min\left\{\max\left\{0, \frac{\phi_2 A^*(\lambda_3-\lambda_5)+\phi_3 I^*(\lambda_4-\lambda_5)}{c_3}\right\}, u_{3\max}\right\}.
\end{aligned} \tag{4.21}$$

Proof. The adjoint system (4.17), minimality conditions (4.18) and transversality conditions (4.19) hold from Pontryagin's Minimum Principle (Pontryagin, 2018). Hence, the system (4.20) can be directly derived from (4.17), (4.15) and (4.12). Also, the convexity of the objective functional in (4.13) with respect to u guarantees the existence of optimal controls (Fleming & Rishel, 2012). Thus, from the optimality conditions

$$\frac{\partial\mathscr{H}}{\partial u_i} = 0, i = 1,2,3 \tag{4.22}$$

it follows that,

$$\begin{aligned}
\frac{\partial \mathscr{H}}{\partial u_1} = 0 &\implies u_1^* = \frac{\left[\frac{\beta_L L^*}{K+L^*} + \beta_A A^* + \beta_I I^*\right](S^*(\lambda_2-\lambda_1) + (1-r)V^*(\lambda_2-\lambda_6))}{c_1}, \\
\frac{\partial \mathscr{H}}{\partial u_2} = 0 &\implies u_2^* = \frac{\phi_1 S^*(\lambda_1-\lambda_6)}{c_2}, \\
\frac{\partial \mathscr{H}}{\partial u_3} = 0 &\implies u_3^* = \frac{\phi_2 A^*(\lambda_3-\lambda_5) + \phi_3 I^*(\lambda_4-\lambda_5)}{c_3}.
\end{aligned} \tag{4.23}$$

The boundedness of u_i^* on $(0, u_{i\max})$ and the minimality condition (4.18), gives (4.21). □

Remark 5. The Hessian matrix, $H(\mathscr{H}) = diag\{c_1, c_2, c_3\}$, of the Hamiltonian function is positive definite with respect to the control u with $c_i > 0, i = 1,2,3$. Hence the optimal control is indeed the minimizer.

4.5.3 Numerical Simulations for Optimal Control

To supplement the analytical findings in subsection 4.5.2 and also better understand the control strategies, several numerical simulations of model (4.1) are carried out in this subsection. For this purpose, we use the GEKKO optimization suite in section B.2, an object-oriented Python library for control problems, to find the optimal numerical solution of our model (Beal et al., 2018). We examined the following seven strategies to investigate the effects of the controls:

- **Strategy 1**: Use of prevention only, $u_2 = u_3 = 0, u_1 \neq 0$.
- **Strategy 2**: Use of vaccination only, $u_1 = u_3 = 0, u_2 \neq 0$.
- **Strategy 3**: Use of treatment only, $u_1 = u_2 = 0, u_3 \neq 0$.
- **Strategy 4**: Use of prevention and vaccination, $u_3 = 0, u_1 \neq 0, u_2 \neq 0$.
- **Strategy 5**: Use of prevention and treatment, $u_2 = 0, u_1 \neq 0, u_3 \neq 0$.
- **Strategy 6**: Use of vaccination and treatment, $u_1 = 0, u_2 \neq 0, u_3 \neq 0$.
- **Strategy 7**: Use of all interventions, $u_1 \neq 0, u_2 \neq 0, u_3 \neq 0$.

For numerical simulations, the initial conditions are chosen as $(S(0), E(0), A(0), I(0), R(0), V(0), L(0))$ = $(300, 60, 30, 10, 0, 100, 10)$ and the parameter values are stated in Table 4.1. Also, we consider $W_1 = 2$, $W_2 = 2$, $W_3 = 1$, $c_1 = 20$, $c_2 = 1$, $c_3 = 10$, $\phi_1 = 0.1$, $\phi_2 = 0.025$, $\phi_3 = 0.05$ and final time $T = 350$ days. Further, since the application of interventions is imperfect, we took the maximum control values as $u_{i\max} = 0.95$, i.e., 95% perfection.

Using the model parameter values in Table 4.1, the effective reproduction number is $\mathscr{R}_e = 2.794$. For the herd with no vaccination program (τ=0), the basic reproduction number $\mathscr{R}_0 = 8.977$ is almost three fold compared to the case when the vaccination program is introduced. This shows that the vaccination program has a critical role in managing leptospirosis in cattle herds, even though its efficacy and coverage have their own impact, as seen in Figure 4.2 above. These results are also in line with Aslan et al. (2021); Okosun et al. (2016). Figures 4.9-4.15 illustrate the effect of seven control strategies on the disease compartments. It can be seen from each of these figures that the number of symptomatic and asymptomatic cattle and the *Leptospira* concentration in the environment decrease significantly over the simulation period. In support of the result in Engida et al. (2023), Figure 4.9 shows that prevention measures such as isolating and separate feeding of infected cattle, restricting cattle from watercourses, and subdividing cattle into smaller batches significantly reduce the exposure of animals to *Leptospira*. Figure 4.10 shows that vaccination is the effective control method for interrupting the transmission of leptospirosis in cattle and reducing its impact (Okosun et al., 2016; Wilson-Welder et al., 2020). Moreover, Figure 4.11 shows treatment can rapidly control the disease compared to other measures. However, Figures 4.12-4.15 show that the infected population rapidly converges to zero with the use of combined controls rather than using a single control. Combining strategies such as prevention, vaccination, and antibiotic treatment can properly manage reproductive consequences and financial risks associated with leptospiral infection in cattle (Martins & Lilenbaum, 2017).

Regarding the control profile, Figures 4.9(d), 4.10(d), and 4.11(d) show that each control should be applied maximally throughout the year when introduced separately to get optimal reduction of the disease. However, combining the controls results in a relatively shorter time for maximum control use, which then gradually decreases to zero. In particular, when all controls are used at the same time, u_1 should be maximum for only 50 days, u_3 should be maximum for about 150 days, and u_2 should be imposed maximum for about 200 days for optimal management of the disease, as seen from Figure 4.15(d).

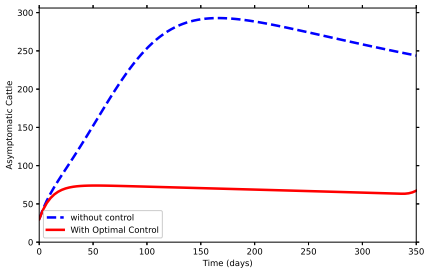

(a) Effect of u_1 on asymptomatic cattle.

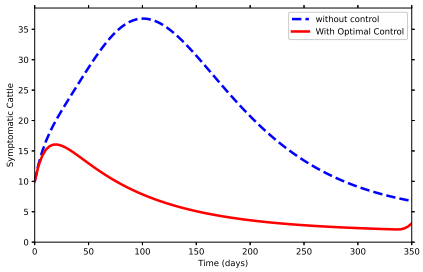

(b) Effect of u_1 on symptomatic cattle.

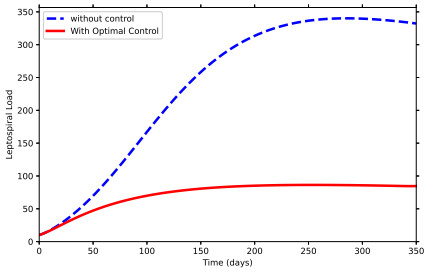

(c) Effect of u_1 on leptospiral load.

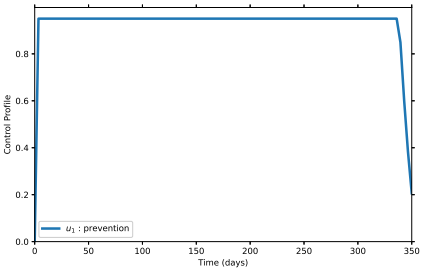

(d) Control profile ($u_1 \neq 0$).

Figure 4.9: Strategy 1: effort of prevention ($u_1 \neq 0$).

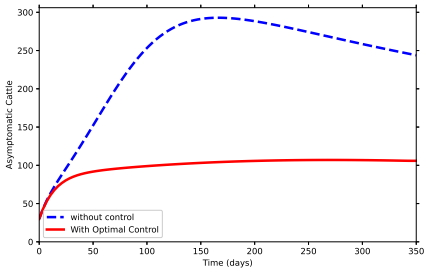

(a) Effect of u_2 on asymptomatic cattle.

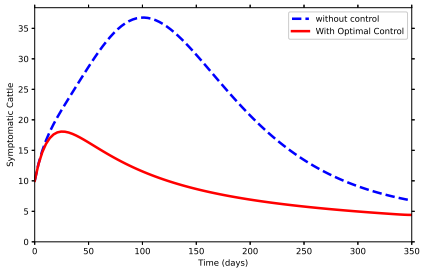

(b) Effect of u_2 on symptomatic cattle.

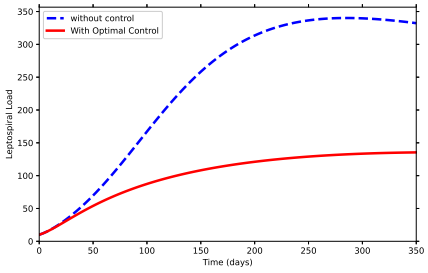

(c) Effect of u_2 on leptospiral load.

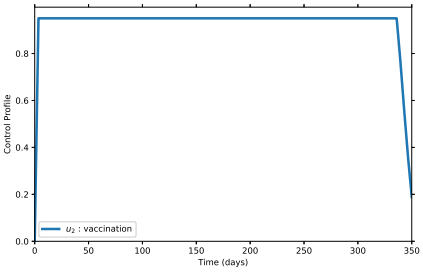

(d) Control profile ($u_2 \neq 0$).

Figure 4.10: Strategy 2: effort of vaccination ($u_2 \neq 0$).

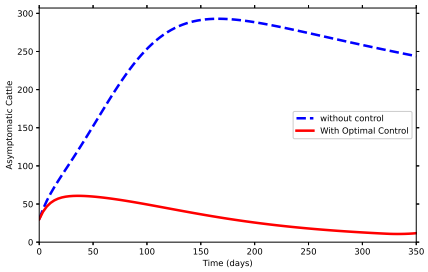

(a) Effect of u_3 on asymptomatic cattle.

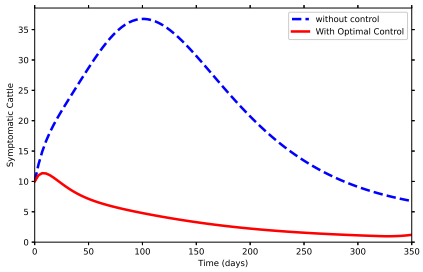

(b) Effect of u_3 on symptomatic cattle.

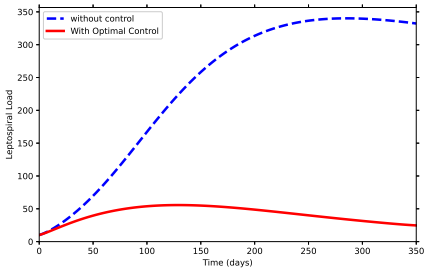

(c) Effect of u_3 on leptospiral load.

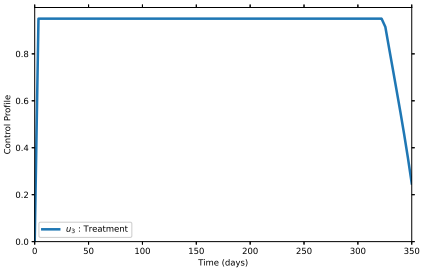

(d) Control profile ($u_3 \neq 0$).

Figure 4.11: Strategy 3: effort of treatment ($u_3 \neq 0$).

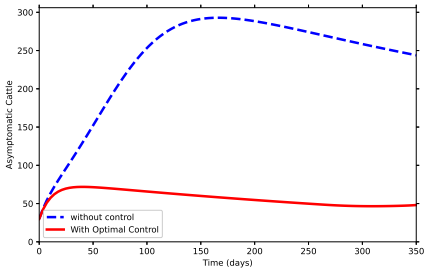

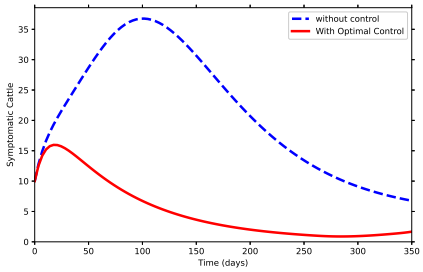

(a) Effect of u_1 and u_2 on asymptomatic cattle.(b) Effect of u_1 and u_2 on symptomatic cattle.

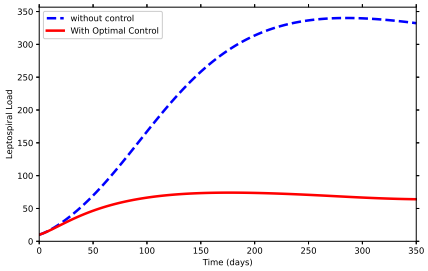

(c) Effect of u_1 and u_2 on leptospiral load.

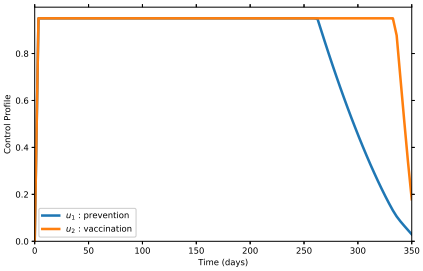

(d) Control profile ($u_1 \neq 0$, $u_2 \neq 0$).

Figure 4.12: Strategy 4: effort of prevention and vaccination ($u_1 \neq 0$, $u_2 \neq 0$).

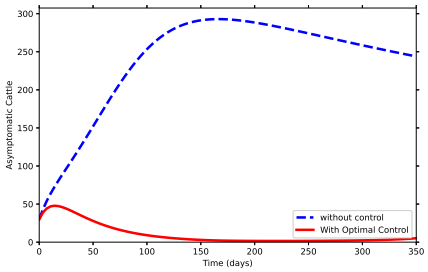

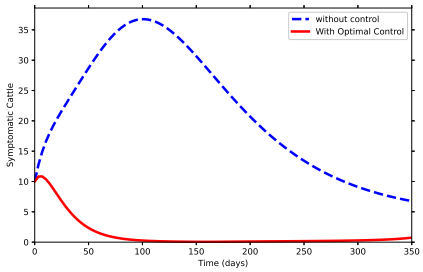

(a) Effect of u_1 and u_3 on asymptomatic cattle.(b) Effect of u_1 and u_3 on symptomatic cattle.

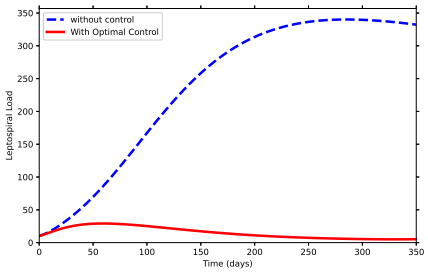

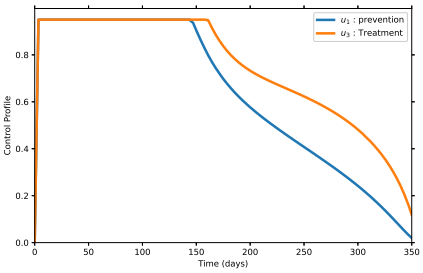

(c) Effect of u_1 and u_3 on leptospiral load. (d) Control profile ($u_1 \neq 0$, $u_3 \neq 0$).

Figure 4.13: Strategy 5: effort of prevention and treatment ($u_1 \neq 0$, $u_3 \neq 0$).

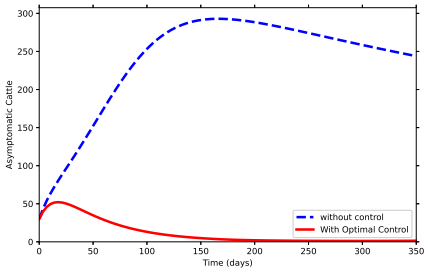

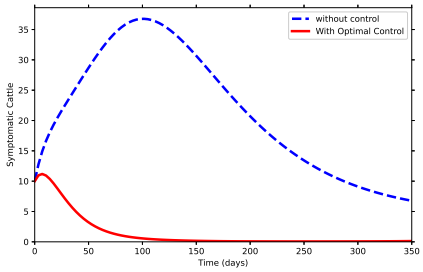

(a) Effect of u_2 and u_3 on asymptomatic cattle.(b) Effect of u_2 and u_3 on symptomatic cattle.

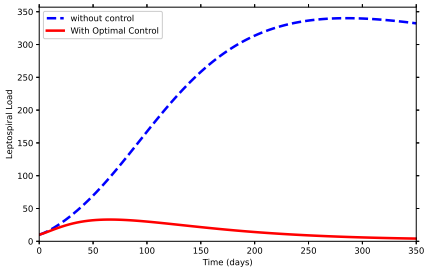

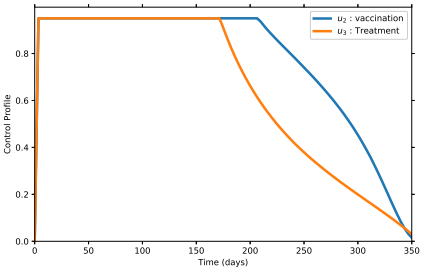

(c) Effect of u_2 and u_3 on leptospiral load. (d) Control profile ($u_2 \neq 0$, $u_3 \neq 0$).

Figure 4.14: Strategy 6: effort of vaccination and treatment ($u_2 \neq 0$, $u_3 \neq 0$).

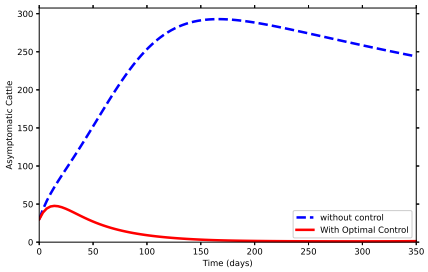

(a) Effect of u_1, u_2 and u_3 on asymptomatic cattle.

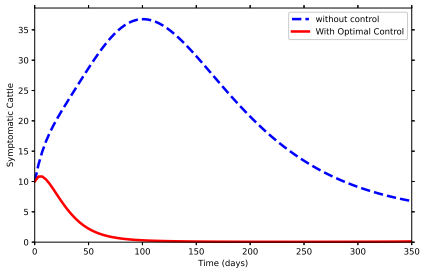

(b) Effect of u_1, u_2 and u_3 on symptomatic cattle.

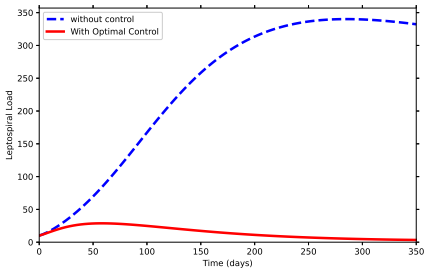

(c) Effect of u_1, u_2 and u_3 on leptospiral load.

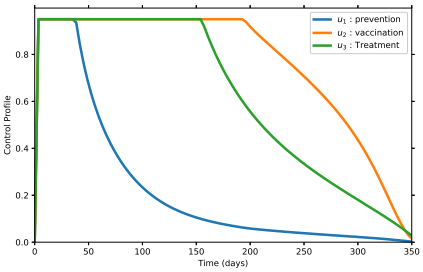

(d) Control profile ($u_1 \neq 0, u_2 \neq 0$ and $u_3 \neq 0$).

Figure 4.15: Strategy 7: effort of prevention, vaccination and treatment ($u_1 \neq 0, u_2 \neq 0$ and $u_3 \neq 0$).

4.6 Cost-effectiveness Analysis

To determine the most cost-effective scenario among all optimal interventions carried out in the preceding subsection, we utilize two methodologies in this section: the average cost-effectiveness ratio (ACER) and the incremental cost-effectiveness ratio (ICER) (Asamoah et al., 2021; Baloba et al., 2023; Engida et al., 2023).

4.6.1 Average Cost-effectiveness Ratio (ACER)

A particular control approach is evaluated by the average cost-effectiveness ratio in relation to its baseline choice. ACER of a certain optimal approach is calculated using the following formula (Asamoah et al., 2022):

$$ACER = \frac{Total\ expenses\ produced\ by\ particular\ intervention\ strategy}{Total\ number\ of\ infections\ averted\ by\ the\ intervention\ strategy} \tag{4.24}$$

Table 4.3: ACER value for different strategies.

Control strategy	Infection Averted	Total expense	ACER
strategy 2 (u_2)	28,903.52	43.85	0.0015
strategy 1 (u_1)	35,275.89	879.09	0.0249
strategy 4 (u_1, u_2)	37,483.34	778.24	0.0208
strategy 3 (u_3)	42,162.70	430.98	0.0102
strategy 6 (u_2, u_3)	46,927.20	304.87	0.0065
strategy 5 (u_1, u_3)	47,354.59	815.61	0.0172
strategy 7 (u_1, u_2, u_3)	47,453.99	431.33	0.0091

where, the overall expenses generated by the specific approach, T_C, is estimated from

$$T_C = \frac{1}{2}\int_0^T \left[c_1 u_1^2 + c_2 u_2^2 + c_3 u_3^2\right] dt. \tag{4.25}$$

Here, the infection averted is the difference between the sum of asymptomatic and symptomatic infected cattle and *Leptospira* concentration without control(s) and with control(s) for the particular strategy. In this study, the total infection averted, (T_A), is determined by

$$T_A = \int_0^T (A(t) + I(t) + L(t))\, dt - \int_0^T (A^*(t) + I^*(t) + L^*(t))\, dt \tag{4.26}$$

where, the $A^*(t), I^*(t)$ and $L^*(t)$ correspond to the optimal solutions associated with the optimal controls (u_1^*, u_2^*, u_3^*) and $A(t), I(t)$ and $L(t)$ are the solutions without optimal controls $(u_1 = u_2 = u_3 = 0)$.

The most economical approach is the one with the lowest ACER (Asamoah et al., 2021). Using the parameter values in Table 4.1, the ACER value for each of the seven control strategies is computed in Table 4.3. From Table 4.3 and Figure 4.16, we conclude that strategy 2 (vaccination) is the most efficient measure of all, and strategy 1 (prevention) is the least efficient measure for this specific model.

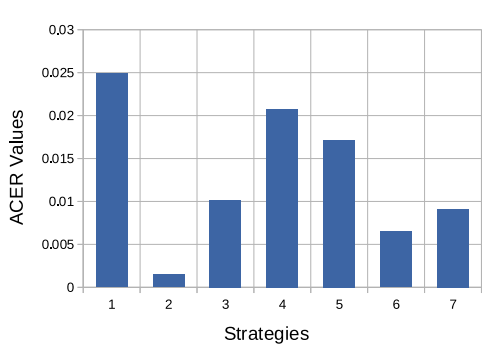

(a) ACER values of control strategies.

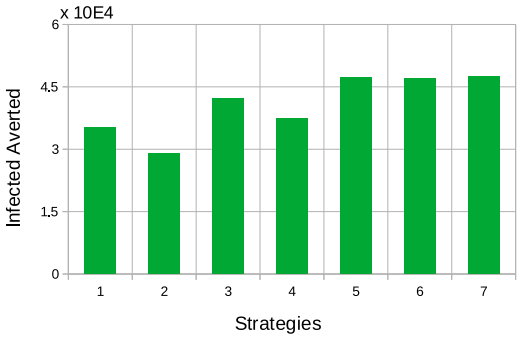

(b) Total number of infection averted.

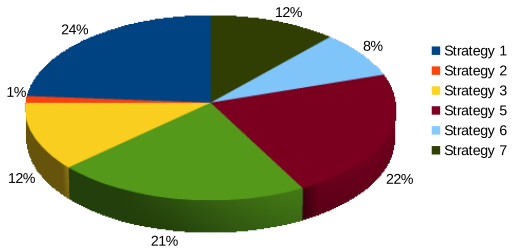

(c) Total cost produced by control strategies.

Figure 4.16: ACER values, infection averted and total cost for each control strategies.

4.6.2 The Incremental Cost-effectiveness Ratio (ICER)

In this subsection, we are going to look at the incremental cost-effectiveness ratio (ICER), which compares the expenses and health outcomes from any two separate intervention strategies seeking the same scarce resource (Asamoah et al., 2022; Baloba et al., 2023; Melese, 2023). Thus, the following formula determines the ICER value for the two cases, i and j (Asamoah et al., 2021):

$$ICER = \frac{Difference\ in\ Cost\ produced\ by\ Strategy\ i\ and\ j}{Difference\ in\ the\ total\ number\ of\ infection\ averted\ in\ Strategy\ i\ and\ j}. \quad (4.27)$$

Next, we compute the ICER values for the seven control intervention strategies to confirm which one is the most economical. Thus, ICER is computed for the competing control strategies as follows based on the results in Table 4.3, shown according to their ascending order of the total number of infections averted:

$$ICER(\textit{strategy 2}) = \frac{43.85 - 0}{28,903.52 - 0} = 0.0015,$$

$$ICER(\textit{strategy 1, strategy 2}) = \frac{879.09 - 43.85}{35,275.89 - 28,903.52} = 0.1311.$$

Since $0.0015 < 0.1311$, strategy 2 is better than strategy 1.

$$ICER(\textit{strategy 4, strategy 2}) = \frac{778.24 - 43.85}{37,483.34 - 28,903.52} = 0.0856.$$

Since $0.0015 < 0.0856$, strategy 2 is better than strategy 4.

$$ICER(\textit{strategy 3, strategy 2}) = \frac{430.98 - 43.85}{42,162.70 - 28,903.52} = 0.0292.$$

Since $0.0015 < 0.0292$, strategy 2 is better than strategy 3.

$$ICER(\textit{strategy 6, strategy 2}) = \frac{304.87 - 43.85}{46,927.20 - 28,903.52} = 0.0145.$$

Since $0.0015 < 0.0145$, strategy 2 is better than strategy 6.

$$ICER(\textit{strategy 5, strategy 2}) = \frac{815.61 - 43.85}{47354.59 - 28,903.52} = 0.0418.$$

Since $0.0015 < 0.0418$, strategy 2 is better than strategy 5.

$$ICER(\textit{strategy 7, strategy 2}) = \frac{431.33 - 43.85}{47,453.99 - 28,903.52} = 0.0209.$$

Since $0.0015 < 0.0209$, strategy 2 is better than strategy 7.

Accordingly, the ICER analysis shows that strategy 2 (vaccination) is the most efficient measure of all strategies to control leptospirosis transmission in cattle herds for the proposed model. Also, these results are in line with the ACER analysis in the above subsection.

4.7 Conclusion

Despite its profound negative health and economic consequences, leptospirosis remains a relatively neglected zoonotic disease. This disease not only leads to the loss of a considerable number of cattle but also threatens breeding stock through instances of abortion. The consequences are especially severe for smallholder farmers in rural areas, resulting in substantial

financial losses. Our study is one of the studies in the area of the leptospirosis model, shedding light on the transmission dynamics and possible mitigation strategies to control its spread. In addition, our study will give insights into the best combinations of interventions to minimize the transmission of leptospirosis disease within the cattle population and to explore the impacts of various intervention strategies.

In the qualitative analysis part of our study, we have proved the well posedness of the proposed model and also found the basic reproduction number. Furthermore, we demonstrated that the disease-free equilibrium point is locally and globally asymptotically stable when $\mathcal{R}_e$ is less than one and unstable otherwise. The existence of endemic equilibrium was also shown using Descartes' rule of sign. Regarding numerical results, the disease-free and endemic equilibriums were stable, as shown in Figure 4.4 and Figure 4.5, which supports the analytical result. Based on the most sensitive parameters (i.e.,β_A, σ and τ), a simulation was conducted. Accordingly, Figure 4.6 shows that decreasing the contact rate β_A results in decreasing the infected cattle population and the leptospiral load in the environment. Hence, any effort to reduce the incidence rate should be emphasized. Figure 4.7 also shows that increasing the recovery rate resulted in a significant decrease in the number of infected cattle. This can be done using pre-diagnosis identification of asymptomatic infected cattle and treatment with appropriate antibiotics. Furthermore, Figure 4.8 shows increasing vaccination rates of susceptible cattle considerably decreased the infected population.

In the control-imposed model, we introduced three control functions that vary with time based on the sensitivity index in Table 4.2. These are control u_1: effort of preventing susceptible and vaccinated cattle from infected cattle and contaminated environments; control u_2: effort of vaccinating susceptible cattle; and control u_3: effort of pre-diagnosis and treating of symptomatic and asymptomatic infected cattle populations. The required conditions for an optimality system were derived using Pontryagin's minimum principle, and the existence of the optimal control triplets was confirmed using standard results. The GEKKO dynamic optimization package in a Python program was implemented to carry out the numerical simulations. The application of all the controls demonstrates that the disease can be reduced by using the suggested control measures effectively. However, our cost-effectiveness analysis shows that strategy 2 (vaccination) is the most efficient control measure among all intervention strategies.

CHAPTER 5

MATHEMATICAL MODEL AND ANALYSIS OF LEPTOSPIROSIS IN CATTLE AND RAT

5.1 Model Formulation

In this section, we will use a system of nonlinear differential equations to provide a mathematical model for the transmission dynamics of leptospirosis in the cattle-rat interface. To develop the model, cattle, rats, and *Leptospira* populations are taken into account. We divide the cattle population into six compartments: susceptible S_C, exposed E_C, asymptomatic infectious A_C, symptomatic infectious I_C, recovered R_C, and vaccinated V_C. The rat population is divided into two compartments: the susceptible S_R and the asymptomatic infectious class A_R. L stands for the concentration of *Leptospira* in the environment. Susceptible cattle population is raised by a constant recruited rate Λ_C and due to the rate of loss of vaccine immunity η. This class becomes exposed by the force of infection $\lambda_C = \beta_{CC}(A_C + I_C) + \beta_{CR}A_R + \frac{\beta_C L}{K+L}$ and also transferred to the vaccinated class at the rate of τ. Furthermore, exposed cattle become infected at the rate of α, and the ν portion becomes symptomatically infected. The vaccinated class becomes exposed by the reduced force of infection $(1-r)\lambda_C$, where r is vaccine efficacy, and becomes susceptible at the rate of η after losing temporary immunity. σ and δ are recovery rates of asymptomatic and symptomatic infected cattle, respectively. Since the natural immunity is not lifelong, the recovered cattle become susceptible at the rate of γ.

Similarly, the susceptible rat population is recruited at a rate of Λ_R and decreased by the force of infection $\lambda_R = \beta_{RR}A_R + \frac{\beta_R L}{K+L}$. The symptomatic and asymptomatic cattle shed *Leptospira* at the rate of ω_C, whereas asymptomatic rats shed at the rate of ω_R. In addition, environmentally free-*Leptospira* contaminates cattle and rats at the rates of β_C and β_R, respectively. Table 5.1 summarizes the description of all parameters used in the model. Further, our model is based on the following controlling assumptions:

i) Vertical transmission is not considered.

ii) While cattle can serve as reservoirs, existing literature does not provide conclusive evidence that they directly transmit leptospirosis to rats. Thus, we assume unidirectional transmission from rats to cattle.

iii) A homogeneous mixing assumption is applied due to the nature of traditional cattle farm-

ing, where livestock share common grazing and water.

Table 5.1: Parameters and their description

Parameter	Description
Λ_C	Cattle recruitment rate
Λ_R	Rat recruitment rate
ρ	Fraction of immunized recruited cattle
K	Environmental *Leptospira* concentration
β_{CC}	*Leptospira* transmission coefficient within cattle
β_{CR}	*Leptospira* transmission coefficient from rat to cattle
β_C	*Leptospira* transmission coefficient from environment to cattle
β_{RR}	*Leptospira* transmission coefficient within rat
β_R	*Leptospira* transmission coefficient from environment to rat
α	Progression rate from E_C to I_C
ν	Portion of cattle goes to I_C
δ	Progression rate from I_C to R_C
σ	Progression rate from A_C to R_C
μ_C	Cattle natural death rate
μ_R	Rat natural death rate
d_C	*Leptospira* induced death rate of infected cattle
ε	*Leptospira* decay rate
ω_C	Shedding rate of A_C and I_C
ω_R	Shedding rate of A_R
η	Vaccine immunity loss
r	Vaccine efficacy
τ	Vaccination rate of susceptible cattle
γ	Natural immunity loss

The dynamics of leptospirosis transmission in cattle and rats is described by the following set of differential equations, based on Figure 5.1.

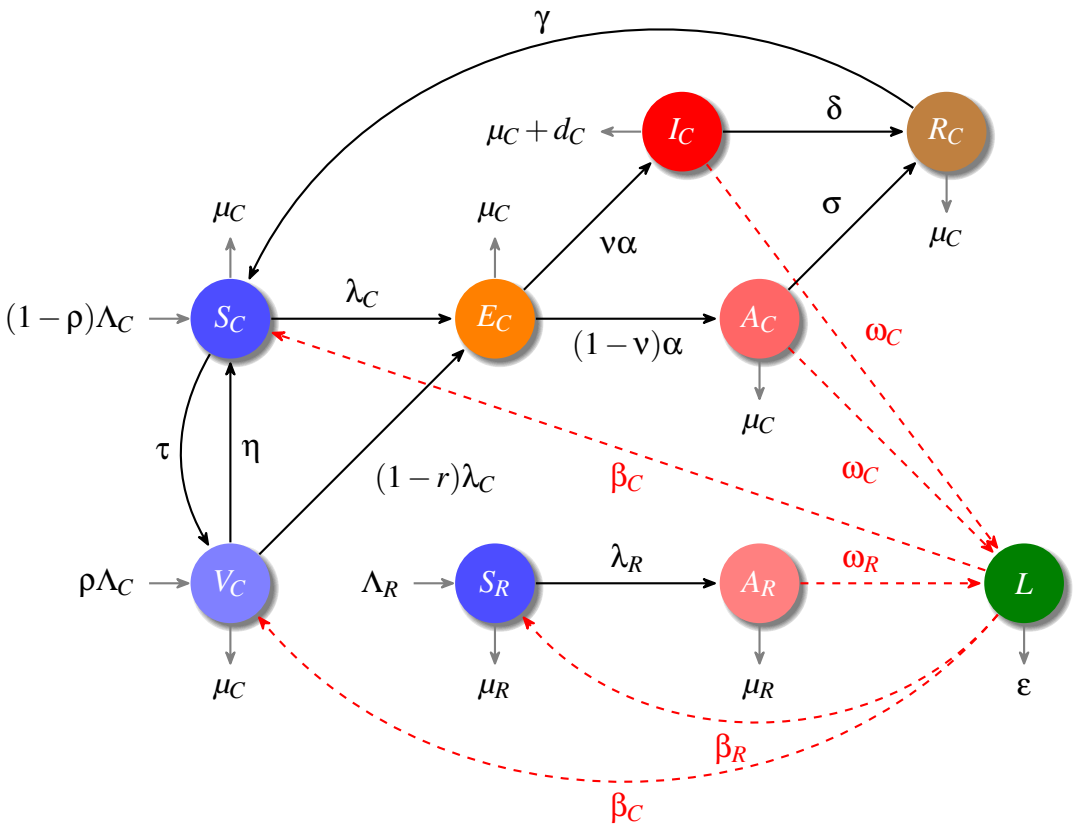

Figure 5.1: *Leptospira* transmission flow diagram in cattle and rat. Subscript 'C' and 'R' refers, cattle and rat population respectively.

$$
\begin{aligned}
\frac{dS_C}{dt} &= (1-\rho)\Lambda_C - \lambda_C S_C + \gamma R_C + \eta V_C - \tau S_C - \mu_C S_C, \\
\frac{dE_C}{dt} &= \lambda_C \left[S_C + (1-r)V_C\right] - (\alpha+\mu_C)E_C, \\
\frac{dA_C}{dt} &= (1-\nu)\alpha E_C - (\sigma+\mu_C)A_C, \\
\frac{dI_C}{dt} &= \nu\alpha E_C - (\delta+\mu_C+d_C)I_C, \\
\frac{dR_C}{dt} &= \sigma A_C + \delta I_C - (\gamma+\mu_C)R_C, \\
\frac{dV_C}{dt} &= \rho\Lambda_C - (1-r)\lambda_C V_C + \tau S_C - \eta V_C - \mu_C V_C, \\
\frac{dS_R}{dt} &= \Lambda_R - \lambda_R S_R - \mu_R S_R, \\
\frac{dA_R}{dt} &= \lambda_R S_R - \mu_R A_R, \\
\frac{dL}{dt} &= \omega_C(A_C + I_C) + \omega_R A_R - \varepsilon L,
\end{aligned}
\tag{5.1}
$$

where

$$
\lambda_C = \beta_{CC}(A_C + I_C) + \beta_{CR}A_R + \frac{\beta_C L}{K+L},
$$

$$
\lambda_R = \beta_{RR}A_R + \frac{\beta_R L}{K+L},
$$

and the initial conditions; $S_C(0) > 0,\ E_C(0) \geq 0,\ A_C(0) \geq 0,\ I_C(0) \geq 0,\ R_C(0) \geq 0,\ V_C(0) \geq 0,\ S_R(0) > 0,\ A_R(0) \geq 0,\ L(0) = L_0 \geq 0.$

5.2 Model Analysis

5.2.1 Existence and Uniqueness of Solutions

Theorem 5.2.1 (Existence and Uniqueness). Consider the initial value problem (4.1) for the leptospirosis transmission model defined by the system:

$$
\frac{d\mathbf{X}}{dt} = \mathbf{F}(\mathbf{X}(t)), \quad \mathbf{X}(0) = \mathbf{X}_0,
$$

where

$$\mathbf{X}(t) = \begin{pmatrix} S_C(t) \\ E_C(t) \\ A_C(t) \\ I_C(t) \\ R_C(t) \\ V_C(t) \\ S_R(t) \\ A_R(t) \\ L(t) \end{pmatrix}, \quad \mathbf{F}(\mathbf{X}) = \begin{pmatrix} (1-\rho)\Lambda_C - \lambda_C S_C + \gamma R_C + \eta V_C - \tau S_C - \mu_C S_C \\ \lambda_C [S_C + (1-r)V_C] - (\alpha+\mu_C)E_C \\ (1-\nu)\alpha E_C - (\sigma+\mu_C)A_C \\ \nu\alpha E_C - (\delta+\mu_C+d_C)I_C \\ \sigma A_C + \delta I_C - (\gamma+\mu_C)R_C \\ \rho\Lambda_C - (1-r)\lambda_C V_C + \tau S_C - \eta V_C - \mu_C V_C \\ \Lambda_R - \lambda_R S_R - \mu_R S_R \\ \lambda_R S_R - \mu_R A_R \\ \omega_C(A_C + I_C) + \omega_R A_R - \varepsilon L \end{pmatrix},$$

with $N_C = S_C + E_C + A_C + I_C + R_C + V_C$, $N_R = S_R + A_R$ and initial conditions satisfying $\mathbf{X}_0 \in \mathbb{R}^9_+$.

Assume that all the parameters are positive constants and the initial conditions satisfy $\mathbf{X}_0 \in \Omega$, where $\Omega = \Omega_C \times \Omega_R \times \Omega_L$ is the biologically feasible region defined by: $\Omega = \Omega_C \text{x} \Omega_R \text{x} \Omega_L \in \mathbb{R}^6_+ \text{x} \mathbb{R}^2_+ \text{x} \mathbb{R}^1_+$, where
$\Omega_C(t) = \{(S_C(t), E_C(t), A_C(t), I_C(t), R_C(t), V_C(t)) : 0 \leq N_C(t) \leq \frac{\Lambda_C}{\mu_C}\}$,
$\Omega_R(t) = \{(S_R(t), A_R(t)) : 0 \leq N_R(t) \leq \frac{\Lambda_R}{\mu_R}\}$, and
$\Omega_L(t) = \{L : 0 \leq L(t) \leq \frac{\Lambda_C \omega_C}{\varepsilon \mu_C} + \frac{\Lambda_R \omega_R}{\varepsilon \mu_R}\}$.

Then the governing model (4.1) admits a unique, nonnegative, and bounded solution $\mathbf{X}(t)$ that exists for all time $t \geq 0$ and remains in the region Ω.

Proof. We establish the result as follows. Note that the function $\mathbf{F}(\mathbf{X})$ is continuously differentiable with respect to all state variables in $\mathbb{R}^9_+$, provided $N_C, N_R > 0$. Since $\mathbf{F}$ and its Jacobian matrix are continuous on the closed, bounded set Ω, they satisfy a Lipschitz condition inside Ω. By the Picard-Lindelöf theorem (Coddington & Levinson, 1955; Hartman, 1964), there exists a unique local solution $\mathbf{X}(t)$ on some maximal interval of existence $[0, t_{\max})$. The derivative of the vector field $\mathbf{F}$ is also nonnegative, for each state variable, when it approaches zero. That is,

$$\left.\frac{dS_C}{dt}\right|_{S_C=0} = (1-\rho)\Lambda_C + \gamma R_C + \eta V_C > 0,$$

$$\left.\frac{dE_C}{dt}\right|_{E_C=0} = \lambda_C(S_C + (1-r)V_C) \geq 0,$$

$$\left.\frac{dS_R}{dt}\right|_{S_R=0} = \Lambda_R > 0, \qquad \left.\frac{dA_R}{dt}\right|_{A_C=0} = \lambda_R S_R \geq 0,$$

and similarly for other compartments. Thus, by the invariance principle for cooperative systems

(Smith, 1995), solutions starting in the nonnegative orthant $\mathbb{R}^9_+$ remain nonnegative for all $t \geq 0$.

Next, define the total cattle population $N_C(t) = S_C(t) + E_C(t) + A_C(t) + I_C(t) + R_C(t) + V_C(t)$. Adding the first six equations yields:

$$\frac{dN_C}{dt} = \Lambda - \mu N_C(t) - dI_C(t) \leq \Lambda - \mu_C N_C.$$

Applying Grönwall's inequality (Gronwall, 1919), we obtain:

$$N_C(t) \leq \frac{\Lambda_C}{\mu_C} + \left(N_C(0) - \frac{\Lambda}{\mu}\right) e^{-\mu t} \leq \max\left\{N_C(0), \frac{\Lambda_C}{\mu_C}\right\}.$$

For rat population N_R, we have:

$$\frac{dN_R}{dt} = \frac{dS_R}{dt} + \frac{dA_R}{dt} = \Lambda_R - \mu N_R(t).$$

and we obtain

$$N_R(t) = N_R(0)e^{-\mu_R t} + \frac{\Lambda_R}{\mu_R}(1 - e^{-\mu_R t}) \leq \max\left\{N_R(0), \frac{\Lambda_R}{\mu_R}\right\}$$

For the pathogen compartment $L(t)$, we have:

$$\frac{dL}{dt} = \omega_C(A_C + I_C) + \omega_R A_R - \varepsilon L,$$

Thus, all state variables remain uniformly bounded on any finite time interval.

Since the right-hand side $\mathbf{F}$ is Lipschitz continuous on Ω and solutions remain bounded, by the continuation theorem for ordinary differential equations (Hirsch et al., 1974), the local solution can be extended to all $t \geq 0$. Specifically, the boundedness of solutions prevents finite-time blow-up, ensuring global existence.

From the bounds derived above, it follows directly that if $\mathbf{X}(0) \in \Omega$, then $\mathbf{X}(t) \in \Omega$ for all $t \geq 0$. Thus, Ω is positively invariant (Hale, 1969).

Therefore, by combining the Picard-Lindelöf theorem, Grönwall's inequality, and the continuation principle, we conclude that the model equations (5.1) has a unique, nonnegative, bounded solution that exists globally in time and remains within the biologically feasible region Ω. □

Remark 6. The mathematical foundation established here follows standard results in dynamical systems theory (Perko, 2013; Wiggins, 2003). The boundedness argument via Grönwall's inequality is particularly crucial, as it ensures that population variables do not grow without

bound which is an important requirement for biological realism. The invariance of Ω confirms that the model respects basic demographic constraints. These features ensure that the model is both mathematically well-posed and biologically realistic.

5.2.2 *Leptospira*-free Equilibrium Point and Effective Reproduction Number

The *Leptospira*-free equilibrium point of model (5.1) can be computed by setting right hand side of the system equals zero in the absence of infection ($E_C^* = A_C^* = I_C^* = R_C^* = A_R^* = L^* = 0$), we have

$$\begin{aligned}(1-\rho)\Lambda_C + \eta V_C^* - \tau S_C^* - \mu_C S_C^* &= 0,\\ \rho\Lambda_C - \eta V_C^* + \tau S_C^* - \mu_C V_C^* &= 0,\\ \Lambda_R - \mu_R S_R^* &= 0.\end{aligned} \tag{5.2}$$

Solving system (5.2) gives

$$S_C^* = \frac{\Lambda_C((1-\rho)\mu_C+\eta)}{\mu_C(\eta+\tau+\mu_C)},\ V_C^* = \frac{\Lambda_C(\rho\mu_C+\tau)}{\mu_C(\eta+\tau+\mu_C)},\ S_R^* = \frac{\Lambda_R}{\mu_R}.$$

Thus, the *Leptospira*-free equilibrium point, $\mathscr{E}^*$, of model (5.1) is given by

$$\mathscr{E}^* = (\frac{\Lambda_C((1-\rho)\mu_C+\eta)}{\mu_C(\eta+\tau+\mu_C)}, 0, 0, 0, 0, \frac{\Lambda_C(\rho\mu_C+\tau)}{\mu_C(\eta+\tau+\mu_C)}, \frac{\Lambda_R}{\mu_R}, 0, 0) \tag{5.3}$$

The effective reproduction number $\mathscr{R}_e$ represents the expected number of secondary infections generated by a single infected individual. To compute the effective reproduction number of model (5.1), we use the next-generation matrix approach presented in Van den Driessche & Watmough (2002). Considering the infected compartments $W = (E_C, A_C, I_C, A_R, L)$ in model (5.1), then we have $\frac{dW}{dt} = \mathscr{F}(t) - \mathscr{V}(t)$,

$$\mathscr{F} = \begin{bmatrix} \lambda_C\left[S_C + (1-r)V_C\right] \\ 0 \\ 0 \\ \lambda_R S_R \\ 0 \end{bmatrix}, \qquad \mathscr{V} = \begin{bmatrix} k_1 E_C \\ k_2 A_C - (1-\nu)\alpha E_C \\ k_3 I_C - \nu\alpha E_C \\ \mu_R A_R \\ \varepsilon L - \omega_C(A_C + I_C) - \omega_R A_R \end{bmatrix} \tag{5.4}$$

where $k_1 = \alpha + \mu_C$, $k_2 = \sigma + \mu_C$ and $k_3 = \delta + \mu_C + d_C$.
The Jacobian of matrices of $\mathscr{F}(t)$ and $\mathscr{V}(t)$ at $\mathscr{E}^*$ are given respectively by,

$$F=\frac{\partial \mathscr{F}_i}{\partial x_j}=\begin{bmatrix}0 & \beta_{CC}P_C^* & \beta_{CC}P_C^* & \beta_{CR}P_C^* & \beta_C P_C^*/K\\ 0 & 0 & 0 & 0 & 0\\ 0 & 0 & 0 & 0 & 0\\ 0 & 0 & 0 & \beta_{RR}S_R^* & \beta_R S_R^*/K\\ 0 & 0 & 0 & 0 & 0\end{bmatrix}, V=\frac{\partial \mathscr{V}_i}{\partial x_j}=\begin{bmatrix}k_1 & 0 & 0 & 0 & 0\\ -(1-\nu)\alpha & k_2 & 0 & 0 & 0\\ -\nu\alpha & 0 & k_3 & 0 & 0\\ 0 & 0 & 0 & \mu_R & 0\\ 0 & -\omega_C & -\omega_C & -\omega_R & \varepsilon\end{bmatrix},$$

where, $P_C^*=\left[S_C^*+(1-r)V_C^*\right]$, $S_C^*=\dfrac{\Lambda_C((1-\rho)\mu_C+\eta)}{\mu_C(\eta+\tau+\mu_C)}$, $V_C^*=\dfrac{\Lambda_C(\rho\mu_C+\tau)}{\mu_C(\eta+\tau+\mu_C)}$, and $S_R^*=\frac{\Lambda_R}{\mu_R}$.
Thus,

$$FV^{-1}=\begin{bmatrix}0 & \beta_{CC}P_C^* & \beta_{CC}P_C^* & \beta_{CR}P_C^* & \beta_C P_C^*/K\\ 0 & 0 & 0 & 0 & 0\\ 0 & 0 & 0 & 0 & 0\\ 0 & 0 & 0 & \beta_{RR}S_R^* & \beta_R S_R^*/K\\ 0 & 0 & 0 & 0 & 0\end{bmatrix}\begin{bmatrix}\frac{1}{k_1} & 0 & 0 & 0 & 0\\ \frac{(1-\nu)\alpha}{k_1k_2} & \frac{1}{k_2} & 0 & 0 & 0\\ \frac{\nu\alpha}{k_1k_3} & 0 & \frac{1}{k_3} & 0 & 0\\ 0 & 0 & 0 & \frac{1}{\mu_R} & 0\\ \frac{((1-\nu)k_3+\nu k_2)\alpha\omega_C}{k_1k_2k_3\varepsilon} & \frac{\omega_C}{k_2\varepsilon} & \frac{\omega_C}{k_3\varepsilon} & \frac{\omega_R}{\mu_R\varepsilon} & \frac{1}{\varepsilon}\end{bmatrix}$$

$$=\begin{bmatrix}y_{11} & y_{12} & y_{13} & y_{14} & y_{15}\\ 0 & 0 & 0 & 0 & 0\\ 0 & 0 & 0 & 0 & 0\\ y_{41} & y_{42} & y_{43} & y_{44} & y_{45}\\ 0 & 0 & 0 & 0 & 0\end{bmatrix} \tag{5.5}$$

where,

$$y_{11}=\frac{P_C^*\alpha}{k_1k_2k_3}\left(\beta_{CC}+\frac{\beta_C\omega_C}{\varepsilon K}\right)((1-\nu)k_3+\nu k_2),\quad y_{12}=\frac{P_C^*}{k_2}\left(\beta_{CC}+\frac{\beta_C\omega_C}{\varepsilon K}\right),\quad y_{13}=\frac{P_C^*}{k_3}\left(\beta_{CC}+\frac{\beta_C\omega_C}{\varepsilon K}\right),$$

$$y_{14}=\frac{P_C^*}{\mu_R}\left(\beta_{CR}+\frac{\beta_C\omega_R}{\varepsilon K}\right),\quad y_{15}=\frac{\beta_C P_C^*}{\varepsilon K},\quad y_{41}=\frac{\beta_R S_R^*\alpha\omega_C}{k_1k_2k_3\varepsilon K}\left((1-\nu)k_3+\zeta k_2\right),\quad y_{42}=\frac{\beta_R S_R^*\omega_C}{k_2\varepsilon K},$$

$$y_{43}=\frac{\beta_R S_R^*\omega_C}{k_3\varepsilon K},\qquad y_{44}=\frac{S_R^*}{\mu_R}\left(\beta_{RR}+\frac{\beta_R\omega_R}{\varepsilon K}\right),\qquad y_{45}=\frac{\beta_R S_R^*}{\varepsilon K}.$$

Computing $|FV^{-1}-\lambda I|=0$, gives $\lambda^3(\lambda^2-(y_{11}+y_{44})\lambda+(y_{11}y_{44}-y_{14}y_{41}))=0$. Thus,
$\lambda_{1,2,3}=0, \lambda_{4,5}=\dfrac{1}{2}\left[(y_{11}+y_{44})\pm\sqrt{(y_{11}-y_{44})^2+4y_{14}y_{41}}\right]$, are eigenvalues of the matrix FV^{-1}.

Therefore, the effective reproduction number, $\mathscr{R}_e$, of the model is given by the dominant eigenvalue of matrix FV^{-1}

$$\mathscr{R}_e = \rho(FV^{-1}) = \frac{1}{2}\left[(\mathscr{R}_e^c + \mathscr{R}_e^r) + \sqrt{(\mathscr{R}_e^c - \mathscr{R}_e^r)^2 + 4\mathscr{R}_e^{cr}}\right] \tag{5.6}$$

where,
$\mathscr{R}_e^c = \frac{P_C^*\alpha}{k_1k_2k_3}\left(\beta_{CC} + \frac{\beta_C\omega_C}{\varepsilon K}\right)((1-\nu)k_3 + \nu k_2)$, $\mathscr{R}_e^r = \frac{S_R^*}{\mu_R}\left(\beta_{RR} + \frac{\beta_R\omega_R}{\varepsilon K}\right)$,
$\mathscr{R}_e^{cr} = \frac{P_C^*}{\mu_R}\left(\beta_{CR} + \frac{\beta_C\omega_R}{\varepsilon K}\right)\left(\frac{\beta_R S_R^*\alpha\omega_C}{k_1k_2k_3\varepsilon K}((1-\nu)k_3 + \nu k_2)\right)$.

Remark 7. The epidemiological implication of each component of $\mathscr{R}_e$ in (5.6) : $\mathscr{R}_e^c$ indicates infections that can be generated by direct contact of susceptible cattle with an infectious cattle and also indirect contact with an environment contaminated by infectious cattle. $\mathscr{R}_e^r$ shows the new infection generated by direct contact of susceptible rats with an infectious rat and indirect contact with the environment that is contaminated by the infectious rat. The first term in $\mathscr{R}_e^{cr}$ indicates the new infection of cattle through direct contact with rats and environments contaminated by rats. The second term shows new infections of rats due to environments contaminated by infected cattle. In particular, for a rat-free environment, $\mathscr{R}_e = \mathscr{R}_e^c$.

5.2.3 Stability of *Leptospira*-free Equilibrium Point

The following section will present two theorems regarding the local and global stability of *Leptospira*-free equilibrium of model (5.1).

Theorem 5.2.2. The *Leptospira*-free equilibrium point, $\mathscr{E}^*$, of model (5.1) is locally asymptotically stable for $\mathscr{R}_e < 1$ and unstable otherwise.

Proof. Theorem 5.2.2 is trivial since the decomposed matrices $\mathscr{F}$ and $\mathscr{V}$ exist, which satisfy axioms (A1)–(A5) of Theorem 2 of Van den Driessche & Watmough (2008). □

Remark 8. Epidemiologically, Theorem 5.2.2 implies that if the initial total numbers of the populations in Equation (5.1) are close to $\mathscr{E}^*$, then $\mathscr{R}_e < 1$ is suffice to limit the spread of leptospirosis in rats and cattle. The *Leptospira*-free equilibrium must be globally asymptotically stable when $\mathscr{R}_e < 1$ in order to guarantee that the disease can be eradicated regardless of the initial population size. We will also show the global stability of the *Leptospira*-free equilibrium exploiting the method developed by Castillo-Chavez (2002),

Theorem 5.2.3. The *Leptospira*-free equilibrium point, $\mathscr{E}^*$, of model (5.1) is globally asymptotically stable for $\mathscr{R}_e < 1$ on its feasible region.

Proof. Re-writing model (5.1) as;

$$\begin{aligned}\frac{d\mathbf{U}}{dt} &= F(\mathbf{U},\mathbf{V}),\\ \frac{d\mathbf{V}}{dt} &= G(\mathbf{U},\mathbf{V}); with, G(\mathbf{U},0)=0,\end{aligned} \tag{5.7}$$

where, $\mathbf{U}=(S_C,R_C,V_C,S_R)\in\mathbb{R}^4$ denotes the uninfected compartment and $\mathbf{V}=(E_C,A_C,I_C,A_R,L)\in\mathbb{R}^5$ denotes the infected compartments. Let $\mathscr{E}^*=(\mathbf{U}^*,0)$ denotes the *Leptospira*-free equilibrium point of model (5.1). The following conditions grants the global stability of the *Leptospira*-free equilibrium point according to Castillo-Chavez (2002),

H_1 : For $\dfrac{d\mathbf{U}}{dt}=F(\mathbf{U},\mathbf{V})$, $\mathbf{U}^*$ is a globally asymptotically stable where $F(\mathbf{U}^*,0)=0$

H_2 : $G(\mathbf{U},\mathbf{V})=B\mathbf{V}-\hat{G}(\mathbf{U},\mathbf{V})$, $\hat{G}(\mathbf{U},\mathbf{V})>0$ for $(\mathbf{U},\mathbf{V})\in\Omega$, where $B=D_YG(\mathbf{U}^*,0)$ is an M-matrix (the matrix with off-diagonal elements non-negative).

To show condition H_1, take a sub-model of our model

$$\frac{d\mathbf{U}}{dt}=F(\mathbf{U},0)=\begin{bmatrix}(1-\rho)\Lambda_C+\gamma R_C+\eta V_C-(\tau+\mu_C)S_C\\ -(\gamma+\mu_C)R_C\\ \rho\Lambda_C+\tau S_C-(\eta+\mu_C)V_C\\ \Lambda_R-\mu_R S_R\end{bmatrix} \tag{5.8}$$

Solving the sub-system (5.8) and taking the limit as $t\to\infty$ gives us,

$S_C(t)\to\dfrac{\Lambda_C((1-\rho)\mu_C+\eta)}{\mu_C(\eta+\tau+\mu_C)}$, $R_C(t)\to 0$, $V_C\to\dfrac{\Lambda_C(\rho\mu_C+\tau)}{\mu_C(\eta+\tau+\mu_C)}$, and $S_R(t)\to\dfrac{\Lambda_R}{\mu_R}$, as $t\to\infty$,

which implies $\mathbf{U}^*$ is globally asymptotically stable on Ω.

On the other hand to show condition H_2,

$$B=D_YG(\mathbf{U}^*,0)=\begin{bmatrix}-(\alpha+\mu_C) & \beta_{CC}\left[S_C^*+(1-r)V_C^*\right] & \beta_{CC}\left[S_C^*+(1-r)V_C^*\right] & \beta_{CR}\left[S_C^*+(1-r)V_C^*\right] & \frac{\beta_C\left[S_C^*+(1-r)V_C^*\right]}{K}\\ (1-\nu)\alpha & -(\sigma+\mu_C) & 0 & 0 & 0\\ \nu\alpha & 0 & -(\delta+\mu_C+d_C) & 0 & 0\\ 0 & 0 & 0 & \beta_{RR}S_R^*-\mu_R & \frac{\beta_R S_R^*}{K}\\ 0 & \omega_C & \omega_C & \omega_R & -\varepsilon\end{bmatrix},$$

where, $S_C^*=\dfrac{\Lambda_C((1-\rho)\mu_C+\eta)}{\mu_C(\eta+\tau+\mu_C)}$, $V_C^*=\dfrac{\Lambda_C(\rho\mu_C+\tau)}{\mu_C(\eta+\tau+\mu_C)}$, $S_R^*=\frac{\Lambda_R}{\mu_R}$, and

$$G(\mathbf{U},\mathbf{V})=\begin{bmatrix}\left(\beta_{CC}(A_C+I_C)+\beta_{CR}A_R+\frac{\beta_C L}{K+L}\right)\left[S_C+(1-\rho)V_C\right]-(\alpha+\mu_C)E_C\\ (1-\nu)\alpha E_C-(\sigma+\mu_C)A_C\\ \nu\alpha E_C-(\delta+\mu_C+d_C)I_C\\ \left(\beta_{RR}A_R+\frac{\beta_R L}{K+L}\right)S_R-\mu_R A_R\\ \omega_C(A_C+I_C)+\omega_R A_R-\varepsilon L\end{bmatrix}$$

Thus,

$$\hat{G}(\mathbf{U},\mathbf{V}) = \begin{bmatrix} (\beta_{CC}A_C + \beta_{CC}I_C + \beta_{CR}A_R)\left[(S_C^* + (1-r)V_C^*) - (S_C + (1-r)V_C)\right] + \beta_C L(\frac{(S_C^* + (1-r)V_C^*)}{K} - \frac{(S_C + (1-r)V_C)}{(K+L)}) \\ 0 \\ 0 \\ \beta_{RR}A_R(S_R^* - S_R) + \beta_R L\left[\frac{S_R^*}{K} - \frac{S_R}{K+L}\right] \\ 0 \end{bmatrix}$$

where, $\hat{G}(\mathbf{U},\mathbf{V}) = B\mathbf{V} - G(\mathbf{U},\mathbf{V})$. For $S_C \leq S_C^*$, $V_C \leq V_C^*$, $S_R \leq S_R^*$ and $\beta_R L\left[\frac{S_R^*}{K} - \frac{S_R}{K+L}\right] = \beta_R L\left[\frac{S_R^* L + K(S_R^* - S_R)}{K(K+L)}\right] \geq 0$ on the feasible region Ω, $\hat{G}(\mathbf{U},\mathbf{V}) \geq 0$. Therefore both H_1 and H_2 conditions are satisfied and $\mathscr{E}^*$ is globally asymptotically stable for $\mathscr{R}_e < 1$. □

5.2.4 *Leptospira*-persistence Equilibrium Point

The equilibrium point of *Leptospira*-persistence can be found by putting the right side of model (5.1) to zero and solving for state variables. If $\mathscr{E}^{**} = (S_C^{**}, E_C^{**}, A_C^{**}, I_C^{**}, R_C^{**}, V_C^{**}, S_R^{**}, A_R^{**}, L^{**})$ is the *Leptospira*-persistence equilibrium point and we write the other state variables in terms of E_C^{**} as follows,

$$\begin{aligned}
S_C^{**} &= \frac{k_1((1-r)\lambda^* + k_6)E_C^{**} - (1-r)\rho\Lambda\lambda_C^{**}}{\lambda_C^{**}((1-\phi)\lambda_C^{**} + k_6 + (1-r)\tau)}, \\
A_C^{**} &= \frac{(1-\nu)\alpha}{k_2}E_C^{**}, \\
I_C^{**} &= \frac{\nu\alpha}{k_3}E_C^{**}, \\
R_C^{**} &= \frac{\sigma(1-\nu)\alpha k_3 + \delta\nu\alpha k_2}{k_2 k_3 k_4}E_C^{**}, \\
V_C^{**} &= \frac{\rho\Lambda + \tau S_C^{**}}{(1-r)\lambda_C^{**} + k_6}, \\
S_R^{**} &= \frac{\Lambda_R}{\lambda_R^{**} + \mu_R}, \\
A_R^{**} &= \frac{\lambda_R^{**}}{\mu_R}S_R^{**}, \\
L_C^{**} &= \frac{\omega_C\alpha\mu_R\left[(1-\nu)k_3 + \nu k_2\right]E_C^{**} + \omega_R\lambda_R^{**}k_2k_3S_R^{**}}{k_2k_3\mu_R\varepsilon},
\end{aligned} \tag{5.9}$$

where,

$\lambda_C^{**} = \beta_{CC}(A_C^{**} + I_C^{**}) + \beta_{CR}A_R^{**} + \frac{\beta_C L^{**}}{K+L^{**}}$, $\lambda_R^{**} = \beta_{RR}A_R^{**} + \frac{\beta_R L^{**}}{K+L^{**}}$, $k_1 = \alpha+\mu$,
$k_2 = \sigma+\mu$, $k_3 = (\delta+\mu+d)$, $k_4 = \gamma+\mu$, $k_5 = \tau+\mu$, $k_6 = \eta+\mu$.

The *Leptospira*-persistence equilibrium point (5.9) is unique, because the *Leptospira*-free equilibrium point is globally asymptotically stable from Theorem 5.2.3. Since the analysis is com-

plicated, we present stability of the unique *Leptospira*-persistence equilibrium point graphically in Section 5.4.

Table 5.2: Parameters values and their sources

Parameter	Value	Unit	Source
Λ_C	0.05	$\frac{cattle}{day}$	Assumed
Λ_R	0.2	$\frac{rat}{day}$	Assumed
ρ	0.5		Assumed
K	10000	*unit*	Engida et al. (2022)
β_{CC}	0.0001	$\frac{1}{(cattle)(day)}$	Aslan et al. (2021)
β_{CR}	0.0002	$\frac{1}{(rat)(day)}$	Assumed
β_C	0.0012	$\frac{1}{day}$	Aslan et al. (2021)
β_{RR}	0.0001	$\frac{1}{(rat)(day)}$	Minter et al. (2019)
β_R	0.005	$\frac{1}{day}$	Holt et al. (2006)
α	0.1	$\frac{1}{day}$	Chadsuthi et al. (2022)
ν	0.2		Assumed
δ	0.00274	$\frac{1}{day}$	Aslan et al. (2021); Okosun et al. (2016)
σ	0.00137	$\frac{1}{day}$	Assumed
μ_C	0.000274	$\frac{1}{day}$	Ndondo et al. (2016)
μ_R	0.00274	$\frac{1}{day}$	Alemneh (2020)
d_C	0.01	$\frac{1}{day}$	Holt et al. (2006)
ε	0.05	$\frac{1}{day}$	Minter et al. (2019)
ω_C	0.014	$\frac{unit}{(cattle)(day)}$	Aslan et al. (2021)
ω_R	0.02	$\frac{unit}{(rat)(day)}$	Assumed
η	0.013	$\frac{1}{day}$	Okosun et al. (2016)
r	0.88		Esteves et al. (2022); Wilson-Welder et al. (2020)
τ	0.05	$\frac{1}{day}$	Assumed
γ	0.00185	$\frac{1}{day}$	Chadsuthi et al. (2022)

5.3 Sensitivity Analysis

Sensitivity analysis is an effective method for determining those parameters that have a major impact on the reproduction number. Additionally, this analysis helps choose the best control measures to minimize rate of the disease spread. The sensitivity analysis determines the resilience of the model prediction to changes in parameter values due to potential errors in data collection and assumed parameter values. The literature has used a variety of methods in this

regard. For this study, we applied normalized forward sensitivity indices presented in Definition A.5.1. $\mathscr{R}_e$ is directly (inversely) impacted by the relevant parameter when the index value is positive (or negative). Definition A.5.1 gives the formulas for the normalized forward sensitivity index for the model's primary parameters: As a result, we used the values in Table 5.2 to quantitatively evaluate the sensitivity index of $\mathscr{R}_e$ with regard to each model parameters. Vaccine efficiency, r, cattle death rate, μ_C, rat death rate, μ_R, cattle recruitment rate, Λ_C, and contact rate with infectious cattle, β_{CC}, are the most sensitive factors, respectively. For instance, if β_{CC} increases by 10%, $\mathscr{R}_e$ increases (or decreases) by 6.4%, and if μ_R increases or decreases by 10%, $\mathscr{R}_e$ decreases (or increases) by 6.8%. In conclusion, the sensitivity analysis indicates that the most influential parameters affecting $\mathscr{R}_e$ are the contact rate among cattle (β_{CC}), rat-to-cattle transmission rate (β_{CR}), and rat mortality rate (μ_R). This suggests that reducing cattle-to-cattle contact and controlling the rat population are effective strategies for mitigating disease spread. Moreover, lowering $\mathscr{R}_e$ is achieved by improving the recovery rate of asymptomatic cattle (σ) through early diagnosis and treatment. These findings reveals that reducing rat density, increasing vaccination coverage, and improving recovery rates significantly reduce $\mathscr{R}_e$, thereby lowering disease prevalence. Table 5.3 provides a summary of the sensitivity indices of $\mathscr{R}_e$ for each parameter value.

5.4 Numerical simulation and Discussion

To validate the theoretical results, numerical simulations were performed using Python's odeint package. The baseline parameter values in Table 5.2 were selected from the literature, with adjustments made based on epidemiological plausibility. The initial conditions are chosen as $(S_C(0), E_C(0), A_C(0), I_C(0), R_C(0), V_C(0), S_R(0), A_R(0), L(0)) = (100, 30, 20, 10, 0, 50, 100, 50, 10)$.

5.4.1 Stability of *Leptospira*-persistence Equilibrium Point

Using the initial condition mentioned above and the parameter values found in Table 5.2, Eq. (5.6) yields $\mathscr{R}_e \approx 2.86937 > 1$. Applying *scipy.optimize.fSolve* (Moruzzi & Moruzzi, 2020), if we solve model (5.1) by setting the right-hand side to zero, we obtain a unique positive *Leptospira*-persistence equilibrium given by $\mathscr{E}^{**} = (S_C^{**}, E_C^{**}, A_C^{**}, I_C^{**}, R_C^{**}, V_C^{**}, S_R^{**}, A_R^{**}, L^{**}) = (5.3031, 1.1226, 54.6261, 1.7252, 37.4598, 19.2827, 27.2986, 45.6941, 34.0560)$. Figure 5.2 (a) and (b) shows the stability of this unique *Leptospira*-persistence equilibrium $\mathscr{E}^{**}$.

Table 5.3: Sensitivity of the parameters

Parameters	Value	Sensitivity index
Λ_C	0.05	0.65988
Λ_R	0.2	0.34012
ρ	0.5	-0.00415
K	10000	-0.02457
β_{CC}	0.0001	+0.63595
β_{CR}	0.0002	+0.02371
β_C	0.0012	+0.00022
β_{RR}	0.0001	+0.31578
β_R	0.005	+0.02435
α	0.1	+0.00180
ν	0.2	-0.13972
δ	0.00274	-0.00425
σ	0.00137	-0.53306
μ_C	0.000274	-0.76629
μ_R	0.00274	-0.68025
d_C	0.01	-0.01552
ε	0.05	-0.02457
ω_C	0.014	+0.02393
ω_R	0.02	+0.00064
η	0.013	+0.31230
r	0.88	-1.52005
τ	0.05	-0.31473

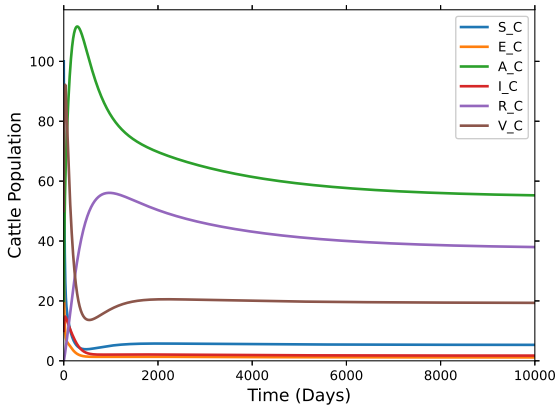

(a) As $t \to \infty$, $(S_C, E_C, A_C, I_C, R_C, V_C) \to (5.303, 1.123, 54.626, 1.725, 37.460, 19.283)$.

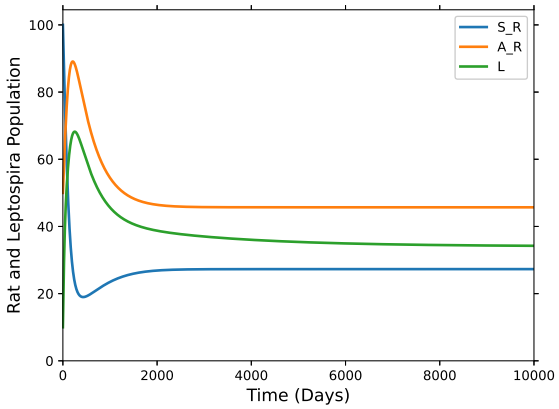

(b) As $t \to \infty$, $(S_R, A_R, L) \to (27.299, 45.694, 34.056)$.

Figure 5.2: $\mathscr{E}^{**} \approx (5.303, 1.123, 54.626, 1.725, 37.460, 19.283, 27.299, 45.694, 34.056)$, when $\mathscr{R}_e = 2.86937 > 1$ with the baseline values in Table 5.2.

5.4.2 Stability of *Leptospira*-free Equilibrium Point

If we adjust the values of $\beta_{CC} = 0.00005$, $\mu_R = 0.0274$, and $\tau = 0.15$, the effective reproduction number becomes $\mathscr{R}_e \approx 0.87227 < 1$. Figures 5.3 (a) and (b) show that the *Leptospira*-free equilibrium, $\mathscr{E}^* = (14.6825, 0, 0, 0, 0, 0, 167.7992, 7.2993, 0)$, calculated using Eq. (5.3), is locally asymptotically stable. Since this situation indicates that there are no infectious animal and free-living *Leptospira* in the soil as time goes on, there won't be any affected animals, and only the susceptible cattle, vaccinated cattle, and susceptible rat population will exist.

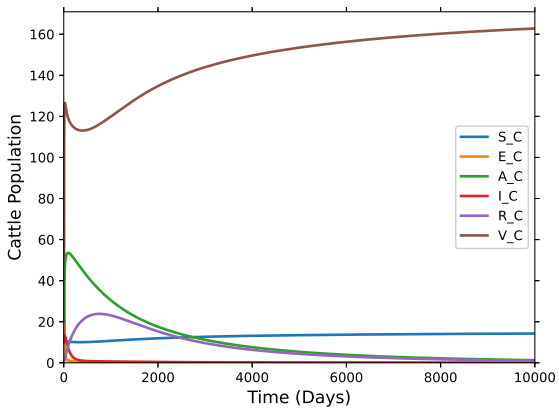

(a) As $t \to \infty$, $(S_C, E_C, A_C, I_C, R_C, V_C)$ $\to (14.683, 0, 0, 0, 0, 167.800)$.

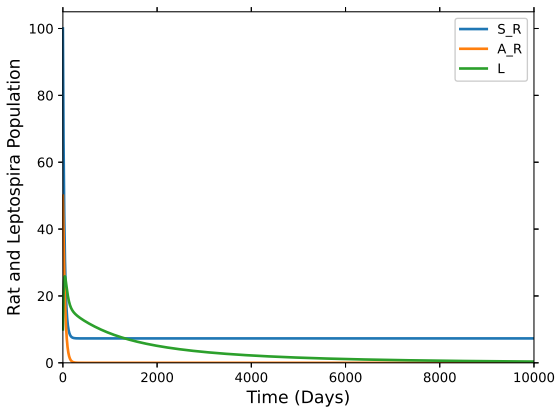

(b) As $t \to \infty$, $(S_R, A_R, L) \to (7.300, 0, 0)$.

Figure 5.3: $\mathscr{E}^* = (14.683, 0, 0, 0, 0, 167.800, 7.300, 0, 0)$, when $\mathscr{R}_e = 0.87227 < 1$ with the baseline values in Table 5.2.

5.4.3 The Impact of the Most Sensitive Parameters

The Impact of Varying Contact Rate within Cattle, β_{CC} and Cattle with Rat, β_{CR}

In this subsection, we demonstrate change in the dynamics of leptospirosis varying contact rate within cattle, β_{CC}. Figure 5.4 (a)-(d) shows the simulation for sensitivities of susceptible, vaccinated, and infectious cattle as well as the *Leptospira* load in the environment with the change of contact rate within cattle ($\beta_{CC} = 0.0002, \beta_{CC} = 0.0001, \beta_{CC} = 0.00005$). These figures clearly indicate that the susceptible and vaccinated cattle population improved significantly in decreasing contact with infectious cattle. In addition, the quantity of infectious cattle and *Leptospira* load in the environment can be reduced and possibly eliminated by lowering the values of β_{CC}. The findings of Engida et al. (2022) support this result, showing that reducing the rate of contact with asymptomatic cattle may be an effective way to manage the expansion of infected cattle and the environmental *Leptospira* burden.

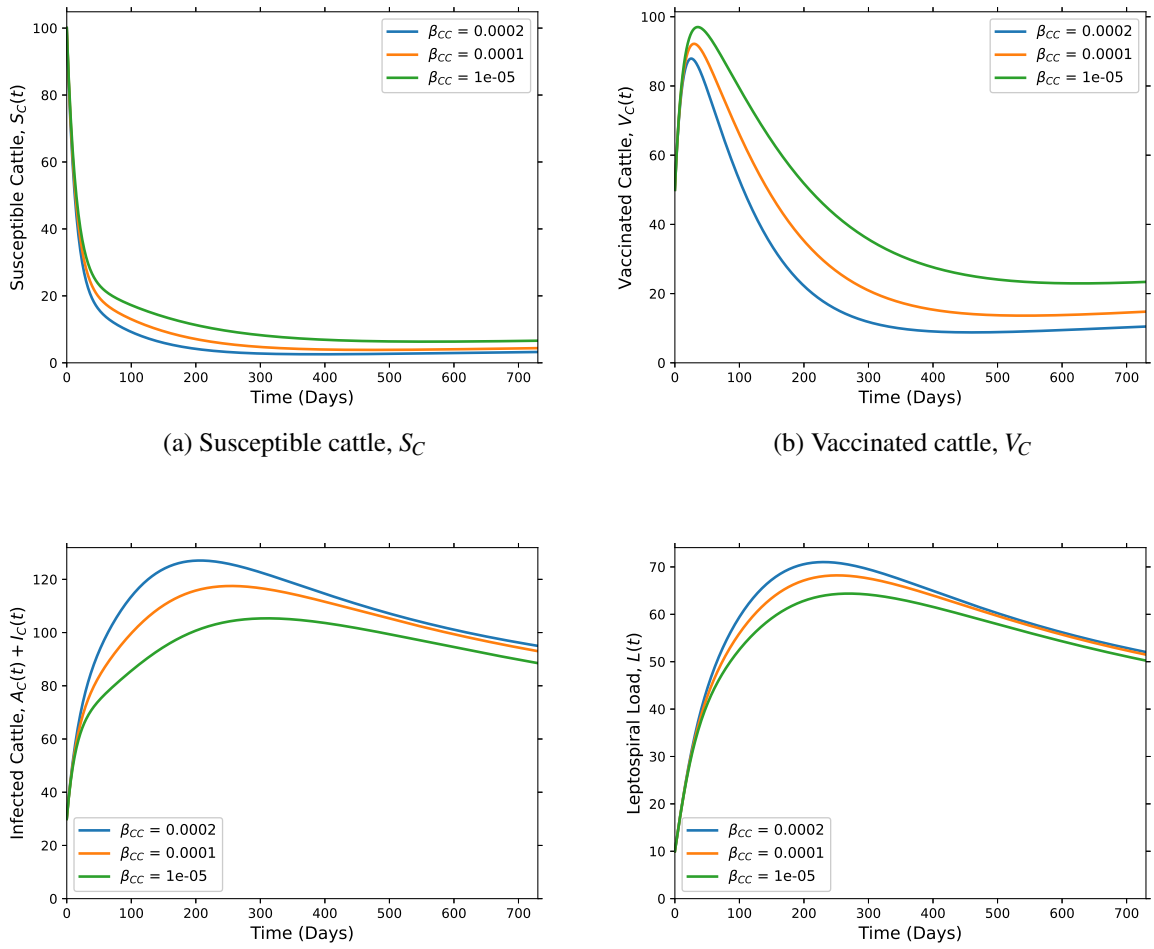

(a) Susceptible cattle, S_C

(b) Vaccinated cattle, V_C

(c) Infected cattle, $A_C + I_C$

(d) Leptospiral Load, L

Figure 5.4: Impact of contact rate within cattle, β_{CC}.

Similarly, Figure 5.5 depicts the dynamic behavior of model (5.1) by varying the contact rate of cattle with rats ($\beta_{CR} = 0.0002, \beta_{CR} = 0.0001, \beta_{CR} = 0.00005$). It can be seen from Figure 5.5 (a) and (b) that decreasing the incidence of cattle with rats increases the sizes of susceptible and vaccinated cattle and vice versa. On the other hand, reducing this parameter reduces the sizes of infectious cattle and *Leptospiral* load in the environment, as shown in Figure 5.5 (c) and (d), respectively.

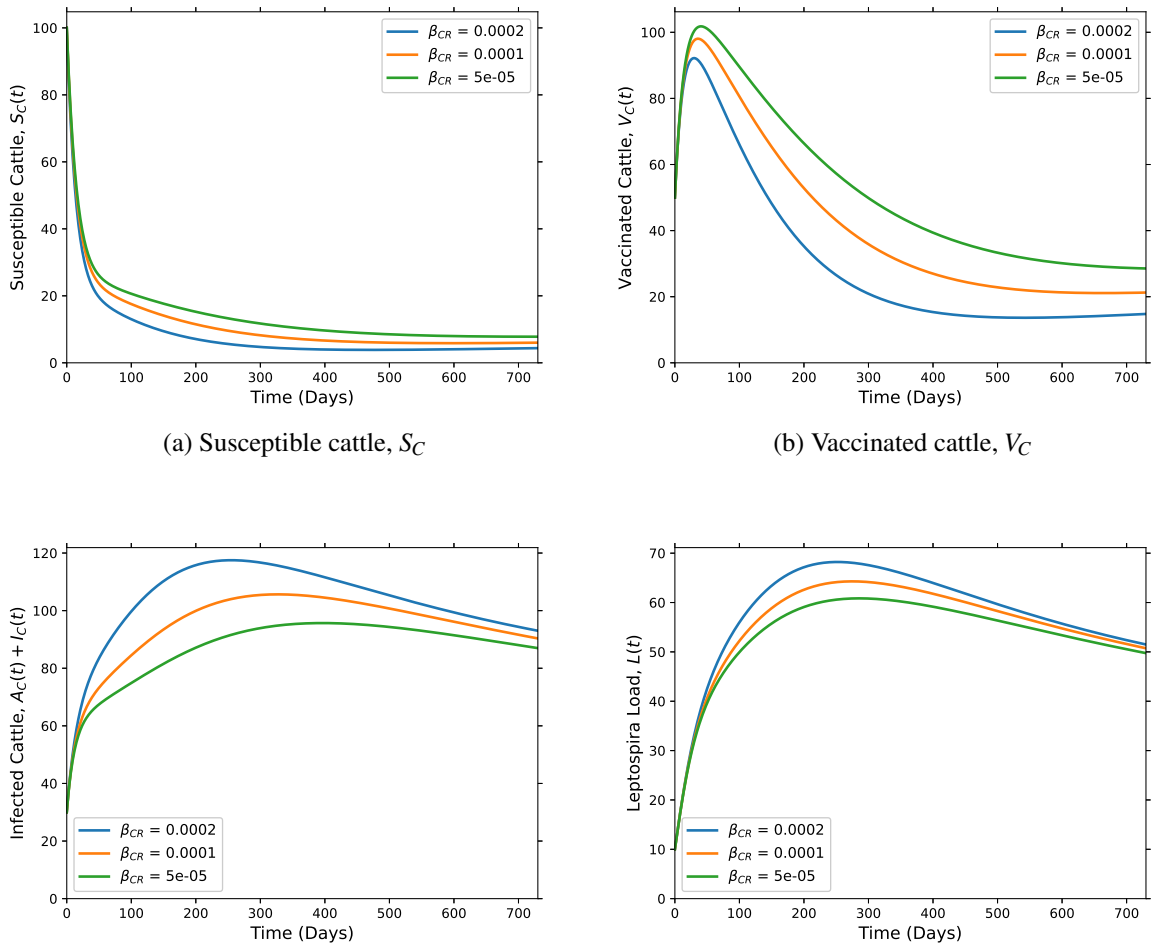

(a) Susceptible cattle, S_C

(b) Vaccinated cattle, V_C

(c) Infected cattle, $A_C + I_C$

(d) Leptospiral Load, L

Figure 5.5: Impact of contact rate of cattle with rat, β_{CR}.

The impact of Varying Death Rate of Rat, μ_R.

The impact of death rate of rats with cattle population and *Leptospira* load is illustrated in this section by varying values of μ_R ($\mu_R = 0.00137, \mu_R = 0.00274, \mu_R = 0.00548$). Reducing the rat population can also lower the environmental concentration of *Leptospira* and the number of cattle infections. It can be observed, from Figure 5.6 (a)-(b), that the number of infected cattle and the amount of *Leptospira* in the environment decrease as μ_R increases. Conversely, decreasing the death rate of rats decreases the number of susceptible and vaccinated cattle. Hence, reducing animal reservoirs(such as rat) is critical for controlling leptospirosis transmission to the cattle population. This can be done through trapping or environmentally friendly rodenticide and this result coincide with work of Engida et al. (2023).

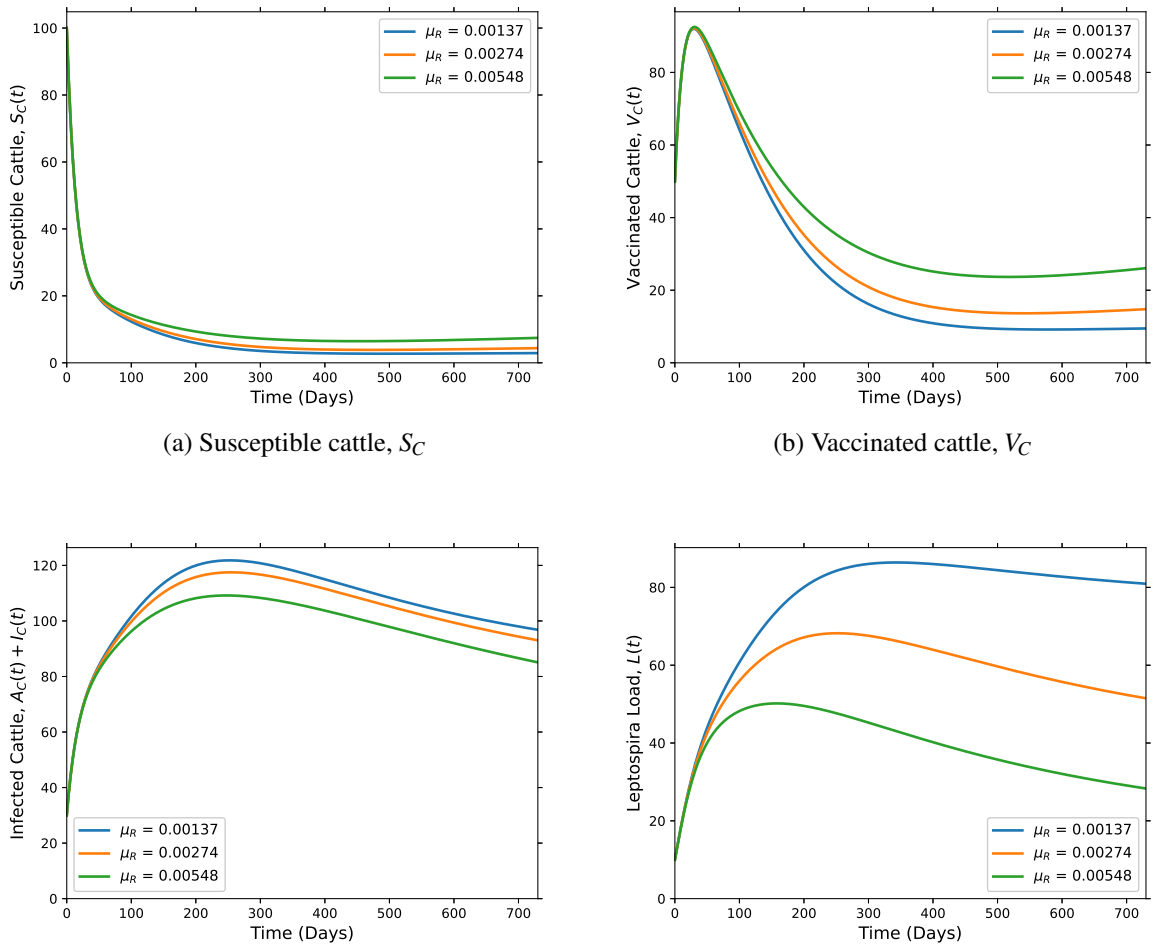

(a) Susceptible cattle, S_C

(b) Vaccinated cattle, V_C

(c) Infected cattle, $A_C + I_C$

(d) Leptospiral Load, L

Figure 5.6: Impact of varying death rate of rat, μ_R.

The Impact of Varying Recovery Rate of Asymptomatic Infectious Cattle, σ.

By raising the recovery rate of asymptomatic infectious cattle, σ by pre-diagnosis treatment, the infectious cattle can be decreased. In this section, we simulate model (5.1) and change the value of σ to observe how it affects bacterial and cattle populations. As shown in Figure 5.7 (a) and (b), we can see from Figure 5.7 that σ is directly proportional to susceptible and vaccinate cattle. Furthermore, Figure 5.7 (c) and (d) show that while the size of σ increases (or decreases, respectively) with time, the infectious cattle population and *Leptospiral* load increase (or decrease).

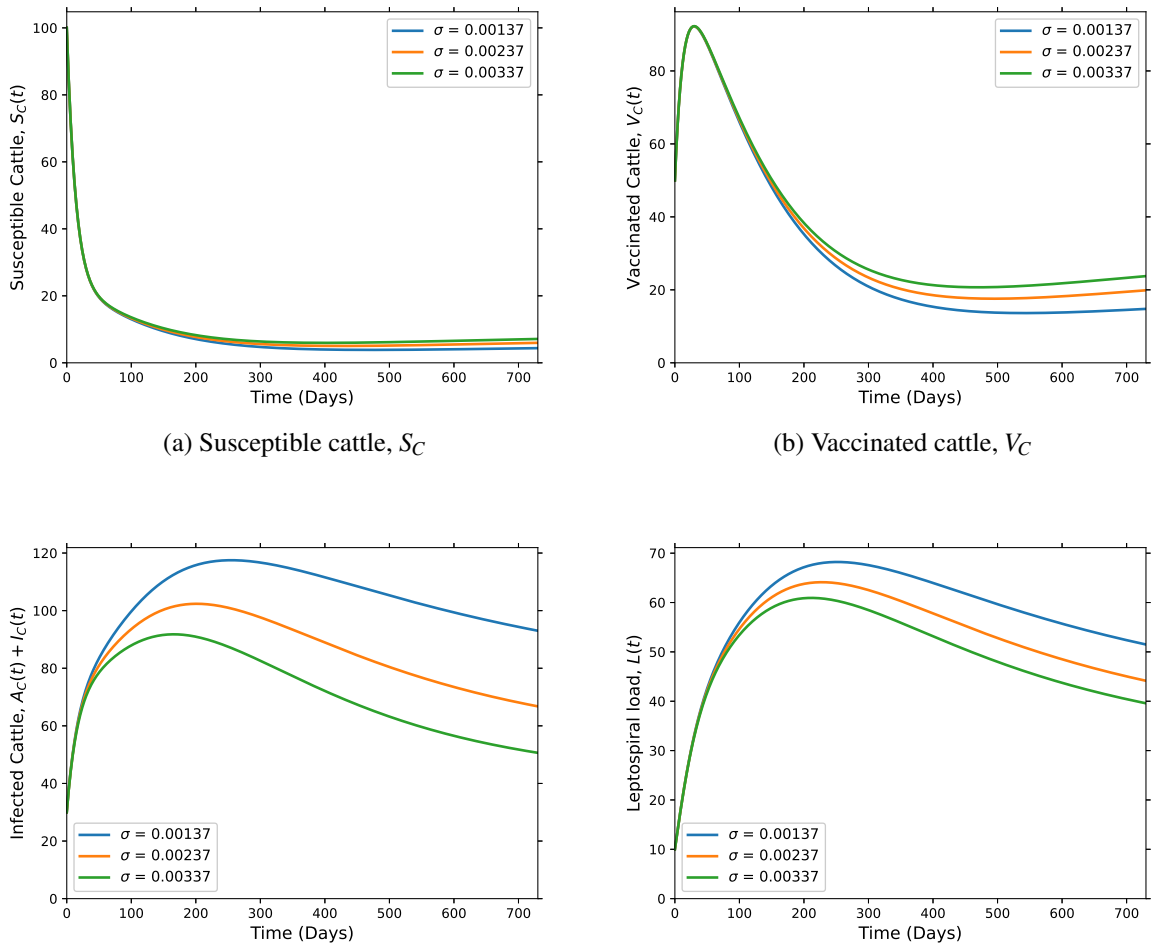

(a) Susceptible cattle, S_C

(b) Vaccinated cattle, V_C

(c) Infected cattle, $A_C + I_C$

(d) Leptospiral Load, L

Figure 5.7: Impact of recovery rate of asymptomatic infectious cattle, σ.

5.5 Conclusion

In conclusion, our study has built and investigated the mathematical modeling of leptospirosis in cattle and rats with free-living *Leptospira* pathogens in the environment. The analysis of the model indicates that there exists a region where the model is mathematically and epidemiologically well posed. The effective reproduction number is computed using the next-generation matrix approach, and its sensitivity is analyzed with respect to model parameters. The simulations confirm that when $\mathscr{R}_e > 1$, the infection persists, but for $\mathscr{R}_e < 1$, the disease dies out over time. Furthermore, the numerical simulations in Figures 5.4 - 5.7 and the sensitivity analysis result in Table 5.3 show that decreasing the contact rate with infected cattle, β_{CC} and with infected rats, β_{CR}, increasing rats' mortality rate, μ_R, and fostering the recovery rate of asymp-

tomatic cattle, σ, can meaningfully reduce the infection status in cattle herds. In particular, our results underscore the contribution of rats in the transmission of cattle leptospirosis. Consistent with our findings, Sunaryo & Priyanto (2022) highlights that a major risk factor for leptospirosis outbreaks in cattle herds and humans is the existence of high rat populations, particularly in agricultural and peridomestic areas where they interact with livestock. Therefore, to interrupt this cycle of transmission, preventive and control methods must focus on both rodent control measures and appropriate livestock management.

CHAPTER 6

FRACTIONAL-ORDER MODELING AND ANALYSIS OF LEPTOSPIROSIS IN CATTLE AND HUMAN

In this chapter, we developed a mathematical model of the Caputo fractional derivative (CFD) that describes the dynamics of leptospirosis in humans and cattle. Fractional-order modeling is especially promising for leptospirosis because it naturally captures the memory effects of asymptomatic carriers, environmental persistence, and relapse dynamics, offering a more realistic representation than classical models. Our model particularly describes the dynamics of indirect transmission from the environment to humans and cattle as well as direct transmission from cattle to humans and cattle to cattle. The model takes into account how various parameters and fractional orders affect the dynamics of leptospirosis transmission. We examine the fundamental characteristics of the model and conduct a qualitative analysis.

6.1 Model Formulation

In this section, we developed a fractional-order mathematical model of leptospirosis dynamics in cattle and humans. The developed model considers the interaction of populations: the susceptible S_c, vaccinated V_c, infected I_c, and recovered R_c for the cattle population and the susceptible S_h, exposed E_h, infected I_h, and recovered R_h for the human population. Also the environmental free-*Leptospira L* is considered as a separate compartment. The cattle population is recruited at the constant rate of Λ_c, of which ρ portion goes to the vaccinated class and the rest goes to the susceptible class. The susceptible class transferred to the infected class by the force of infection $\lambda_c = \beta_{cc} I_c + \frac{\beta_c L}{K+L}$ and recovered at the rate of σ_c. Due to vaccine imperfection, the vaccinated class becomes infected at the reduced force of infection $(1-r)\lambda_c$, where r is vaccine efficacy. Also, the recovered class lose their natural immunity and become susceptible at the rate of γ_c. We introduced parameter τ, which measures the vaccination rate of susceptible cattle, and the vaccinated class becomes susceptible at the rate of η_c due to loss of temporary immunity.

Similarly, for human populations, which are recruited by the rate Λ_h, the susceptible class is transferred to the exposed class by the force of infection $\lambda_h = \beta_{hc} I_c + \frac{\beta_h L}{K+L}$, and the exposed become infected at the rate of α_h. Moreover, the infected class recovered at the rate of δ_h and recovered loss of its natural immunity at the rate of γ_h. The parameters used in our model are summarized in Table 6.1, and the transmission dynamics are represented by the flow diagram given by Figure 6.1. Furthermore, the formulated mathematical model is governed by the fol-

lowing assumptions.

1. Incubation period for cattle is assumed negligible since it too small compared with infection period.

2. Human to human and human to cattle transmission are neglected (Artiono et al., 2024; Oguntolu et al., 2024).

3. Both population are assumed homogeneous.

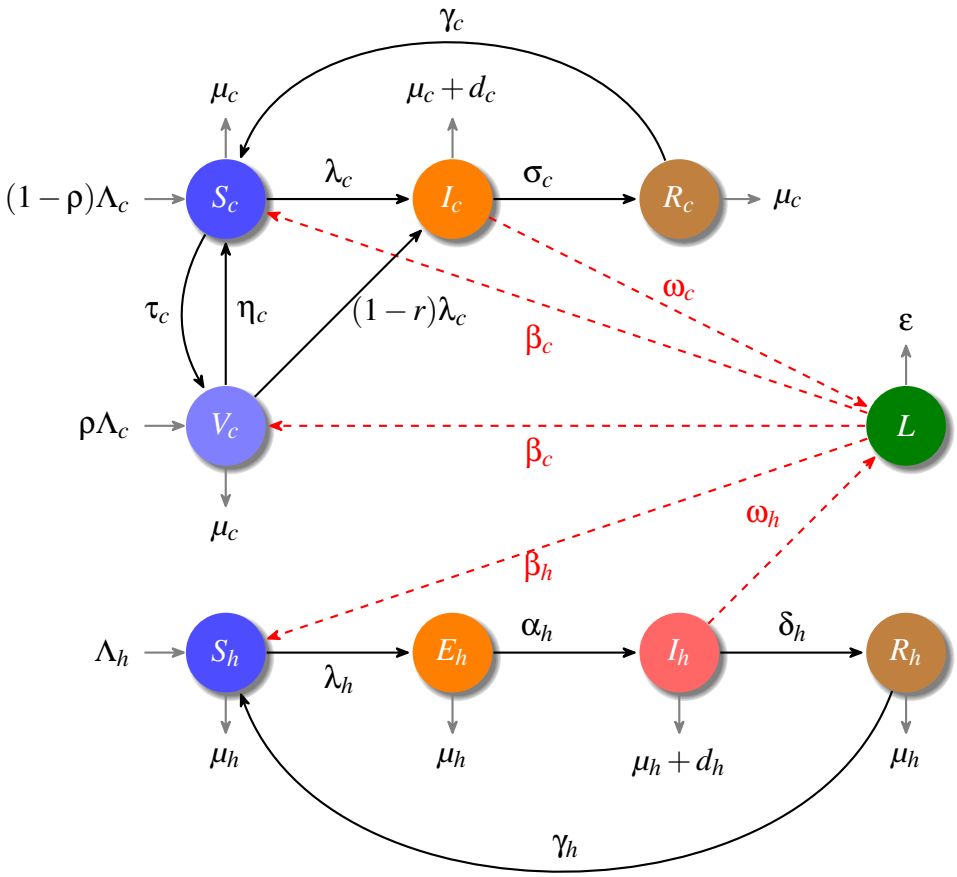

Figure 6.1: Flow diagram of leptospirosis dynamics in cattle and human

The system of non-linear, Caputo fractional-order differential equations that follows the dynamics of the proposed model is:

$$
\begin{aligned}
{}_0^C D_t^{\psi} S_c &= (1-\rho)\Lambda_c - \lambda_c S_c + \gamma_c R_c + \eta_c V_c - \tau_c S_c - \mu_c S_c, \\
{}_0^C D_t^{\psi} V_c &= \rho\Lambda_c - (1-r)\lambda_c V_c + \tau_c S_c - \eta_c V_c - \mu_c V_c, \\
{}_0^C D_t^{\psi} I_c &= \lambda_c [S_c + (1-r)V_c] - (\sigma_c + \mu_c + d_c) I_c, \\
{}_0^C D_t^{\psi} R_c &= \sigma_c I_c - (\gamma_c + \mu_c) R_c, \\
{}_0^C D_t^{\psi} S_h &= \Lambda_h - \lambda_h S_h + \gamma_h R_h - \mu_h S_h, \\
{}_0^C D_t^{\psi} E_h &= \lambda_h S_h - (\alpha_h + \mu_h) E_h, \\
{}_0^C D_t^{\psi} I_h &= \alpha_h E_h - (\delta_h + \mu_h + d_h) I_h, \\
{}_0^C D_t^{\psi} R_h &= \delta_h I_h - (\gamma_h + \mu_h) R_h, \\
{}_0^C D_t^{\psi} L &= \omega_c I_c + \omega_h I_h - \varepsilon L
\end{aligned}
\tag{6.1}
$$

where $\psi \in (0,1]$, ${}_0^C D_t^{\psi}$ denotes left Caputo fractional order derivative, where $\lambda_c = \beta_{cc} I_c + \frac{\beta_c L}{K+L}$, $\lambda_h = \beta_{hc} I_c + \frac{\beta_h L}{K+L}$, and the initial conditions;
$S_c(0) > 0$, $I_c(0) \geq 0$, $R_c(0) \geq 0$, $V_c(0) \geq 0$, $S_h(0) > 0$, $E_h(0) \geq 0$, $I_h(0) \geq 0$, $R_h(0) \geq 0$ $L(0) \geq 0$.

6.2 Model Analysis

6.2.1 Existence and Uniqueness of Solution

Theorem 6.2.1. The fractional dynamical system (6.1) with the initial value has a unique solution $\forall t > 0$.

Proof. Consider the region $\mathfrak{C} = [0,t]\text{x}\Omega$, where $t < \infty$ and
$\Omega = \{(S_c, V_c, I_c, R_c, S_h, E_h, I_h, R_h, L) \in \mathbb{R}_+^9 : \max\{|S_c|, |V_c|, |I_c|, |R_c|, |S_h|, |E_h|, |I_h|, |R_h|, |L|\} \leq M, M \in \mathbb{R}^+$.
Denote $\phi_1(t) = (S_c, V_c, I_c, R_c, S_h, E_h, I_h, R_h, L)$ and $\phi_2(t) = (\overline{S}_c, \overline{V}_c, \overline{I}_c, \overline{R}_c, \overline{S}_h, \overline{E}_h, \overline{I}_h, \overline{R}_h, \overline{L})$. Consider a mapping $f : \mathbb{R}_+^9 \to \mathbb{R}_+$:

$$
f(t, \phi(t)) = (f_1(t,\phi(t)), f_2(t,\phi(t)), f_3(t,\phi(t)), f_4(t,\phi(t)), f_5(t,\phi(t)), f_6(t,\phi(t)), f_7(t,\phi(t)), f_8(t,\phi(t), f_9(t,\phi(t)))^T
$$

where a function $f_i(t,\phi(t))$ is given by

$$
f_i(t,\phi(t)) = {}_0^C D_t^{\psi} \phi_i(t), \forall i = 1, ..., 9.
$$

For any $\phi_1, \phi_2 \in \Omega$, we have $\|f_1(t,\phi_1) - f_1(t,\phi_2)\| = \|\{(1-\rho)\Lambda_c - \lambda_c S_c + \gamma_c R_c + \eta_c V_c - \tau_c S_c - \mu_c S_c\} - \{(1-\rho)\Lambda_c - \lambda_c \overline{S}_c + \gamma_c R_c + \eta_c V_c - \tau_c \overline{S}_c - \mu_c \overline{S}_c\}\| \leq \|(\lambda_c + \tau_c + \mu_c)\| \|(S_c - \overline{S}_c)\| = M_1 \|(S_c - \overline{S}_c)\|$
where, $M_1 = \|(\lambda_c + \tau_c + \mu_c)\| = \|(\beta_{cc}\|I_c\| + \frac{\beta_c \|L\|}{K + \|L\|} + \tau_c + \mu_c)\|$.

Table 6.1: Parameters description

Parameter	Description
Λ_c	Cattle recruitment rate
Λ_h	Human recruitment rate
ρ	Fraction of immunized recruited cattle
K	Environmental *Leptospira* concentration
β_{cc}	Contact rate between infected cattle and susceptible cattle
β_{hc}	Contact rate between infected cattle and susceptible human
β_c	Contact rate between contaminated environment and susceptible cattle
β_h	Contact rate between contaminated environment and susceptible human
α_h	Rate of progression from exposed to infected human compartments
δ_h	Rate of progression from infected to Recovered human compartments
σ_c	Rate of progression from infected to recovered cattle compartments
μ_c	Cattle natural death rate
μ_h	Human natural death rate
d_c	*Leptospira* induced death rate of infected cattle
d_h	*Leptospira* induced death rate of infected human
ε	*Leptospira* decay rate
ω_c	*Leptospira* shedding rate from infected cattle
ω_h	*Leptospira* shedding rate from infected human
η_c	Rate of loss of vaccine immunity
r	Vaccine efficacy
τ_c	Vaccination rate of susceptible cattle
γ_c	Rate of loss of natural immunity for cattle
γ_h	Rate of loss of natural immunity for human

Utilizing this approach for all compartments, we have

$$\begin{aligned}\|f(t,\phi_1)-f(t,\phi_2)\| &= \|f_1(t,\phi_1)-f_1(t,\phi_2)\|+\|f_2(t,\phi_1)-f_2(t,\phi_2)\|+\|f_3(t,\phi_1)-f_3(t,\phi_2)\|\\ &+\|f_4(t,\phi_1)-f_4(t,\phi_2)\|+\|f_5(t,\phi_1)-f_5(t,\phi_2)\|+\|f_6(t,\phi_1)-f_6(t,\phi_2)\|\\ &+\|f_7(t,\phi_1)-f_7(t,\phi_2)\|+\|f_8(t,\phi_1)-f_8(t,\phi_2)\|+\|f_9(t,\phi_1)-f_9(t,\phi_2)\|\\ &\leq M_1\|S_c-\overline{S}_c\|+M_2\|V_c-\overline{V}_c\|+M_3\|I_c-\overline{I}_c\|+M_4\|R_c-\overline{R}_c\|+M_5\|S_h-\overline{S}_h\|\\ &+M_6\|E_h-\overline{E}_h\|+M_7\|I_h-\overline{I}_h\|+M_8\|R_h-\overline{R}_h\|+M_9\|L-\overline{L}\|\end{aligned}$$

where $M_1=\|(\beta_{cc}\|I_c\|+\frac{\beta_c\|L\|}{K+\|L\|}+\tau_c+\mu_c)\|$, $M_2=\|((1-r)(\beta_{cc}\|I_c\|+\frac{\beta_c\|L\|}{K+\|L\|})+\eta_c+\mu_c)\|$, $M_3=\|(\sigma_c+\mu_c+d_c)\|$, $M_4=\|(\gamma_c+\mu_c)\|$, $M_5=\|(\beta_{hc}\|I_c\|+\frac{\beta_h\|L\|}{K+\|L\|}+\mu_h)\|$, $M_6=\|(\alpha_h+\mu_h)\|$, $M_7=\|(\delta_h+\mu_h+d_h)\|$, $M_8=\|(\gamma_h+\mu_h)\|$, and $M_9=\|\varepsilon\|$, which yields
$\|f(t,\phi_1)-f(t,\phi_2)\|\leq M\|\phi_1-\phi_2\|$, where $M=\max\{M_1,M_2,M_3,M_4,M_5,M_6,M_7,M_8,M_9\}$. The Lipschitz's condition is thus satisfied by $f(t,\phi(t))$, confirming that the fractional dynamical

system (6.1) has a unique solution $\phi(t)$ with the initial data $\phi(0)$. □

6.2.2 Boundedness and Positivity of Solution

Theorem 6.2.2. The fractional dynamical system (6.1) has a biologically feasible region Ω_{ch} $\forall t > 0$, where

$$\Omega_{ch} = \left\{ (S_c, V_c, I_c, R_c, S_h, E_h, I_h, R_h, L) \in \mathbb{R}^9_+ : N_c \leq \frac{\Lambda_c}{\mu_c}, N_h \leq \frac{\Lambda_h}{\mu_h} \text{ and } L \leq \frac{\Lambda_c \omega_c}{\mu_c \varepsilon} + \frac{\Lambda_h \omega_h}{\mu_h \varepsilon} \right\}$$

Proof. The total cattle population is given by

$$N_c(t) = S_c(t) + V_c(t) + I_c(t) + R_c(t)$$

For $\psi \in (0,1]$, taking CFD and substituting the values of Eq. (6.1), we obtain

$${}^{C}_{0}D^{\psi}_{t} N_c(t) = \Lambda_c - \mu_h N_c(t) - d_c I_c.$$

If $N_c(0) \geq \frac{\Lambda_c}{\mu_c}$, then ${}^{C}_{0}D^{\psi}_{t} N_c(t) \leq 0$ and applying the Laplace transform (A.8.7) of Eq. (6.1), we obtain

$$\mathscr{L}\left[{}^{C}_{0}D^{\psi}_{t} N_c(t) + \mu_c N_c(t) \right] = \mathscr{L}(\Lambda_c)$$

$$\implies s^{\psi}\mathscr{L}(N_c(t)) - s^{\psi-1}(N_c(0)) + \mu_c \mathscr{L}(N_c(t)) = \frac{\Lambda_c}{s^{\psi}}$$

$$\implies (\mu_c + s^{\psi})\mathscr{L}(N_c(t)) = \left[\frac{\Lambda_c}{s^{\psi}} + s^{\psi-1}(N_c(0)) \right].$$

$$\implies \mathscr{L}(N_c(t)) \leq \left[\frac{\Lambda_c}{s^{\psi}(\mu_c + s^{\psi})} + \frac{s^{\psi-1}}{(\mu_c + s^{\psi})}(N_c(0)) \right]. \tag{6.2}$$

Applying the inverse Laplace transform of Eq. (6.2), we have

$$N_c(t) \leq \Lambda_c t^{\psi} E_{\psi,\psi+1}(-\mu_c t^{\psi}) + N_c(0) E_{\psi,1}(-\mu_c t^{\psi}). \tag{6.3}$$

Using the property of Mittag-Leffler function (A.12) on Eq. (6.3), we obtain

$$N_c(t) \leq \frac{\Lambda_c}{\mu_c}\left[E_{\psi,1}(-\mu_c t^{\psi}) + t^{\psi} E_{\psi,\psi+1}(-\mu_c t^{\psi}) \right] = \frac{\Lambda_c}{\mu_c}.$$

Hence, for the cattle population the invariant region is given by

$$\Omega_c = \left\{ (S_c, V_c, I_c, R_c) \in \mathbb{R}^4_+ \middle| N_c(t) \leq \frac{\Lambda_c}{\mu_c} \right\}.$$

Similarly, for human population

$$N_h(t) \leq \frac{\Lambda_h}{\mu_h}.$$

with invariant region given by

$$\Omega_h = \left\{ (S_h, E_h, I_h, R_h) \in \mathbb{R}^4_+ \middle| N_h(t) \leq \frac{\Lambda_h}{\mu_h} \right\}.$$

and, for free-*Leptospira* population

$$L(t) \leq \frac{\Lambda_c \omega_c}{\mu_c \varepsilon} + \frac{\Lambda_h \omega_h}{\mu_h \varepsilon}.$$

with invariant region given by

$$\Omega_L = \left\{ L \in \mathbb{R}_+ \middle| L(t) \leq \frac{\Lambda_c \omega_c}{\mu_c \varepsilon} + \frac{\Lambda_h \omega_h}{\mu_h \varepsilon} \right\}.$$

Taking the product of invariant regions for the cattle, human, and *Leptospira* population at any time, which is then given by

$$\begin{aligned} \Omega_{ch} &= \Omega_c \times \Omega_h \times \Omega_L \subset \mathbb{R}^4_+ \times \mathbb{R}^4_+ \times \mathbb{R}_+ \\ &= \left\{ (S_c, V_c, I_c, R_c, S_h, E_h, I_h, R_h, L) \in \mathbb{R}^9_+ : N_c \leq \frac{\Lambda_c}{\mu_c},\ N_h \leq \frac{\Lambda_h}{\mu_h} \text{ and } L \leq \frac{\Lambda_c \omega_c}{\mu_c \varepsilon} + \frac{\Lambda_h \omega_h}{\mu_h \varepsilon} \right\} \end{aligned}$$

Showing the biologically feasible region for the system (6.1). This completes the proof.

□

Theorem 6.2.3. The solution of system (6.1), which is $X(t) = (S_c(t), I_c(t), R_c(t), S_h(t), E_h(t), I_h(t), R_h(t), L(t))$ is always non-negative $\forall t > 0$ provided that the initial value $X(0)$ is non-negative.

Proof. In order to prove positivity, it needs to be established that the system (6.1) fulfills the following condition on $\mathbb{R}^9_+$:

$$
\begin{cases}
{}_0^C D_t^{\Psi} S_c = (1-\rho)\Lambda_c + \gamma_c R_c + \eta_c V_c \geq 0, \\
{}_0^C D_t^{\Psi} V_c = \rho\Lambda_c + \tau_c S_c \geq 0 \\
{}_0^C D_t^{\Psi} I_c = \lambda_c [S_c + (1-r)V_c] \geq 0 \\
{}_0^C D_t^{\Psi} R_c = \sigma_c I_c \geq 0 \\
{}_0^C D_t^{\Psi} S_h = \Lambda_h + \gamma_h R_h \geq 0 \\
{}_0^C D_t^{\Psi} E_h = \lambda_h S_h \geq 0 \\
{}_0^C D_t^{\Psi} I_h = \alpha_h E_h \geq 0 \\
{}_0^C D_t^{\Psi} R_h = \delta_h I_h \geq 0 \\
{}_0^C D_t^{\Psi} L = \omega_c I_c + \omega_h I_h \geq 0
\end{cases}
$$

Lemma 1 states that the solution remains within Ω_{ch} since the desired target set has been effectively reached. This implies that the solution of the system (6.1) is bounded because all terms in the sum are positive. □

6.3 Stability Analysis

This section will identify the equilibria of model (6.1) and identify the effective reproduction number. The model's equilibria will then be subjected to evaluation of both local and global stability. We first calculate the effective reproduction number of system (6.1) before looking at the linear stability of the equilibria. The effective reproduction number, which is determined using the next-generation matrix technique and the *Leptospira*-free equilibrium (LFE), quantifies the possibility for transmission of any infectious disease.

To calculate LFE, we set the right hand side of system (6.1) equal to zero and solve the system obtained. Thus, the *Leptospira*-free equilibrium point,
$\mathscr{E}^* = (S_c^*, V_c^*, I_c^*, R_c^*, S_h^*, E_h^*, I_h^*, R_h^*, L^*)$, of model (6.1) is given by

$$
\mathscr{E}^* = \left(\frac{\Lambda_c(\eta_c + (1-\rho)\mu_c)}{\mu_c(\eta_c + \tau_c + \mu_c)}, \frac{\Lambda_c(\tau_c + \rho\mu_c)}{\mu_c(\eta_c + \tau_c + \mu_c)}, 0, 0, \frac{\Lambda_h}{\mu_h}, 0, 0, 0, 0 \right) \tag{6.4}
$$

Here we used the next-generation matrix method to derive the effective reproduction number from integer-order model structure (Van den Driessche & Watmough, 2002). We made the implicit assumption that this dimensionless quantity remains a valid threshold value applicable to Caputo fractional-order models, provided the model retains a positive invariant set and satisfies standard assumptions for equilibrium analysis (Agbata et al., 2025). Hence, applying the next-generation matrix technique and establishing the matrices F and V, which represent

the new infection factors and the transfer factors, respectively, at the LFE point (6.4). Re-write $k_1 = \sigma_c + \mu_c + d_c$, $k_2 = \alpha_h + \mu_h$, and $k_3 = \delta_h + \mu_h + d_h$ for convenience. Consequently, we have

$$F = \begin{bmatrix} \beta_{cc}P_c^* & 0 & 0 & \beta_c P_c^*/K \\ \beta_{hc}S_h^* & 0 & 0 & \beta_h S_h^*/K \\ 0 & 0 & 0 & 0 \\ 0 & 0 & 0 & 0 \end{bmatrix}, \text{and } V = \begin{bmatrix} k_1 & 0 & 0 & 0 \\ 0 & k_2 & 0 & 0 \\ 0 & -\alpha_h & k_3 & 0 \\ -\omega_c & 0 & -\omega_h & \varepsilon \end{bmatrix},$$

where, $P_c^* = [S_c^* + (1-r)V_c^*]$, $S_c^* = \dfrac{\Lambda_c(\eta_c + (1-\rho)\mu_c)}{\mu_c(\eta_c + \tau_c + \mu_c)}$, $V_c^* = \dfrac{\Lambda_c(\tau_c + \rho\mu_c)}{\mu_c(\eta_c + \tau_c + \mu_c)}$, and $S_h^* = \frac{\Lambda_h}{\mu_h}$. Since F is Metzler matrix and V is invertible matrix. Thus, V^{-1} is given by

$$V^{-1} = \begin{pmatrix} \frac{1}{k_1} & 0 & 0 & 0 \\ 0 & \frac{1}{k_2} & 0 & 0 \\ 0 & \frac{\alpha_h}{k_1 k_2} & \frac{1}{k_3} & 0 \\ \frac{-\omega_c}{k_1\varepsilon} & \frac{\alpha_h\omega_h}{k_2 k_3 \varepsilon} & \frac{-\omega_h}{k_3\varepsilon} & \frac{1}{\varepsilon} \end{pmatrix}.$$

The next-generation matrix is hence computed as

$$FV^{-1} = \begin{pmatrix} (\frac{\beta_{cc}P_c^*}{k_1} - \frac{\omega_c\beta_c P_c^*}{Kk_1\varepsilon}) & \frac{\omega_h\alpha_h\beta_c P_c^*}{Kk_2k_3\varepsilon} & \frac{-\omega_h\beta_c P_c^*}{Kk_3\varepsilon} & \frac{\beta_c P_c^*}{K\varepsilon} \\ \frac{\beta_{hc}S_h^*}{k_1} - \frac{\omega_c\beta_h S_h^*}{Kk_1\varepsilon} & \frac{\omega_h\alpha_h\beta_h S_h^*}{Kk_2k_3\varepsilon} & \frac{-\omega_h\beta_h S_h^*}{Kk_3\varepsilon} & \frac{\beta_h S_h^*}{K\varepsilon} \\ 0 & 0 & 0 & 0 \\ 0 & 0 & 0 & 0 \end{pmatrix}. \tag{6.5}$$

The dominant eigenvalue $\rho(FV^{-1})$ of Eq. (6.5), defined as the effective reproduction number $\mathscr{R}_e$, is given by:

$$\mathscr{R}_e = \frac{1}{2}\left[(\frac{\beta_{cc}P_c^*}{k_1} - \frac{\omega_c\beta_c P_c^*}{Kk_1\varepsilon} + \frac{\omega_h\alpha_h\beta_h S_h^*}{Kk_2k_3\varepsilon}) + \sqrt{\left(\frac{\beta_{cc}P_c^*}{k_1} - \frac{\omega_c\beta_c P_c^*}{Kk_1\varepsilon} - \frac{\omega_h\alpha_h\beta_h S_h^*}{Kk_2k_3\varepsilon}\right)^2 + 4\left(\frac{\omega_h\alpha_h\beta_c P_c^*}{Kk_2k_3\varepsilon}\right)\left(\frac{\beta_{hc}S_h^*}{k_1} - \frac{\omega_c\beta_h S_h^*}{Kk_1\varepsilon}\right)}\right]. \tag{6.6}$$

The other type of equilibrium point of the model (6.1) is the *Leptospira*-persistent equilibrium (LPE). To find LPE we set Eq. (6.1) to zero with at least one of the infectious classes should be nonzero. If $\mathscr{E}^{**} = (S_c^{**}, V_c^{**}, I_c^{**}, R_c^{**}, S_h^{**}, E_h^{**}, I_h^{**}, R_h^{**}, L^{**})$ is LPE point, it is implicitly given by,

$$
\begin{aligned}
S_c^{**} &= \frac{[(1-\rho)\mu_c+\eta_c]\Lambda_c+[(\mu_c+\eta_c)]\gamma_c R_c^{**}-k_1\eta_c I_c^{**}}{\mu_c(\lambda_c^{**}+\tau_c+\mu_c)+\eta_c},\\
V_c^{**} &= \frac{\Lambda_c-k_1 I_c^{**}+\gamma_c R_c^{**}}{\mu_c}-S_c^{**},\\
R_c^{**} &= \frac{\sigma_c I_c^{**}}{k_5},\\
S_h^{**} &= \frac{k_2}{\lambda_h^{**}}E_h^{**},\\
E_h^{**} &= \frac{k_3}{\alpha_h}I_h^{**},\\
R_h^{**} &= \frac{\delta_h}{k_4}I_h^{**},\\
L^{**} &= \frac{\omega_c I_c^{**}+\omega_h I_h^{**}}{\varepsilon},
\end{aligned}
\tag{6.7}
$$

where,

$\lambda_c^{**}=\beta_{cc}I_c^{**}+\frac{\beta_c L^{**}}{K+L^{**}}$, $\lambda_h^{**}=\beta_{hc}I_c^{**}+\frac{\beta_h L^{**}}{K+L^{**}}$, $k_1=\sigma_c+\mu_c+d_c$,
$k_2=\alpha_h+\mu_h$, $k_3=\delta_h+\mu_h+d_h$, $k_4=\gamma_h+\mu_h$, $k_5=\gamma_c+\mu_c$.

Theorem 6.3.1. The *Leptospira*-persistent equilibrium $\mathscr{E}^{**}$ of model (6.1) is globally asymptotically stable if $\mathscr{R}_e>1$.

Proof. We adopt a multi-step approach integrating linear stability theory, fractional Lyapunov analysis, and numerical validation.

Step 1: Local Stability via Matignon's Criterion

We linearize the system near $\mathbf{x}^*=\mathscr{E}^{**}$:

$$
{}^{C}D_t^{\psi}y(t)=J(\mathbf{x}^{**})y(t)+g(\mathbf{y}(t)),
$$

where $\mathbf{y}(t)=\mathbf{x}(t)-\mathbf{x}^{**}$, $J(\mathbf{x}^{**})$ denotes the Jacobian matrix at equilibrium, and g contains higher-order nonlinear terms.

Let λ_i be the eigenvalues of $J(\mathbf{x}^{**})$. By Matignon's theorem, the linearized system is locally asymptotically stable if:

$$
|\arg(\lambda_i)|>\frac{\psi\pi}{2},\quad \text{for all } i=1,\ldots,9.
$$

Numerical evaluation with parameters from Table 6.2 confirms that this condition holds when $\mathscr{R}_e>1$.

Step 2: Lyapunov Function Construction

Consider the quadratic Lyapunov candidate:

$$V(\mathbf{y}) = \frac{1}{2}\|\mathbf{y}\|^2 = \frac{1}{2}\sum_{i=1}^{9} y_i^2.$$

Due to the non-local nature of fractional derivatives, we invoke lemma 2 and there exist a constant $K(\psi) > 0$ such that:

$${}^{C}D_t^{\psi} V(\mathbf{y}(t)) \leq \sum_{i=1}^{n} y_i(t) \cdot {}^{C}D_t^{\psi} y_i(t) + K(\psi)\|y(t)\|^2.$$

Step 3: Evaluation of the Lyapunov Derivative

Using the system dynamics, we compute:
$\sum_{i=1}^{9} y_i \cdot {}^{C}D_t^{\psi} y_i = y_1\left[(1-\rho)\Lambda_c - \lambda_c S_c + \gamma_c R_c + \eta_c V_c - \tau_c S_c - \mu_c S_c\right]$
$+ y_2\left[\rho\Lambda_c - (1-r)\lambda_c V_c + \tau_c S_c - \eta_c V_c - \mu_c V_c\right] + \cdots + y_9\left[\omega_c I_c + \omega_h I_h - \varepsilon L\right].$

Step 4: Application of Equilibrium Conditions

At $\mathscr{E}^{**}$, the following hold:

$$(1-\rho)\Lambda_c + \gamma_c R_c^{**} + \eta_c V_c^{**} = (\lambda_c^{**} + \tau_c + \mu_c)S_c^{**}, \quad \rho\Lambda_c + \tau_c S_c^{**} = ((1-r)\lambda_c^{**} + \eta_c + \mu_c)V_c^{**}, \quad \cdots$$

Substituting these into the derivative expression and simplifying yields:

$$\sum_{i=1}^{9} y_i \cdot {}^{C}D_t^{\psi} y_i \leq -\sum_{i=1}^{9} c_i y_i^2 + \mathcal{R}(\mathbf{y}),$$

where $c_i > 0$ and $\mathcal{R}(\mathbf{y})$ denotes bounded cross terms.

Step 5: Bounding Cross Terms

Applying Yong's inequality:

$$|y_i y_j| \leq \frac{\varepsilon}{2} y_i^2 + \frac{1}{2\varepsilon} y_j^2$$

we bound $\mathcal{R}(\mathbf{y})$ and absorb in to the main negative definite term. Thus using Lemma 2

$${}^{C}D_t^{\psi} V(\mathbf{y}(t)) \leq -c\|y\|^2,$$

for some $c > 0$

Step 6: Numerical Validation

To complement the analytical approach, we perform simulations using the fractional Adams-Bashforth-Moulton method. Key observations from Figure 6.2 include:

- All trajectories from diverse initial conditions converge to a Leptospira-persistent equilibrium point, i.e., $\mathscr{E}^{**} = (65.8, 127.9, 9.12, 11.8, 60933.8, 3330.1, 4229.8, 3420.1, 848.5)$.
- The convergence speed demonstrated dependence on the fractional order ψ.
- The hereditary properties of the Caputo operator captured the unique epidemiological features of leptospirosis, such as asymptomatic carriers, environmental persistence, multi-host transmission, and relapse behavior, that make its dynamics strongly dependent on past states.

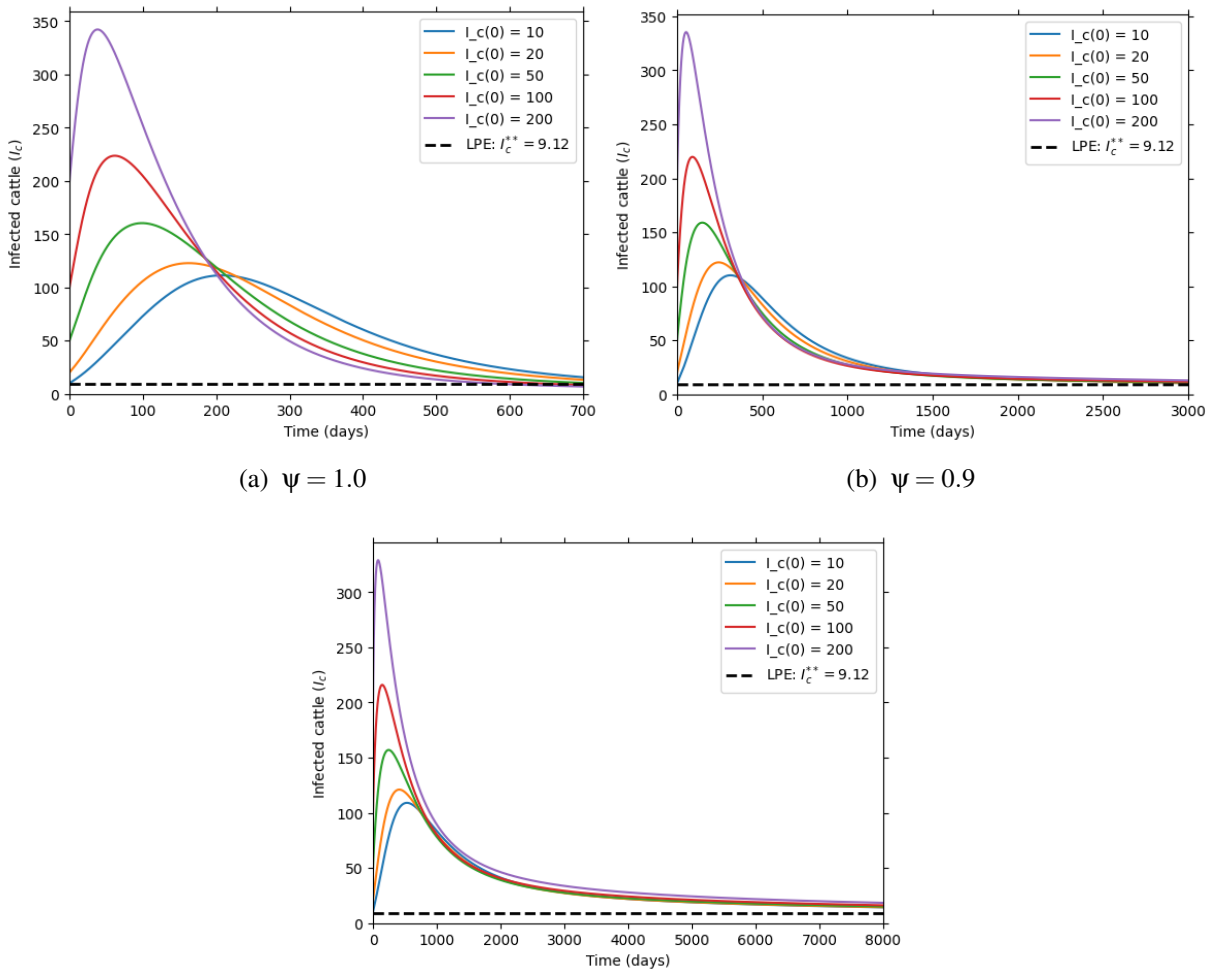

(a) $\psi = 1.0$

(b) $\psi = 0.9$

(c) $\psi = 0.8$

Figure 6.2: Global stability of *Leptospira*-Persistent Equilibrium point

□

Table 6.2: Parameters values and their sources

Parameter	Value	Unit	Source
Λ_c	0.15	$\frac{cattle}{day}$	Assumed
Λ_h	5	$\frac{human}{day}$	Assumed
ρ	0.5		Assumed
K	1000	*unit*	Holt et al. (2006)
β_{cc}	0.0001	$\frac{1}{(cattle)(day)}$	Aslan et al. (2021)
β_{hc}	0.0003	$\frac{1}{(human)(day)}$	Assumed
β_c	0.0012	$\frac{1}{day}$	Aslan et al. (2021)
β_h	0.005	$\frac{1}{day}$	Assumed
α_h	0.092	$\frac{1}{day}$	Oguntolu et al. (2024)
δ_h	0.072	$\frac{1}{day}$	Engida et al. (2022)
σ_c	0.00274	$\frac{1}{day}$	Aslan et al. (2021)
μ_c	0.000274	$\frac{1}{day}$	Ndondo et al. (2016)
μ_h	0.000046	$\frac{1}{day}$	Ngoma et al. (2022); Okosun et al. (2016)
d_c	0.01	$\frac{1}{day}$	Holt et al. (2006)
d_h	0.0004	$\frac{1}{day}$	Oguntolu et al. (2024)
ε	0.05	$\frac{1}{day}$	Minter et al. (2019)
ω_c	0.014	$\frac{unit}{(cattle)(day)}$	Aslan et al. (2021)
ω_h	0.01	$\frac{unit}{(human)(day)}$	Assumed
η_c	0.013	$\frac{1}{day}$	Okosun et al. (2016)
r	0.88		Esteves et al. (2022); Wilson-Welder et al. (2020)
τ_c	0.025	$\frac{1}{day}$	Assumed
γ_c	0.00185	$\frac{1}{day}$	Chadsuthi et al. (2022)
γ_h	0.089	$\frac{1}{day}$	Khan et al. (2014); Oguntolu et al. (2024)

6.4 Sensitivity Analysis

The sensitivity analysis determines the resilience of the model prediction to changes in parameter values due to potential errors in data collection and assumed parameters. For this study, we applied normalized forward sensitivity indices presented in Definition A.5.1. $\mathscr{R}_e$ is directly (inversely) impacted by the relevant parameter when the index value is positive (or negative). Definition A.5.1 gives the formulas for the normalized forward sensitivity index for the model's primary parameters:

Table 6.3: Sensitivity of the parameters

Parameters	Value	Sensitivity index
Λ_c	0.15	+0.5583
Λ_h	5	+0.4417
ρ	0.5	-0.0042
K	1000	-0.4396
β_{cc}	0.0001	+0.3552
β_{hc}	0.0003	+0.4095
β_c	0.0012	+0.0012
β_h	0.005	+0.2365
α_h	0.092	+0.2043
δ_h	0.072	-0.6420
σ_c	0.00274	-0.1175
μ_c	0.000274	-0.5687
μ_h	0.000046	-0.4422
d_c	0.01	-0.4290
d_h	0.0004	-0.0036
ε	0.05	-0.4396
ω_c	0.014	+0.0022
ω_h	0.01	+0.4417
η_c	0.013	+0.2597
r	0.88	-0.7645
τ_c	0.025	-0.2610

As a result, we used the values in Table 6.2 to quantitatively evaluate the sensitivity index of $\mathscr{R}_e$ with regard to each model parameters. Vaccine efficiency, r, human recovery rate, δ_h, cattle recruitment rate, Λ_c, and contact rate of human with infectious cattle, β_{hc}, are the most sensitive parameters, respectively. For instance, if β_{hc} increases by 10%, $\mathscr{R}_e$ increases (or decreases) by 4.1%, and if μ_c increases or decreases by 10%, $\mathscr{R}_e$ decreases (or increases) by 5.7%. In conclusion, the sensitivity analysis of the most influential parameters affecting $\mathscr{R}_e$ are summarized in Table 6.3.

6.5 Results and Discussions

In this section, we have performed numerical simulations of system (6.1) using python program and the fractional Adams-Bashforth-Moulton predictor-evaluator-corrector-evaluator (PECE) algorithm developed in Diethelm et al. (2004); Diethelm & Freed (1998) to support the analytical conclusions of our model.

The effectiveness of the obtained theoretical outcomes are established by the following ex-

amples. The initial conditions are chosen as $(S_c(0), V_c(0), I_c(0), R_c(0), S_h(0), E_h(0), I_h(0), R_h(0), L(0)) = (500, 100, 20, 0, 100000, 1000, 100, 0, 100)$ and the fractional values $\psi = [1.00, 0.95, 0.90, 0.85, 0.80]$ were used to study the effect of the fractional-order on our model. Accordingly, Figure 6.3 represents the dynamics of susceptible, vaccinated, infected and recovered cattle respectively with the change of fractional order. Then, Figure 6.4 describes the impact of susceptible, exposed, infected and recovered human population respectively with the change of fractional order. Finally, Figure 6.5 shows the impact of *Leptospira* load in the environment with the change of fractional order. In each of these figures, as the order of the derivative takes smaller fractional values, the system experiences slow dynamics which inline with the result of Farman et al. (2023). The rate of convergence toward the equilibrium points is more for higher-order derivatives in comparison to the smaller-order derivatives. Thus, to achieve faster convergence toward an equilibrium point, a higher-order system should be considered or the vice-verse. Therefore, the consideration of different fractional orders provides valuable insights into the model's behavior, highlighting its variability and sensitivity to changes in the ordering.

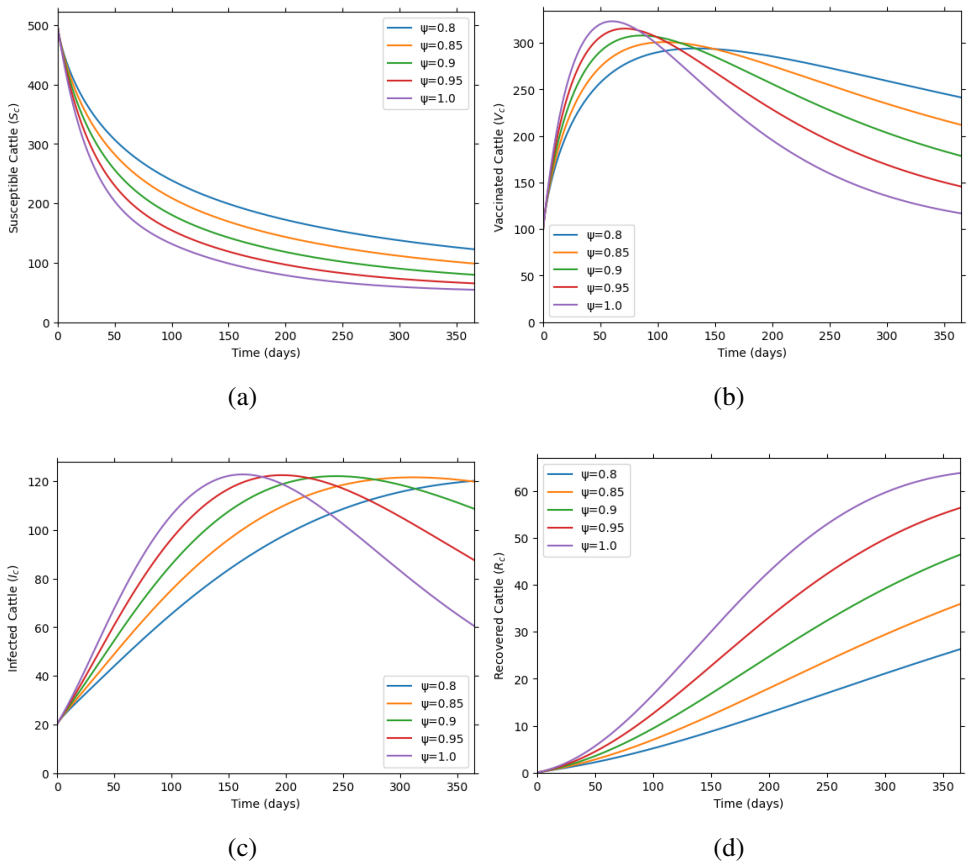

Figure 6.3: Impact of ψ on cattle population (**a**) S_c, (**b**) V_c, (**c**) I_c, and (**d**) R_c, for $\mathscr{R}_e = 2.7904$ using values in Table 6.2.

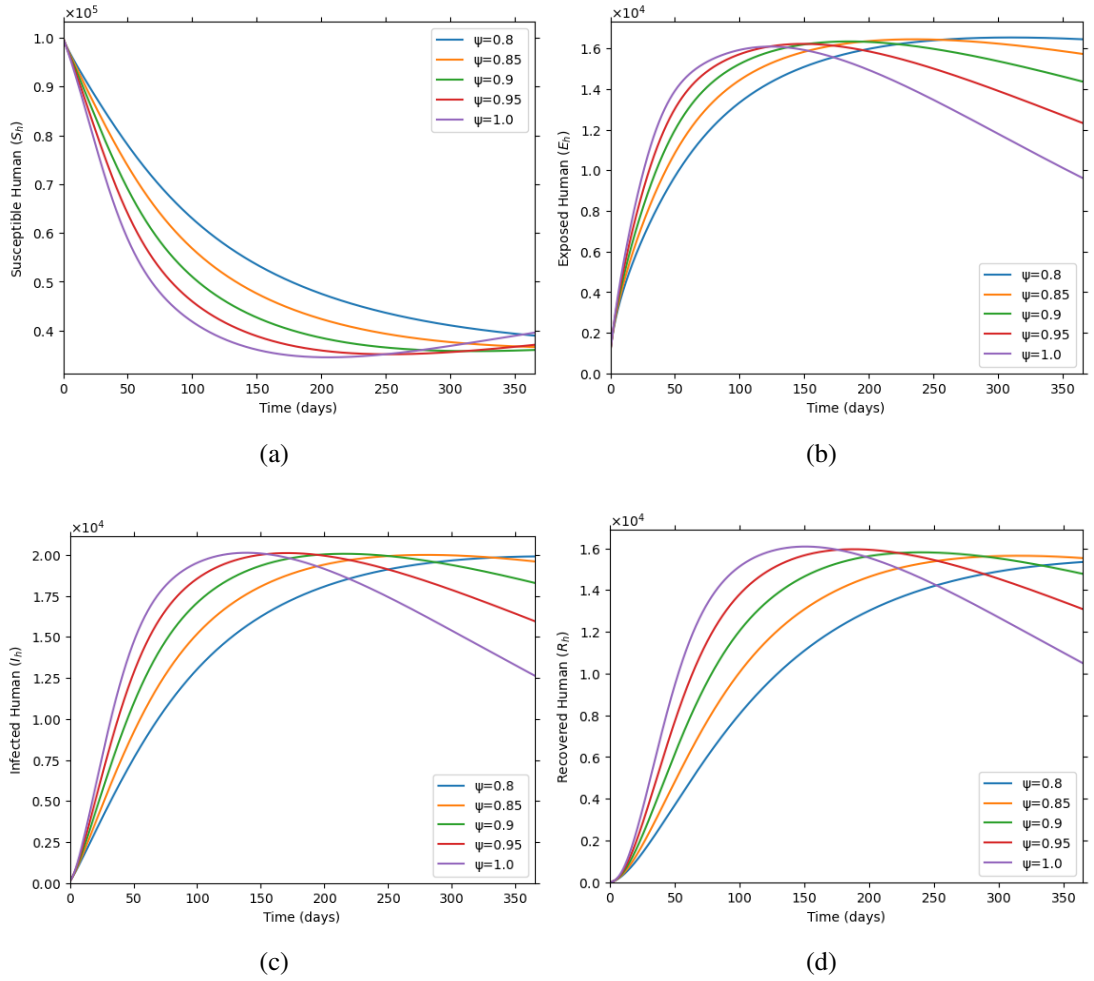

Figure 6.4: Impact of ψ on human population, (**a**) S_h, (**b**) E_h, (**c**) I_h, and (**d**) R_h, for $\mathscr{R}_e = 2.7904$ using values in Table 6.2.

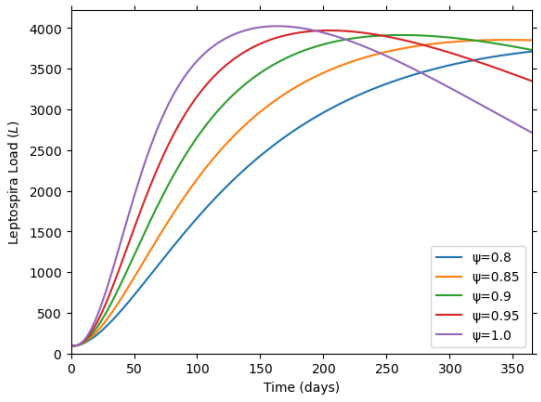

Figure 6.5: Impact of ψ on leptospiral load L, for $\mathscr{R}_e = 2.7904$ using values in Table 6.2.

6.5.1 Impact of Varying Cattle to Cattle Transmission Coefficient, β_{cc}.

In this subsection, we examined the impact of varying cattle-to-cattle transmission coefficient, β_{cc}, on the number of infected cattle, infected humans, and environmental leptospiral load for $\psi = 1$ and $\psi = 0.9$. From the sensitivity analysis in section 6.4, we observed that the parameter β_{cc} has a positive sensitivity index, meaning it is directly proportional to the effective reproduction number, $\mathscr{R}_e$. Figure 6.6 shows the effect of varying β_{cc} on I_C. The graph demonstrates that as we decrease the the contact rate from 0.0003 to 0.00005, the maximum infected population significantly reduced from 300 to 50. Moreover, in Figure 6.6(b) for $\psi = 1$ the graph dropped fastly but in Figure 6.6(a) for $\psi = 0.9$ it dropped slowly because of memory effect. Similarly, Figure 6.7 depicts that the infected human population is also reduced well by the reduction of β_{cc}. This shows that controlling cattle-to-cattle control is indirectly controlling transmission of leptospirosis to farmers, veterinarians and other stockholders. Also Figure 6.8 demonstrates the significant reduction of environmental leptospiral load by the reduction of β_{cc}. Controlling *Leptospira* in soil and water could help the possible occurrence of leptospirosis outbreak through flood.

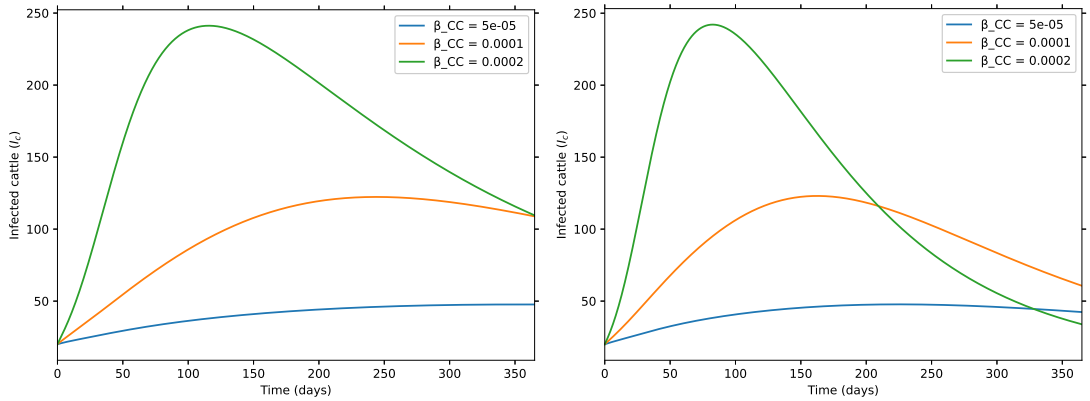

(a) $\psi = 0.9$ (b) $\psi = 1.0$

Figure 6.6: Impact of varying β_{cc} on infected cattle (I_c).

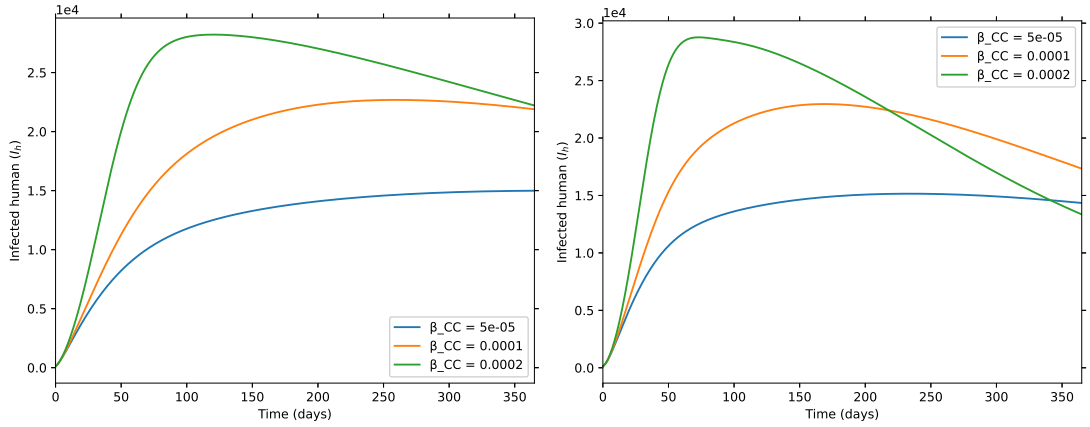

(a) $\psi = 0.9$ (b) $\psi = 1.0$

Figure 6.7: Impact of varying β_{cc} on infected human (I_h).

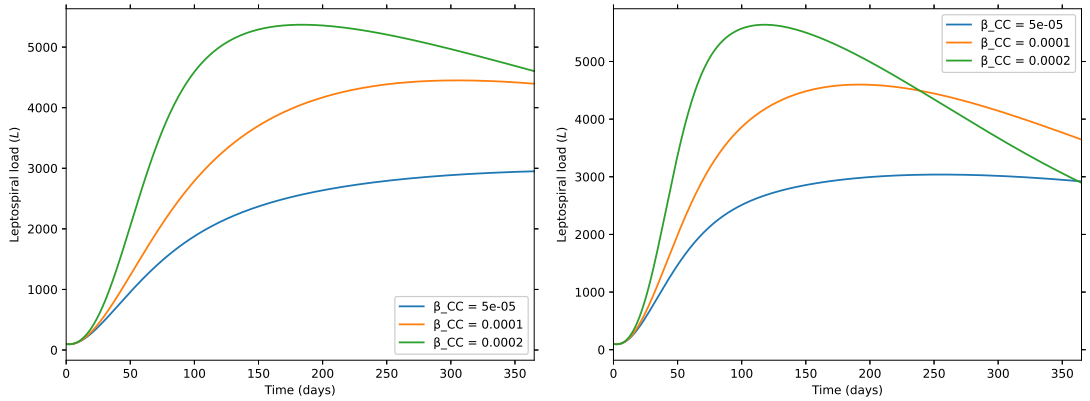

(a) $\psi = 0.9$ (b) $\psi = 1.0$

Figure 6.8: Impact of varying β_{cc} on leptospiral load (L).

6.5.2 Impact of Varying Cattle to Human Transmission Coefficient, β_{ch}

This subsection discuss the impact of varying cattle-to-human transmission coefficient, β_{ch}, on the number of infected cattle, infected humans, and environmental *Leptospira* load. Accordingly, Figure 6.9 shows that I_h decreased slightly by the decrease of β_{ch}. However, Figure 6.10 demonstrates radical drop of infected human, I_h. Figure 6.11 also depicts significant drop of environments *Leptospira* load, L. This shows appropriate preventive measure such as wearing rubber boots, waterproof overalls to cover wounds or skin, goggles, rubber gloves to reduce cattle-to-human direct transmission could be best intervention for human leptospirosis (Engida et al., 2023).

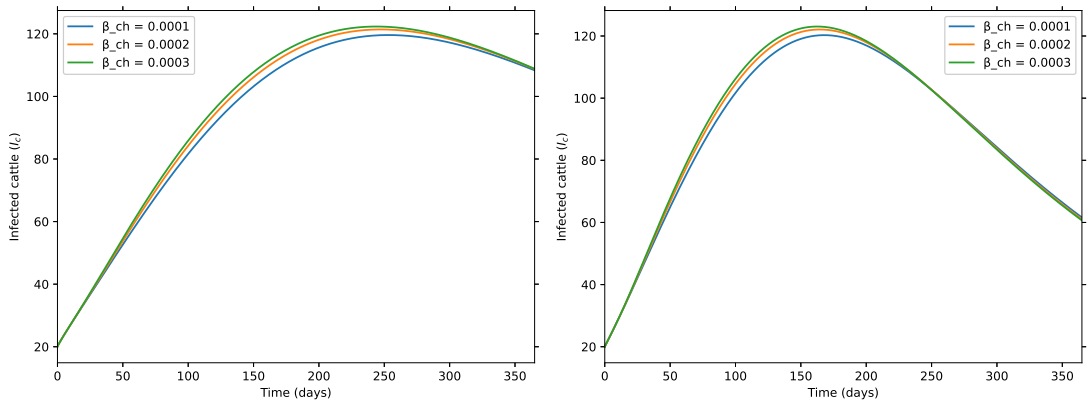

(a) $\psi = 0.9$ (b) $\psi = 1.0$

Figure 6.9: Impact of varying β_{ch} on infected cattle (I_c).

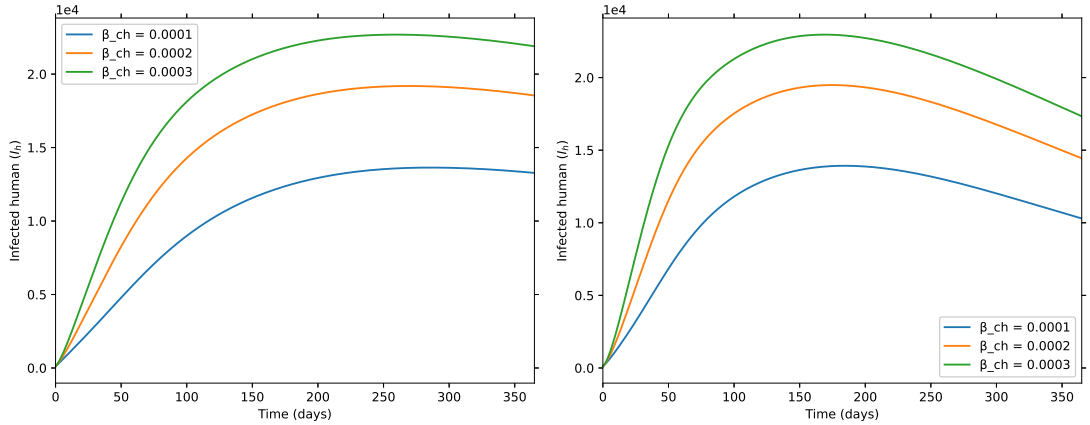

(a) $\psi = 0.9$ (b) $\psi = 1.0$

Figure 6.10: Impact of varying β_{ch} on infected human (I_h).

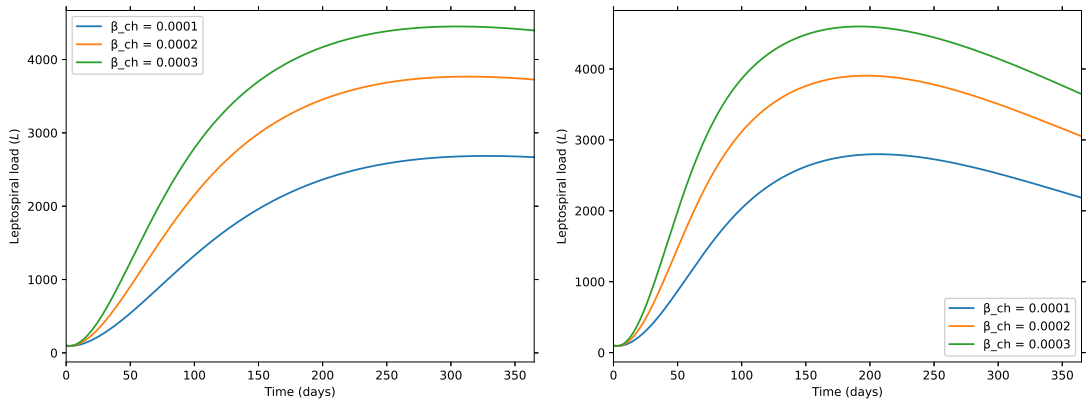

(a) $\psi = 0.9$ (b) $\psi = 1.0$

Figure 6.11: Impact of varying β_{ch} on leptospiral load (L).

6.5.3 Impact of Varying *Leptospira* Decay Rate, ε

Figure 6.12, Figure 6.13, and Figure 6.14 show the decrease in cattle, human, and *Leptospira* populations, respectively, while we increase the *Leptospira* decay rate, ε. The growth of the *Leptospira* pathogen can be reduced through environmental sanitation practices, which involve the clearance of drainage and removal of trash from the surroundings (Oguntolu et al., 2024).

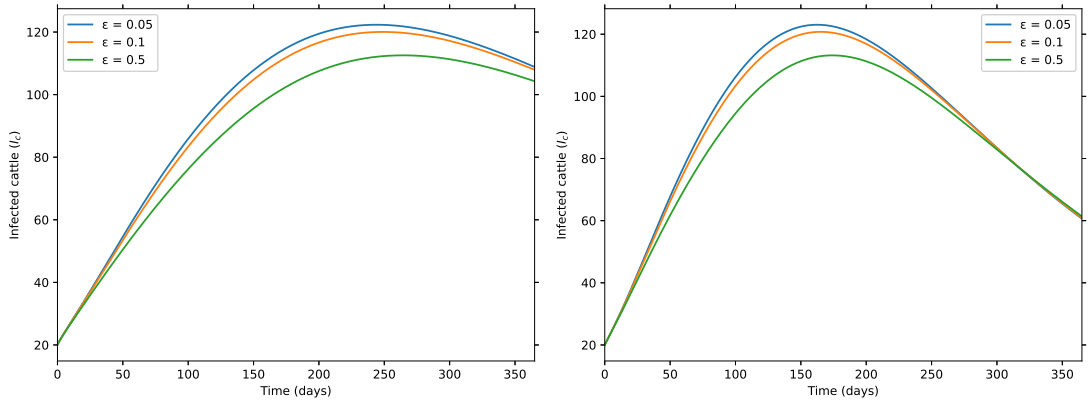

(a) $\psi = 0.9$ (b) $\psi = 1.0$

Figure 6.12: Impact of varying ε on infected cattle (I_c).

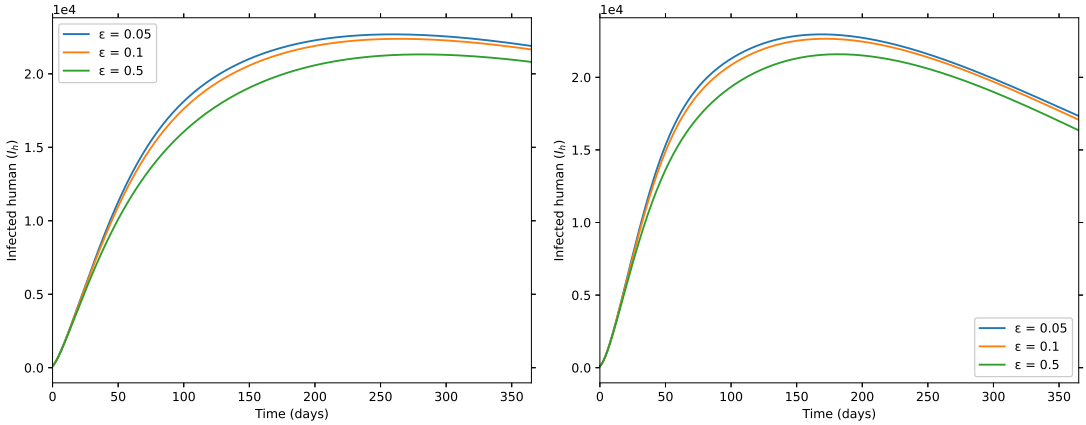

(a) $\psi = 0.9$ (b) $\psi = 1.0$

Figure 6.13: Impact of varying ε on infected human (I_h).

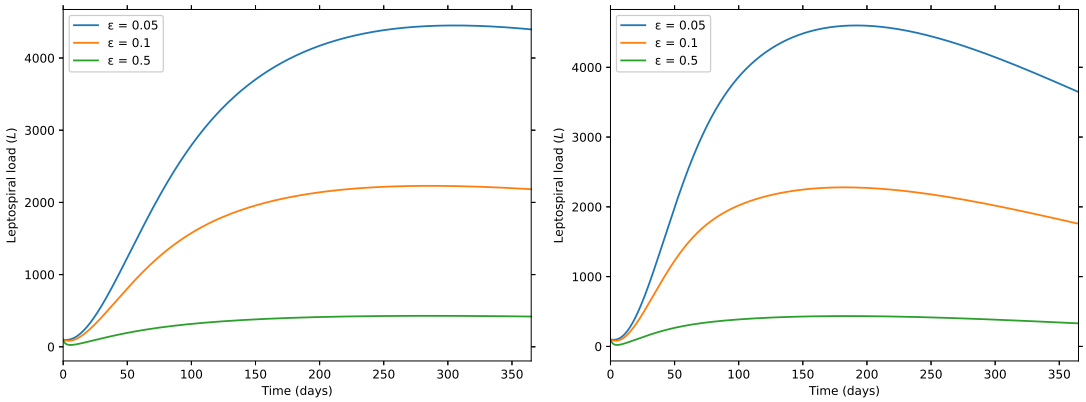

(a) $\psi = 0.9$ (b) $\psi = 1.0$

Figure 6.14: Impact of varying ε on leptospiral load (L).

6.6 Conclusion

In this chapter, a fractional-order leptospirosis disease transmission model is examined to investigate its impact on human beings. The steady-state and fundamental characteristics of the model equilibria are investigated. The existence and uniqueness of solutions for the proposed model are derived. The Lyapunov function is used to analyze global stability. The Adams-Bashforth-Moulton fractional predictor-evaluator-corrector-evaluator (PECE) algorithm in the Python program is used to generate the numerical solution of the model. The graphical outcomes of the proposed fractional model, shown in Figures 6.3-6.5, consistently depend on the fractional order, and it provides valuable and adaptable information for studying the dynamics of

leptospirosis infection. Furthermore, the numerical results of the model (6.1) shown in Figures 6.6-6.14 indicate that leptospirosis infection can be effectively reduced by reducing cattle-to-cattle and cattle-to-human contact rate as well as increasing *Leptospira* decay rate. In all the above simulations, comparisons are made between integer order derivative and fractional order derivative. It is observed that the fractional order method provide reliable findings for all compartment according to steady state at non-integer order derivatives as compare to classical derivative.

CHAPTER 7

SUMMARY, CONCLUSIONS AND RECOMMENDATIONS

This chapter offers a concise overview of the research findings, presents key conclusions, and proposes recommendations based on the study. The dissertation mainly focused on formulating epidemiological mathematical models to enhance understanding of the transmission dynamics of leptospirosis and effective control strategies. The contributions emanating from the findings in this dissertation are summarized and concluded as follows.

7.1 Summary and Conclusion

Leptospirosis poses a significant public health challenge, with a growing incidence in both human and animal populations. The complex interplay between reservoir hosts, environmental factors, and human activities complicates efforts to curb the spread of the disease. Consequently, to give a good insight into the problem, our first model incorporates the role of asymptomatic cattle as well as environmental free-living *Leptospira*. The qualitative and quantitative results shows that the *Leptospira*-free equilibrium point is locally and globally asymptotically stable when $\mathscr{R}_e$ is less than unity and is otherwise unstable. Sensitivity analysis given in Table 4.2 showed that the contact rate with asymptomatic infected cattle, β_A, is the most sensitive parameter in the stated model, followed by the recovery rate of asymptomatic infected cattle, σ, and the vaccination rate of susceptible cattle, τ. Numerical simulations also revealed that a reduction in contact rate with asymptomatic infected cattle, fostering the recovery rate of asymptomatic infected cattle, and augmenting the vaccination rate among susceptible cattle resulted in a notable decrease in disease prevalence within the herd.

Furthermore, we have extended our first model into an optimal control to investigate strategies that minimize the disease burden and related costs. Various simulations of optimal control strategies were performed and graphically shown, both with and without controls. According to the numerical results, applying a combination of prevention, vaccination, and treatment measures could significantly reduce the risk of leptospirosis outbreaks in cattle herds more than the application of a single control measure. However, our cost-effectiveness analysis shows that strategy 2 (vaccination-only) is the most efficient control measure among all intervention strategies in cases of limited resources.

On the other hand, we have formulated and analyzed a mathematical model that takes into account the direct contact within cattle and with rats as well as the indirect transmission via the

environmental free-living *Leptospira*. The stability analysis revealed that the *Leptospira*-free equilibrium point is locally and globally asymptotically stable if $\mathscr{R}_e < 1$ and unstable otherwise. The normalized forward sensitivity index presented in Table 5.3 shows that contact rate within cattle β_{CC}, with rats β_{CR}, rat mortality rate μ_R, and asymptomatic cattle recovery rate σ are the most impactful parameters on the model. Hence, our results show that controlling the rat population by increasing its mortality significantly mitigates disease spread in cattle and humans. Moreover, the simulation results clearly show that the reduction of cattle-to-cattle and cattle-to-rat contact rates, as well as cattle recovery rates through treatment, could significantly reduce the disease spread.

Our final model is dedicated in formulating a fractional order model of leptospirosis. The model analyzes the role of cattle and environmental *Leptospira* load in the transmission of animal and human leptospirosis using a Caputo fractional-order system of differential equations. According to sensitivity analysis conducted on the proposed model, the rate of contact between cattle β_{cc}, the rate of contact between cattle and humans β_{ch}, the rate of recovery of cattle σ_c, the recovery rate of humans δ_h, and the environmental *Leptospira* decay rate ε are the most sensitive parameters. Numerical simulations revealed that a reduction in the rate of contact between cattle and humans, fostering the recovery rate of infected cattle and humans, and maximizing *Leptospira* decay rate resulted in a notable decrease in the prevalence of the disease. Also, the consideration of different fractional orders provides valuable insights into the model's behavior, highlighting its variability and sensitivity to changes in the ordering.

7.2 Recommendations

Leptospirosis, a serious public health concern in Ethiopia and other Sub-Saharan African countries, often remains under-diagnosed. It is a major cause of acute illness, with estimated annual cases reaching over a million and thousands of deaths and significant productivity losses. Here, we want to make some recommendations that might bring positive changes to minimize the prevalence of the diseases. Our study suggests that leptospirosis can be significantly managed in cattle herds by minimizing contact with infected cattle, increasing recovery rate, and enhancing vaccination efforts. Specifically, improved animal husbandry practices such as disinfection of cattle sheds and feeding equipment, quarantine of new cattle before mixing with the herd, regular vaccination, and regular veterinary check-ups and early treatment are efficient methods to manage the disease burden. Additionally, if there are financial limitations to implement all intervention strategies, farmers or ranchers should concentrate on herd vaccination, according to the cost-effectiveness analysis among optimal control strategies (i.e., prevention effort, vaccination, and treatment).

On the other hand, it's crucial to increase rat mortality through trapping or using rodenticide, in careful and ethical manner. Although reducing the rat population can lower the risk of leptospirosis transmission, it's important to consider the potential negative impacts of broad-scale rodent culling. Moreover, our study suggest that leptospirosis can be controlled by implementing environmental sanitation programs that reduce the persistence of *Leptospira* bacteria. This can be done by proper sanitation, improving water quality, controlling flooding and runoff, and using disinfectants for contaminated environments.

Therefore, stakeholders such as farmers, veterinary professionals, and policymakers should prioritize reducing interspecies contact, implementing regular vaccination programs for cattle herds, increasing rodent control efforts, and promoting sanitation measures that accelerate *Leptospira* decay in the environment. In addition, strengthening antibiotic treatment for both humans and animals is essential. Together, these interventions can substantially enhance cattle productivity, lower healthcare costs, and reduce human exposure to leptospirosis.

7.3 Future Works

Although we considered such a comprehensive study of leptospirosis in different species, our study did not cover the effect of weather and temperature variability on the transmission dynamics. We also recognize the significance of validating our model using real data, which represents a limitation of this study stemming from the lack of such data. Future research can incorporate real-world data to validate the proposed models. Further, this dissertation can be extended by considering the following aspects:

- In chapter 5 and chapter 6, it is important to include all the necessary control strategies and their cost-effectiveness analysis;
- The models may give a more realistic result if the impact of temperature and weather variability are considered;
- The co-infection model dynamics can be done by including other livestock diseases, such as brucellosis and Q-fever.

Contribution of the Dissertation

The dissertation reports original results that contribute knowledge to the scientific advancement in mathematics. Two of the contributions were published in peer reviewed journals indexed in Web of Science and Scopus.

Regassa, A.G., Obsu, L.L.(2024). The role of asymptomatic cattle for leptospirosis dynamics in a herd with imperfect vaccination. Sci Rep 14, 23775.

Available at: https://doi.org/10.1038/s41598-024-72613-7

Regassa, A.G., Obsu, L.L., Melese, A.S.(2025). Optimal control of leptospirosis dynamics in cattle herds with cost-effectiveness analysis. Modeling Earth Systems and Environment 11(3), 210

Available at: https://doi.org/10.1007/s40808-025-02380-5

Regassa, A.G., Obsu, L.L., Melese, A.S.(2025). Cattle-rat transmission dynamics of leptospirosis. International Journal of Dynamics and Control. (under review)

Regassa, A.G., Obsu, L.L., Melese, A.S.(2025). Fractional model analysis of leptospirosis in cattle and human. Infectious Disease Modelling. (Submitted)

References

Adler, B. (2014). History of leptospirosis and leptospira. In *Leptospira and leptospirosis* (pp. 1–9). Springer.

Agbata, B. C., Dervishi, R., Agbebaku, D. F., Cenaj, E., Collins, O. C., Ezeafulukwe, A. U., ... Mbah, G. C. E. (2025). A comprehensive analysis of fractional-order model of tuberculosis with treatment intervention. *BMC Infectious Diseases*, *25*(1), 1070.

Alalhareth, F. K., Atta, U., Ali, A. H., Ahmad, A., & Alharbi, M. H. (2023). Analysis of leptospirosis transmission dynamics with environmental effects and bifurcation using fractional-order derivative. *Alexandria Engineering Journal*, *80*, 372–382.

Alemneh, H. T. (2020). A co-infection model of dengue and leptospirosis diseases. *Advances in Difference Equations*, *2020*(1), 664.

Alemu, S. T., Ero, D., & Mor, S. M. (2023). One health insights into pastoralists' perceptions on zoonotic diseases in ethiopia: perspectives from south omo zone of snnp region. *Pastoralism*, *13*(1), 13.

Artiono, R., Prawoto, B. P., Savitri, D., Maulana, D. A., Hamdan, N. I., Latif, N. S. A., & Hadi, N. A. (2024). Mathematical analysis and numerical simulation on free-living leptospira: A mathematical modeling perspective. *European Journal of Pure and Applied Mathematics*, *17*(3), 1637–1658.

Asamoah, J. K. K., Jin, Z., & Sun, G.-Q. (2021). Non-seasonal and seasonal relapse model for q fever disease with comprehensive cost-effectiveness analysis. *Results in Physics*, *22*, 103889.

Asamoah, J. K. K., Oduro, F. T., Bonyah, E., & Seidu, B. (2017). Modelling of rabies transmission dynamics using optimal control analysis. *Journal of Applied Mathematics*, *2017*(1), 2451237.

Asamoah, J. K. K., Okyere, E., Abidemi, A., Moore, S. E., Sun, G.-Q., Jin, Z., ... Gordon, J. F. (2022). Optimal control and comprehensive cost-effectiveness analysis for covid-19. *Results in Physics*, *33*, 105177.

Aslan, I. H., Baca-Carrasco, D., Lenhart, S., & Velasco-Hernandez, J. X. (2021). An age structure model with impulse actions for leptospirosis in livestock cattle. *Journal of Biological Systems*, *29*(01), 75–105.

Aymée, L., Mendes, J., & Lilenbaum, W. (2024). Bovine genital leptospirosis: An update of this important reproductive disease. *Animals*, *14*(2), 322.

Babylon, A., Roberts, M., & Wake, G. (2018). Modelling leptospirosis in livestock. *Theoretical Population Biology*, *121*, 26–32.

Baca-Carrasco, D., Olmos, D., & Barradas, I. (2015). A mathematical model for human and animal leptospirosis. *Journal of Biological Systems*, *23*(supp01), S55–S65.

Baloba, E. B., Seidu, B., & Bornaa, C. S. (2020). Mathematical analysis of the effects of controls on the transmission dynamics of anthrax in both animal and human populations. *Computational and Mathematical Methods in Medicine*, *2020*, 1–14.

Baloba, E. B., Seidu, B., Bornaa, C. S., & Okyere, E. (2023). Optimal control and cost-effectiveness analysis of anthrax epidemic model. *Informatics in Medicine Unlocked*, *42*, 101355.

Barragan, V., Nieto, N., Keim, P., & Pearson, T. (2017). Meta-analysis to estimate the load of leptospira excreted in urine: beyond rats as important sources of transmission in low-income rural communities. *BMC research notes*, *10*, 1–7.

Bautista, J. M., Aranda Estrada, M., Gutiérrez Olvera, L., Lopez Ordaz, R., & Sumano López, H. (2022). Treatment of bovine leptospirosis with enrofloxacin hcl 2h2o (enro-c): A clinical trial. *Animals*, *12*(18), 2358.

Beal, L. D., Hill, D. C., Martin, R. A., & Hedengren, J. D. (2018). Gekko optimization suite. *Processes*, *6*(8), 106.

Bernoulli, D., & Chapelle, D. (2023). Essai d'une nouvelle analyse de la mortalité causée par la petite vérole, et des avantages de l'inoculation pour la prévenir.

Bhalraj, A., & Azmi, A. (2019). Mathematical modelling of the spread of leptospirosis. In *Aip conference proceedings* (Vol. 2184).

Bierque, E., Soupé-Gilbert, M.-E., Thibeaux, R., Girault, D., Guentas, L., & Goarant, C. (2020). Leptospira interrogans retains direct virulence after long starvation in water: E. bierque et al. *Current microbiology*, *77*(10), 3035–3043.

Birkhoff, G., Rota, G.-C., et al. (1989). Ordinary differential equations.

Boey, K., Shiokawa, K., & Rajeev, S. (2019). Leptospira infection in rats: A literature review of global prevalence and distribution. *PLoS neglected tropical diseases*, *13*(8), e0007499.

Bussell, E. H., Dangerfield, C. E., Gilligan, C. A., & Cunniffe, N. J. (2019). Applying optimal control theory to complex epidemiological models to inform real-world disease management. *Philosophical Transactions of the Royal Society B*, *374*(1776), 20180284.

Caley, P., & Ramsey, D. (2001). Estimating disease transmission in wildlife, with emphasis on leptospirosis and bovine tuberculosis in possums, and effects of fertility control. *Journal of Applied Ecology*, 1362–1370.

Caputo, M., & Fabrizio, M. (2015). A new definition of fractional derivative without singular kernel. *Progress in Fractional Differentiation & Applications*, *1*(2), 73–85.

Castillo-Chavez, C. (2002). On the computation of r. and its role on global stability carlos castillo-chavez*, zhilan feng, and wenzhang huang. *Mathematical approaches for emerging and reemerging infectious diseases: an introduction*, *1*, 229.

CDC. (2025). Center for disease control. *https://www.cdc.gov/leptospirosis/pets/index.html*.

Chadsuthi, S., Chalvet-Monfray, K., Kodjo, A., Wiratsudakul, A., & Bicout, D. J. (2022). Modeling of the combined dynamics of leptospirosis transmission and seroconversion in herds. *Scientific Reports*, *12*(1), 15620.

Chadsuthi, S., Chalvet-Monfray, K., Wiratsudakul, A., & Modchang, C. (2021). *The effects of flooding and weather conditions on leptospirosis transmission in thailand. sci. rep. 11, 1486.*

Chakraverty, S., Jena, R. M., & Jena, S. K. (2020). *Time-fractional order biological systems with uncertain parameters* (Vol. 12). Springer.

Chitnis, N., Hyman, J. M., & Cushing, J. M. (2008). Determining important parameters in the spread of malaria through the sensitivity analysis of a mathematical model. *Bulletin of mathematical biology*, *70*, 1272–1296.

Coddington, E. A., & Levinson, N. (1955). *Theory of ordinary differential equations*. McGraw-Hill New York.

Davignon, G., Cagliero, J., Guentas, L., Bierque, E., Genthon, P., Gunkel-Grillon, P., ... others (2023). Leptospirosis: toward a better understanding of the environmental lifestyle of leptospira. *Frontiers in Water*, *5*, 1195094.

Denipitiya, D., Chandrasekharan, N., Abeyewickreme, W., Hartskeerl, R., & Hapugoda, M. (2017). Identification of cattle, buffaloes and rodents as reservoir animals of leptospira in the district of gampaha, sri lanka. *BMC research notes*, *10*, 1–5.

Desa, G., Deneke, Y., Begna, F., & Tolosa, T. (2021). Seroprevalence and associated risk factors of leptospira interrogans serogroup sejroe serovar hardjo in dairy farms in and around jimma town, southwestern ethiopia. *Veterinary Medicine International*, *2021*(1), 6061685.

Descartes, R. (1937). La geometrie, discours de la methode. *Jan Maire, Leiden (1637)*.

De Vries, S. G., Visser, B. J., Nagel, I. M., Goris, M. G., Hartskeerl, R. A., & Grobusch, M. P. (2014). Leptospirosis in sub-saharan africa: a systematic review. *International Journal of Infectious Diseases*, *28*, 47–64.

Diagne, M., Rwezaura, H., Tchoumi, S., & Tchuenche, J. (2021). A mathematical model of covid-19 with vaccination and treatment. *Computational and Mathematical Methods in Medicine*, *2021*(1), 1250129.

Diethelm, K., Ford, N. J., & Freed, A. D. (2004). Detailed error analysis for a fractional adams method. *Numerical algorithms*, *36*(1), 31–52.

Diethelm, K., & Freed, A. D. (1998). The fracpece subroutine for the numerical solution of differential equations of fractional order. *Forschung und wissenschaftliches Rechnen*, *1999*, 57–71.

Engida, H. A., Theuri, D. M., Gathungu, D., Gachohi, J., & Alemneh, H. T. (2022). A mathematical model analysis for the transmission dynamics of leptospirosis disease in human and rodent populations. *Computational and Mathematical Methods in Medicine*, *2022*(1), 1806585.

Engida, H. A., Theuri, D. M., Gathungu, D. K., & Gachohi, J. (2023). Optimal control and cost-effectiveness analysis for leptospirosis epidemic. *Journal of Biological Dynamics*, *17*(1), 2248178.

Esteves, S. B., Santos, C. M., Salgado, F. F., Goncales, A. P., Guilloux, A. G. A., Martins, C. M., ... Miotto, B. A. (2022). Efficacy of commercially available vaccines against canine leptospirosis: A systematic review and meta-analysis. *Vaccine*, *40*(12), 1722–1740.

Falowo, O. D., Olaniyi, S., & Oladipo, A. T. (2023). Optimal control assessment of rift valley fever model with vaccination and environmental sanitation in the presence of treatment delay. *Modeling Earth Systems and Environment*, *9*(1), 457–471.

Farman, M., Jamil, S., Nisar, K. S., & Akgul, A. (2023). Mathematical study of fractal-fractional leptospirosis disease in human and rodent populations dynamical transmission. *Ain Shams Engineering Journal*, 102452.

Fleming, W. H., & Rishel, R. W. (2012). *Deterministic and stochastic optimal control* (Vol. 1). Springer Science & Business Media.

Fraga, T. R., Carvalho, E., Isaac, L., & Barbosa, A. S. (2015). Leptospira and leptospirosis. In *Molecular medical microbiology* (pp. 1973–1990). Elsevier.

Gallego, M. A., & Simoy, M. V. (2021). Mathematical modeling of leptospirosis: A dynamic regulated by environmental carrying capacity. *Chaos, Solitons & Fractals*, *152*, 111425.

Grassly, N. C., & Fraser, C. (2008). Mathematical models of infectious disease transmission. *Nature Reviews Microbiology*, *6*(6), 477–487.

Gronwall, T. H. (1919). Note on the derivatives with respect to a parameter of the solutions of a system of differential equations. *Annals of Mathematics*, *20*(4), 292–296.

Gruber, K. (2021). Preventing zoonotic pandemics: are we there yet? *The Lancet Microbe*, *2*(8), e352.

Hale, J. K. (1969). *Ordinary differential equations*. Wiley-Interscience.

Hartman, P. (1964). *Ordinary differential equations*. John Wiley and Sons.

Hartskeerl, R., Collares-Pereira, M., & Ellis, W. (2011). Emergence, control and re-emerging leptospirosis: dynamics of infection in the changing world. *Clinical microbiology and infection*, *17*(4), 494–501.

Hirsch, M. W., Devaney, R. L., & Smale, S. (1974). *Differential equations, dynamical systems, and linear algebra* (Vol. 60). Academic press.

Hirsch, M. W., Smale, S., & Devaney, R. L. (2012). *Differential equations, dynamical systems, and an introduction to chaos*. Academic press.

Holt, J., Davis, S., & Leirs, H. (2006). A model of leptospirosis infection in an african rodent to determine risk to humans: seasonal fluctuations and the impact of rodent control. *Acta tropica*, *99*(2-3), 218–225.

Igoe, M., Casagrandi, R., Gatto, M., Hoover, C. M., Mari, L., Ngonghala, C. N., ... others (2023). Reframing optimal control problems for infectious disease management in low-income countries. *Bulletin of Mathematical Biology*, *85*(4), 31.

Karpagam, K. B., & Ganesh, B. (2020). Leptospirosis: a neglected tropical zoonotic infection of public health importance—an updated review. *European Journal of Clinical Microbiology & Infectious Diseases*, *39*, 835–846. doi: 10.1007/s10096-019-03797-4

Kermack, W. O., & McKendrick, A. G. (1927). A contribution to the mathematical theory of epidemics. *Proceedings of the royal society of london. Series A, Containing papers of a mathematical and physical character*, *115*(772), 700–721.

Khairullah, A. R., Kusala, M. K. J., Fauziah, I., Furqoni, A. H., Suhendro, I., Effendi, M. H., ... others (2024). Deciphering leptospirosis: Insights into an emerging global threat. *Journal of Advanced Veterinary Research*, *14*(6), 1065–1071.

Khan, M. A., Islam, S., Khan, S. A., Khan, I., Shafie, S., Gul, T., et al. (2014). Prevention of leptospirosis infected vector and human population by multiple control variables. In *Abstract and applied analysis* (Vol. 2014).

Khan, M. A., Saddiq, S. F., Islam, S., Khan, I., & Shafie, S. (2016). Dynamic behavior of leptospirosis disease with saturated incidence rate. *International Journal of Applied and Computational Mathematics*, *2*, 435–452.

Kifle, Z. S., & Lemecha Obsu, L. (2023). Optimal control analysis of a covid-19 model. *Applied Mathematics in Science and Engineering*, *31*(1), 2173188.

Ko, A. I., Goarant, C., & Picardeau, M. (2009). Leptospira: the dawn of the molecular genetics era for an emerging zoonotic pathogen. *Nature Reviews Microbiology*, *7*(10), 736–747.

Kretzschmar, M., & Wallinga, J. (2009). Mathematical models in infectious disease epidemiology. In *Modern infectious disease epidemiology: Concepts, methods, mathematical models, and public health* (pp. 209–221). Springer.

Lemecha Obsu, L., & Feyissa Balcha, S. (2020). Optimal control strategies for the transmission risk of covid-19. *Journal of biological dynamics*, *14*(1), 590–607.

Li, M., Chen, C., & Li, F.-B. (2010). On fractional powers of generators of fractional resolvent families. *Journal of Functional Analysis*, *259*(10), 2702–2726.

Lilenbaum, W., & Martins, G. (2014). Leptospirosis in cattle: a challenging scenario for the understanding of the epidemiology. *Transboundary and emerging diseases*, *61*, 63–68.

Martcheva, M. (2015). *An introduction to mathematical epidemiology* (Vol. 61). Springer.

Martins, G., & Lilenbaum, W. (2017). Control of bovine leptospirosis: Aspects for consideration in a tropical environment. *Research in veterinary science*, *112*, 156–160.

Mata, A. S., & Dourado, S. M. (2021). Mathematical modeling applied to epidemics: an overview. *São Paulo Journal of Mathematical Sciences*, *15*(2), 1025–1044.

MedicalNews. (2025). . *https://www.medicalnewstoday.com/articles/246829*.

Melese, A. S. (2023). Vaccination model and optimal control analysis of novel corona virus transmission dynamics. *Journal of Mathematical Sciences*, *271*(1), 76–97.

Milici, C., Drăgănescu, G., & Machado, J. T. (2018). *Introduction to fractional differential equations* (Vol. 25). Springer.

Minter, A., Costa, F., Khalil, H., Childs, J., Diggle, P., Ko, A. I., & Begon, M. (2019). Optimal control of rat-borne leptospirosis in an urban environment. *Frontiers in Ecology and Evolution*, *7*, 209.

Monti, G., Montes, V., Tortosa, P., Tejeda, C., & Salgado, M. (2023). Urine shedding patterns of pathogenic leptospira spp. in dairy cows. *Veterinary Research*, *54*(1), 64.

Moruzzi, G., & Moruzzi, G. (2020). Numerical solution of ordinary differential equations (ode). *Essential Python for the Physicist*, 89–113.

Mughini-Gras, L., Bonfanti, L., Natale, A., Comin, A., Ferronato, A., La Greca, E., ... Marangon, S. (2014). Application of an integrated outbreak management plan for the control of leptospirosis in dairy cattle herds. *Epidemiology & Infection*, *142*(6), 1172–1181.

Muhammad Altaf, K., & Atangana, A. (2019). Dynamics of ebola disease in the framework of different fractional derivatives. *Entropy*, *21*(3), 303.

Mukdasai, K., Sabir, Z., Raja, M. A. Z., Sadat, R., Ali, M. R., & Singkibud, P. (2022). A numerical simulation of the fractional order leptospirosis model using the supervise neural network. *Alexandria Engineering Journal*, *61*(12), 12431–12441.

Murray, C. K., & Hospenthal, D. R. (2004, Oct). Determination of susceptibilities of 26 leptospira sp. serovars to 24 antimicrobial agents by a broth microdilution technique. *Antimicrobial Agents and Chemotherapy*, *48*(10), 4002–4005. doi: 10.1128/AAC.48.10.4002-4005 .2004

Ndondo, A., Munganga, J., Mwambakana, J., Saad-Roy, C., Van den Driessche, P., & Walo, R. (2016). Analysis of a model of gambiense sleeping sickness in humans and cattle. *Journal of biological dynamics*, *10*(1), 347–365.

Ngoma, H. D., Kiogora, R., & Chepkwony, I. (2022). A fractional order model of leptospirosis transmission dynamics with environmental compartment. *Global Journal of Pure and Applied Mathematics*, *18*(1), 81–110.

Nogueira, D. B., da Costa, F. T. R., de Sousa Bezerra, C., Soares, R. R., da Costa Barnabé, N. N., Falcão, B. M. R., ... others (2020). Leptospira sp. vertical transmission in ewes maintained in semiarid conditions. *Animal Reproduction Science*, *219*, 106530.

Nyokabi, N. S., Moore, H., Berg, S., Lindahl, J., Phelan, L., Gimechu, G., ... Wood, J. L. (2023). Implementing a one health approach to strengthen the management of zoonoses in ethiopia. *One Health*, *16*, 100521.

Oguntolu, F. A., Peter, O. J., Omede, B. I., Balogun, G. B., & Ayoola, T. A. (2024). Mathematical model on the transmission dynamics of leptospirosis in human and animal population with optimal control strategies using real statistical data. *Quality & Quantity*, 1–40.

Okosun, K. O., Mukamuri, M., & Makinde, D. O. (2016). Global stability analysis and control of leptospirosis. *Open Mathematics*, *14*(1), 567–585.

Orjuela, A. G., Parra-Arango, J. L., & Sarmiento-Rubiano, L. A. (2022). Bovine leptospirosis: effects on reproduction and an approach to research in colombia. *Tropical Animal Health and Production*, *54*(5), 251.

Otaka, D., Penna, B., Martins, G., Hamond, C., Lilenbaum, W., & Medeiros, M. A. (2012). Rapid diagnostic of leptospirosis in an aborted bovine fetus by pcr in rio de janeiro, brazil. *Veterinary Microbiology*, *162*(2-4), 1001–1002.

Paixão, G., Botelho-Fontela, S., Gandra, F., & Reis, J. (2025). Acute leptospirosis outbreak in cattle: A case report. *Veterinary Medicine and Science*, *11*(2), e70206.

Perko, L. (2013). *Differential equations and dynamical systems (3rd ed.)*. Springer.

Pieracci, E. G., Hall, A. J., Gharpure, R., Haile, A., Walelign, E., Deressa, A., ... Belay, E. (2016). Prioritizing zoonotic diseases in ethiopia using a one health approach. *One Health*, *2*, 131–135.

Pimenta, C. L. R. M., da Costa, D. F., Silva, M. L. C. R., Pereira, H. D., Júnior, J. P. A., Malossi, C. D., ... de Azevedo, S. S. (2019). Strategies of the control of an outbreak of leptospiral infection in dairy cattle in northeastern brazil. *Tropical animal health and production*, *51*, 237–241.

Pongsumpun, P., Pongsumpun, P., Tang, I.-M., & Lamwong, J. (2025). The role of a vaccine booster for a fractional order model of the dynamic of covid-19: a case study in thailand. *Scientific Reports*, *15*(1), 1162.

Pontryagin, L. S. (2018). *Mathematical theory of optimal processes*. Routledge.

Pyskun, A., Ukhovskyi, V., Pyskun, O., Nedosekov, V., Kovalenko, V., Nychyk, S., ... Iwaniak, W. (2019, September). Presence of antibodies against leptospira interrogans serovar hardjo in serum samples from cattle in ukraine. *Polish Journal of Microbiology*, *68*(3), 295–302. Retrieved from https://doi.org/10.33073/pjm-2019-031 doi: 10.33073/pjm-2019-031

Rajapakse, S., Fernando, N., Dreyfus, A., et al. (2025). Leptospirosis. *Nature Reviews Disease Primers*, *11*(1), 32. Retrieved from https://doi.org/10.1038/s41572-025-00614-5 doi: 10.1038/s41572-025-00614-5

Rajeev, S., Ilha, M., Woldemeskel, M., Berghaus, R. D., & Pence, M. E. (2014). Detection of asymptomatic renal leptospira infection in abattoir slaughtered cattle in southeastern georgia, united states. *SAGE Open Medicine*, *2*, 2050312114544696.

Robi, D. T., Bogale, A., Urge, B., & Aleme, M. (2024). Seroprevalence of coxiella burnetii, leptospira interrogans serovar hardjo, and brucella species and associated reproductive disorders in cattle in southwest ethiopia. *Heliyon*, *10*(3).

Robichaud, M. V., de Passillé, A., Pellerin, D., & Rushen, J. (2011). When and where do dairy cows defecate and urinate? *Journal of dairy science*, *94*(10), 4889–4896.

Rojas, P., Monahan, A. M., Schuller, S., Miller, I. S., Markey, B. K., & Nally, J. E. (2010). Detection and quantification of leptospires in urine of dogs: a maintenance host for the zoonotic disease leptospirosis. *European Journal of Clinical Microbiology & Infectious Diseases*, *29*(10), 1305–1309. doi: 10.1007/s10096-010-0991-2

Ross, R. (1911). *The prevention of malaria*. John Murray.

Salyer, S. J., Silver, R., Simone, K., & Behravesh, C. B. (2017). Prioritizing zoonoses for global health capacity building—themes from one health zoonotic disease workshops in 7 countries, 2014–2016. *Emerging infectious diseases*, *23*(Suppl 1), S55.

Samrot, A. V., Sean, T. C., Bhavya, K. S., Sahithya, C. S., Chan-Drasekaran, S., Palanisamy, R., ... Mok, P. L. (2021). Leptospiral infection, pathogenesis and its diagnosis—a review. *Pathogens*, *10*(2), 145.

Selim, A., Marzok, M., Gattan, H. S., Abdelhady, A., Salem, M., & Hereba, A. M. (2024). Seroprevalence and associated risk factors for bovine leptospirosis in egypt. *Scientific Reports*, *14*(1), 4645.

Sharomi, O., & Malik, T. (2017). Optimal control in epidemiology. *Annals of Operations Research*, *251*, 55–71.

Siegenfeld, A. F., Kollepara, P. K., & Bar-Yam, Y. (2022). Modeling complex systems: A case study of compartmental models in epidemiology. *Complexity*(1), 3007864. Retrieved from https://onlinelibrary.wiley.com/doi/abs/10.1155/2022/3007864 doi: https://doi.org/10.1155/2022/3007864

Smith, H. L. (1995). *Monotone dynamical systems: an introduction to the theory of competitive and cooperative systems* (No. 41). American Mathematical Soc.

Sohm, C., Steiner, J., Jöbstl, J., Wittek, T., Firth, C., Steinparzer, R., & Desvars-Larrive, A. (2023). A systematic review on leptospirosis in cattle: A european perspective. *One Health*, 100608.

Sontakke, B., & Shaikh, A. (2015). Properties of caputo operator and its applications to linear fractional differential equations. *Int. J. Eng. Res. Appl*, *5*(5), 22–27.

Sun, Z.-S., Wan, E.-Y., Agbana, Y. L., Zhao, H.-Q., Yin, J.-X., Jiang, T.-G., ... others (2024). Global one health index for zoonoses: A performance assessment in 160 countries and territories. *IScience*, *27*(4).

Sunaryo, S., & Priyanto, D. (2022). Leptospirosis in rats and livestock in bantul and gunungkidul district, yogyakarta, indonesia. *Veterinary World*, *15*(6), 1449.

Sweileh, W. M. (2022). Global research activity on mathematical modeling of transmission and control of 23 selected infectious disease outbreak. *Globalization and Health*, *18*(1), 1–14.

Tang, J. W., Bahnfleth, W. P., Bluyssen, P. M., Buonanno, G., Jimenez, J. L., Kurnitski, J., ... others (2021). Dismantling myths on the airborne transmission of severe acute respiratory syndrome coronavirus-2 (sars-cov-2). *Journal of Hospital Infection*, *110*, 89–96.

Thibeaux, R., Iraola, G., Ferrés, I., Bierque, E., Girault, D., Soupé-Gilbert, M.-E., ... Goarant, C. (2018). Deciphering the unexplored leptospira diversity from soils uncovers genomic evolution to virulence. *Microbial genomics*, *4*(1), e000144.

Torres, D. F. M. (2021). A brief introduction to optimal control theory with python. *Unpublished Book*.

ul Rehman, A., Singh, R., Abdeljawad, T., Okyere, E., & Guran, L. (2021). Modeling, analysis and numerical solution to malaria fractional model with temporary immunity and relapse. *Advances in Difference Equations*, *2021*(1), 390.

van den Brink, K. M., Aalberts, M., Fabri, N. D., & Santman-Berends, I. M. (2023). Effectiveness of the leptospira hardjo control programme and detection of new infections in dairy cattle in the netherlands. *Animals*, *13*(5), 831.

Van den Driessche, P., & Watmough, J. (2002). Reproduction numbers and sub-threshold endemic equilibria for compartmental models of disease transmission. *Mathematical biosciences*, *180*(1-2), 29–48.

Van den Driessche, P., & Watmough, J. (2008). Further notes on the basic reproduction number. *Mathematical epidemiology*, 159–178.

WHO. (2020). World health organization. *https://www.who.int/news-room/fact-sheets/detail/zoonoses*.

Wiggins, S. (2003). *Introduction to Applied Nonlinear Dynamical Systems and Chaos* (Vol. 2). Springer Science & Business Media.

Wilson-Welder, J. H., Boggiatto, P., Nally, J. E., Wafa, E. I., Alt, D. P., Hornsby, R. L., ... others (2020). Bovine immune response to leptospira antigen in different novel adjuvants and vaccine delivery platforms. *Vaccine*, *38*(18), 3464–3473.

Wu, M., Abdurahman, X., & Teng, Z. (2022). Optimal control strategy analysis for an human-animal brucellosis infection model with multiple delays. *Heliyon*, *8*(12).

Yang, L., Su, Y., Li, X., & Ye, Y. (2020). Analysis and simulation of a fractional order optimal control model for hbv. *Journal of Function Spaces*, *2020*.

Yimer, E., Koopman, S., Messele, T., Wolday, D., Newayeselassie, B., Gessesse, N., ... Sanders, E. J. (2004). Human leptospirosis in ethiopia: a pilot study in wonji. *Ethiopian Journal of Health Development*, *18*(1), 48–51. doi: 10.4314/ejhd.v18i1.9866

Zewdie, A. D., Gakkhar, S., & Gupta, S. K. (2022). Model for transmission and optimal control of anthrax involving human and animal population. *Journal of Biological Systems*, *30*(03), 605–630.

APPENDIX A

MATHEMATICAL PRELIMINARIES

In this chapter, we present some important mathematical definitions and theorems which will be used in this study.

A.1 Existence and uniqueness theorem

Theorem A.1.1. (Hirsch et al., 2012). Consider the initial value problem

$$\mathbf{X}' = f(\mathbf{X}),$$
$$\mathbf{X}(0) = \mathbf{X}_0$$

where $\mathbf{X}_0 \in \mathbb{R}^n$, $f : \mathbb{R}^n \to \mathbb{R}^n$ and $f \in \mathbf{C}^1$ (i.e f and its first partial derivatives exist and are continuous functions on $\mathbb{R}^n$). Then there exists a unique solution of this initial value problem.

A.2 Stability of system of ODE

Theorem A.2.1. (Birkhoff et al., 1989). Suppose the autonomous initial value problem

$$\mathbf{X}' = f(\mathbf{X}),$$
$$\mathbf{X}(0) = \mathbf{X}_0$$

has an equilibrium point at $\mathbf{X} = \mathbf{X}^*$ (i.e $f(X^*) = 0$) and that $J(\mathbf{X}^*)$ is the Jacobian of f evaluated at $\mathbf{X}^*$. Then

i. the system is asymptotically stable at $\mathbf{X} = \mathbf{X}^*$, if all eigenvalues of $J(\mathbf{X}^*)$ have negative real part.

ii. the system is unstable at $\mathbf{X} = \mathbf{X}^*$,if $J(\mathbf{X}^*)$ has at least one eigenvalue with a positive real part.

A.3 Basic Reproduction number

The basic reproduction number, $\mathscr{R}_0$, is defined as an average number of secondary infections produced by one infected individual in a uniformly distributed population. This number is a measure of the potential for disease spread within a population (Tang et al., 2021). If $\mathscr{R}_0 < 1$, then a few infected individuals introduced into a completely susceptible population will, on average, fail to replace themselves, and the disease will not spread. If, on the other hand $\mathscr{R}_0 > 1$, then the number of infected individuals will increase with each generation and the disease will spread. Note that the basic reproduction number is a threshold parameter for invasion of a disease organism into a completely susceptible population. A large number of $\mathscr{R}_0$ may indicate the possibility of a major epidemic.

$\mathscr{R}_0$ can be calculated by using different method and the most common one is th next generation matrix method (Van den Driessche & Watmough, 2002). It is obtained by taking the largest (dominant) eigenvalues (spectral radius) of

$$FV^{-1} = \left[\frac{\partial \mathscr{F}_i(\mathscr{E}_0)}{\partial x_j}\right]\left[\frac{\partial \mathscr{V}_i(\mathscr{E}_0)}{\partial x_j}\right]^{-1} \tag{A.1}$$

where $\mathscr{F}_i$ is the rate of appearance of new infections in compartment i, $\mathscr{V}_i$ is the transfer of infection from one compartment to other compartment and $\mathscr{E}_0$ is disease free equilibrium point.

Furthermore, $\mathscr{F}$ is nonnegative, $\mathscr{V}$ is non-singular nxn matrices. To interpret the entries of FV^{-1} and develop a meaningful definition of reproduction number $\mathscr{R}_0$, consider the fate of an infected individual introduced into compartment k of a disease free population. The (i, j) entry of F is the rate at which infected individuals in compartment j produce new infections in compartment i. The (j,k) entry of V^{-1} is the average length of time this individual spends in compartment j during its life time, assuming that the population remains near the $\mathscr{E}_0$ and barring reinfection. Hence, the (i,k) entry of the product FV^{-1} is the expected number of new infections in compartment i produced by the infected individual originally introduced into compartment k.

A.4 Effective Reproductive Rate

The effective reproductive rate, $\mathscr{R}_e$ is the number of secondary cases produced on average by one infected animal when a fraction of the population are susceptible. Simply, when S out of N are susceptible. Mathematically, $\mathscr{R}_e$ is given by

$$\mathscr{R}_e = \mathscr{R}_0\left(\frac{S}{N}\right) \tag{A.2}$$

Assuming the population mix randomly. The disease persists for $\mathscr{R}_e \geq 1$ and dies out for $\mathscr{R}_e < 1$. The effective reproduction rate, $\mathscr{R}_e$ is more realistic because in every population, not everyone is susceptible. There are those who are infected denoted by I and others who are immune denoted by V. The effective reproductive rate must always be less than unity to ensure that the disease dies out of the population. It is important to achieve $\mathscr{R}_e < 1$. This can only be possible if a fraction of the population are treated or vaccinated large enough. As equation (A.2), the number of the susceptible must be reduce so that $\mathscr{R}_e < 1$.

A.5 Sensitivity Analysis

The goal of sensitivity analysis is to decide qualitatively which parameters are most influential in the model output. To implement the sensitivity analysis of epidemic model, we calculate the sensitivity indices of the reproduction number,$\mathscr{R}_0$ to the parameters in the model. These indices tell us how crucial each parameter is to disease transmission and prevalence. The normalized forward sensitivity index of a variable to a parameter is the ratio of the relative change in the variable to the relative change in the parameter.

Definition A.5.1. (Chitnis et al., 2008; Martcheva, 2015). The normalized forward sensitivity index of $\mathscr{R}_0$ to a parameter,p, is denoted by $\Omega_p^{\mathscr{R}_0}$ is given by

$$\Omega_p^{\mathscr{R}_0} = \frac{\partial \mathscr{R}_0}{\partial p}\left(\frac{p}{\mathscr{R}_0}\right) \tag{A.3}$$

A.6 Castillo-Chavez global stability theorem

Let the system of differential equation be,

$$\frac{dX}{dt} = F(\mathbf{X},\mathbf{Y}) \tag{A.4}$$

Rewriting (A.4)

$$\begin{aligned} \frac{d\mathbf{X}}{dt} &= F(\mathbf{X},\mathbf{Y}) \\ \frac{d\mathbf{Y}}{dt} &= G(\mathbf{X},\mathbf{Y}); with, G(\mathbf{X},0) = 0 \end{aligned} \tag{A.5}$$

where $\mathbf{X}$ denotes the uninfected compartment and $\mathbf{Y}$ denotes the infected compartments.

Theorem A.6.1. (Castillo-Chavez, 2002). The Disease free equilibrium of the system (A.4) is globally asymptotically stable for $\mathscr{R}_0 < 1$ on its feasible region, if H_1 and H_2 below are satisfied.

H_1 : For $\dfrac{dX}{dt} = F(\mathbf{X},\mathbf{Y})$, $\mathbf{X}^*$ is a globally asymptotically stable where $F(\mathbf{X}^*,0) = 0$
H_2 : $G(\mathbf{X},\mathbf{Y}) = B\mathbf{Y} - \hat{G}(\mathbf{X},\mathbf{Y})$, $\hat{G}(\mathbf{X},\mathbf{Y}) > 0$ for $(\mathbf{X},\mathbf{Y}) \in \Omega$, where $B = D_Y G(\mathbf{X}^*,0)$ is an M-matrix (the matrix with off-diagonal elements non-negative).

A.7 Bounded Control and Pontryagin's Maximum Principle

To solve optimal control problems with bounds on the values of the controls, we need the full power of Pontryagin's Maximum Principle (PMP).

Theorem A.7.1. (Pontryagin Maximum Principle)(Torres, 2021). Let (x^*,u^*) be a maximizer for the optimal control problem

$$\begin{aligned} J[x(.),u(.)] = \int_{t_0}^{t_1} f(t,x(t),u(t))dt \to max, \\ x'(t) = g(t,x(t),u(t)), x(.) \in PC([t_0,t_1];R); \\ x(t_0) = x_0, t \in [t_0,t_1], u(.) \in PC([t_0,t_1];R), u(t) \in \Omega, \end{aligned} \tag{A.6}$$

where Ω is a closed subset of R^m. Then, there exists a vector-valued function $\lambda(.) \in PC'([t_0,t_1];R^n)$ such that the triple (x^*,u^*,λ) satisfies:

1. the maximality condition

$$\mathscr{H}(t,x^*(t),u^*(t),\lambda(t)) = \max_{w\in\Omega} \mathscr{H}(t,x^*(t),w,\lambda(t)) \tag{A.7}$$

   at every point $t \in (t_0,t_1)$ of continuity of the control u ;

2. the Hamiltonian system

$$\begin{cases} x'^*(t) = \dfrac{\partial \mathscr{H}}{\partial \lambda} \\ \lambda'^*(t) = -\dfrac{\partial \mathscr{H}}{\partial x} \end{cases} \tag{A.8}$$

3. the transversality condition

$$\lambda(t_1) = 0 \tag{A.9}$$

where the Hamiltonian $\mathscr{H}$ is defined by $\mathscr{H}(t,x,u,\lambda) = f(t,x,u) + \lambda.g(t,x,u)$.

A.8 Fractional Calculus

Below are necessary definitions and theorems of fractional calculus.

Definition A.8.1. (Chakraverty et al., 2020). **Gamma function**. The gamma function is most important in fractional-order calculus, and it is written as

$$\Gamma(n) = \int_0^\infty e^{-x} x^{n-1} dx \tag{A.10}$$

The gamma function satisfy the property $\Gamma(x+1) = x\Gamma(x)$, $x > 0$. For any positive integer n, $\Gamma(n) = (n-1)!$.

Definition A.8.2. (Chakraverty et al., 2020). **Mittag–Leffler function (MLF)**.
One-parameter MLF is defined as

$$E_\alpha(z) = \sum_{n=0}^{\infty} \frac{z^n}{\Gamma(1+n\alpha)} \tag{A.11}$$

for $z \in C$ and $\alpha > 0$, where C is set complex number.
Two-parameter representation of the MLF may be written as

$$E_{\alpha,\beta}(z) = \sum_{n=0}^{\infty} \frac{z^n}{\Gamma(\beta+n\alpha)} \tag{A.12}$$

for $z \in C$ and $\alpha, \beta > 0$.

Definition A.8.3. (Muhammad Altaf & Atangana, 2019). For a function $f : \mathbb{R}^+ \to \mathbb{R}$, then the fractional integral of order $\alpha > 0$ is given by

$$I^\psi f(t) = \frac{1}{\Gamma(\psi)} \int_0^t (t-z)^{\psi-1} f(z) dz \tag{A.13}$$

where $\Gamma(\psi)$ is a gamma function.

Definition A.8.4

Definition A.8.4. (Sontakke & Shaikh, 2015). The **Riemann-Liouville fractional derivative** or Riemann-Liouville fractional differential of function $f(t)$ with order $\psi > 0$ is defined as

$$D^\psi f(t) = \frac{1}{\Gamma(n-\psi)} \frac{d^n}{dt^n} \int_a^t \frac{f(z)}{(t-z)^{\psi+n-1}} dz, n-1 < \psi < n, t > a, \psi, a, t \in R \tag{A.14}$$

Definition A.8.5. (Muhammad Altaf & Atangana, 2019). Given a function $f \in C^n$, then the **Caputo fractional derivative** with order ψ is given as

$$ {}^{C}D_t^{\psi}(f(t)) = I^{n-\psi}D^n f(t) = \frac{1}{\Gamma(n-\psi)}\int_a^t \frac{f^n(z)}{(t-z)^{\psi+n-1}}dz \tag{A.15} $$

that is defined for the absolute continuous functions and $n-1 < \psi < n \in N$. Clearly, ${}^{C}D_{\psi}^{t}(f(t))$ approaches $f'(t)$ as ψ approaches 1.

Definition A.8.6. Consider the Caputo fractional IVP

$$ \begin{cases} {}_{t_0}^{C}D_t^{\psi}x(t) = f(t,x(t)), \\ x(t_0) = x_0, \quad \psi \in (0,1), \end{cases} \tag{A.16} $$

where $\Psi \in C([\mathbb{R}^+ \times \mathbb{R}^n, \mathbb{R}^n])$. Then the integral representation of Eq. (A.16) is given by

$$ x(t) = x_0 + \frac{1}{\Gamma(\psi)}\int_0^t (t-\tau)^{\psi-1} f(\tau, x(\tau))\, d\tau, \tag{A.17} $$

If the solution of the integral Eq. (A.17) exists and is unique, then the solution of IVP (A.16) also exists and is unique.

Definition A.8.7. (Milici et al., 2018) The Laplace transform of the Caputo fractional derivative of order ψ for a function $f(t)$ is defined as:

$$ \mathscr{L}\left\{ {}^{C}D_t^{\psi} f(t) \right\} = s^{\psi}F(s) - \sum_{k=0}^{n-1} s^{\psi-k-1} f^{(k)}(0), $$

where $n-1 < \psi \leq n$ and $F(s)$ is the Laplace transform of $f(t)$, defined as:

$$ F(s) = \mathscr{L}\{f(t)\} = \int_0^{\infty} e^{-st} f(t) dt. $$

Theorem A.8.1. (Yang et al., 2020). Let a nonlinear fractional-order system in the sense of Caputo derivative is

$$ {}^{C}D_{\psi}^{t}x(t) = f(t,x(t)), x(t_0) = x_0 \tag{A.18} $$

where $0 < \psi < 1$. If a point x^* satisfies $f(x^*) = 0$, then x^* is called an equilibrium point of the system. The equilibrium x^* is said to be locally asymptotically stable if all eigenvalues λ_i of the Jacobian matrix $J = \dfrac{\partial f}{\partial x}$ evaluated at x^* satisfy the conditions $|arg(\lambda_i)| > \dfrac{\psi\pi}{2}$.

Lemma 1. ul Rehman et al. (2021) Let $f(t) \in C[0,T]$ and ${}_0^{C}D_t^{\psi} f(t) \in (0,T]$ for $0 < \psi \leq 1$. Then,

- if ${}_0^C D_t^{\psi} f(t) \leq 0$ for all $t \in (0,T]$, then $f(t)$ is non-increasing, and
- if ${}_0^C D_t^{\psi} f(t) \geq 0$ for all $t \in (0,T]$, then $f(t)$ is non-decreasing.

Lemma 2 (Fractional Derivative Inequality). Li et al. (2010) Let $V(\mathbf{y}(t)) = \frac{1}{2}\|\mathbf{y}(t)\|^2$. Then, for the Caputo derivative, there exists a constant $K(\psi) > 0$ such that:

$$ {}^C D_t^{\psi} V(\mathbf{y}(t)) \leq \sum_{i=1}^{n} y_i(t) \cdot {}^C D_t^{\psi} y_i(t) + K(\psi)\|y(t)\|^2. $$

A.9 Local Stability of Leptospira-Free Equilibrium

Proof. The Jacobian matrices of model Eq.(4.1) at *Leptospira*-free equilibrium (LFE), $\mathscr{E}^*$, is given by

$$ J = \begin{bmatrix} -k_1 & 0 & -\beta_A S^* & -bq - \beta_I S^* & \gamma & \eta & \frac{-\beta_L S^*}{K} \\ 0 & -k_2 & \beta_A(S^* + (1-r)V^*) & \beta_I(S^* + (1-r)V^*) & 0 & 0 & \frac{\beta_L(S^* + (1-r)V^*)}{K} \\ 0 & (1-\nu)\alpha & -k_3 & 0 & 0 & 0 & 0 \\ 0 & \nu\alpha & 0 & -k_4 & 0 & 0 & 0 \\ 0 & 0 & \sigma & \delta & -k_5 & 0 & 0 \\ \tau & 0 & -\beta_A(1-r)V_0^* & -\beta_I(1-r)V_0^* & 0 & -k_6 & \frac{-\beta_L(1-r)V_0^*}{K} \\ 0 & 0 & \omega_A & \omega_I & 0 & 0 & -\varepsilon \end{bmatrix} \tag{A.19} $$

where,

$k_1 = \tau + \mu,\ k_2 = \alpha + \mu,\ k_3 = \sigma + \mu,\ k_4 = (\delta + \mu + d) - bq,\ k_5 = \gamma + \mu,\ k_6 = \eta + \mu,$

$V^* = \dfrac{\Lambda(\rho\mu + \tau)}{\mu(\eta + \tau + \mu)}$ and $S^* = \dfrac{\Lambda((1-\rho)\mu + \eta)}{\mu(\eta + \tau + \mu)}$.

The eigenvalues of Jacobian of the matrix in Eq. (A.19) satisfy the following characteristic polynomial equation.

$$ \lambda^7 + D_6\lambda^6 + D_5\lambda^5 + D_4\lambda^4 + D_3\lambda^3 + D_2\lambda^2 + D_1\lambda + D_0 = 0, \tag{A.20} $$

where,

$D_0 = \mu\varepsilon k_2 k_3 k_4 k_5 (k_6 + \tau)(1 - \mathscr{R}_e) > 0$, for $\mathscr{R}_e < 1$.

$D_1 = (k_1 k_2 k_3 k_4 k_5 \varepsilon + \mu(k_6 + \tau)(k_2 k_3 k_4 k_5 + k_2 k_3 k_4 \varepsilon))(1 - \mathscr{R}_e) + \mu(k_6 + \tau)k_2 k_3 k_5 \varepsilon(1 - (\mathscr{R}_A + \mathscr{R}_L')) + \mu(k_6 + \tau)k_2 k_4 k_5 \varepsilon(1 - (\mathscr{R}_I + \mathscr{R}_L'')) + k_2 k_3 k_4 k_5 k_6 \varepsilon(1 - \mathscr{R}_L) + k_3 k_4 k_5 \varepsilon\mu(k_6 + \tau) > 0$, for $\mathscr{R}_0 < 1$ (i.e $\mathscr{R}_A < 1, \mathscr{R}_I < 1, \mathscr{R}_L' < 1, \mathscr{R}_L'' < 1$),

$D_2 = \mu(k_6 + \tau)k_2 k_3 k_5(1 - \mathscr{R}_A) + \mu(k_6 + \tau)k_2 k_4 k_5(1 - \mathscr{R}_I) + [\mu(k_6 + \tau) + k_1\varepsilon + k_1 k_5 + k_5\varepsilon +$

$k_6\varepsilon][1-(\mathscr{R}_A+\mathscr{R}_I)]+k_2k_3\varepsilon[\mu(k_6+\tau)+k_1k_5+k_5k_6][1-(\mathscr{R}_A+\mathscr{R}'_L)]+k_2k_4\varepsilon[\mu(k_6+\tau)+k_1k_5+k_5k_6][1-(\mathscr{R}_I+\mathscr{R}''_L)]+\mu(k_6+\tau)[k_2k_3k_4+k_3k_4k_5+k_3k_4\varepsilon+k_3k_5\varepsilon+k_4k_5\varepsilon]+k_1k_2k_3k_4k_5+k_1k_2k_3k_4\varepsilon+k_1k_2k_3k_5\varepsilon+k_1k_2k_3k_6\varepsilon+k_2k_3k_4k_5k_6+k_3k_4k_5k_6\varepsilon>0$, for $\mathscr{R}_e<1$ (i.e $\mathscr{R}_A<1$, $\mathscr{R}_I<1$, $\mathscr{R}'_L<1$, $\mathscr{R}''_L<1$),

$D_3=(k_1k_5+k_5k_6+\mu(k_6+\tau))[k_2k_3(1-\mathscr{R}_A)+k_2k_4(1-\mathscr{R}_I)]+k_1k_3k_3(k_4+k_5+k_6)[1-(\mathscr{R}_A+\mathscr{R}_I)]+(k_1\varepsilon+k_5\varepsilon+k_6\varepsilon)[k_2k_3(1-(\mathscr{R}_A+\mathscr{R}'_L))+k_2k_4(1-(\mathscr{R}_I+\mathscr{R}''_L))]+k_2k_3k_4\varepsilon(1-\mathscr{R}_0)+\mu(k_6+\tau)(k_2k_5+k_2\varepsilon+k_3k_4+k_3k_5+k_3\varepsilon+k_4k_5+k_4\varepsilon+k_5\varepsilon)>0$, for $\mathscr{R}_e<1$ (i.e $\mathscr{R}_A<1$, $\mathscr{R}_I<1$, $\mathscr{R}'_L<1$, $\mathscr{R}''_L<1$),

$D_4=(k_1k_2+k_2k_5+k_2k_6)(k_3(1-\mathscr{R}_A)+k_4(1-\mathscr{R}_I))+k_2k_3k_4(1-(\mathscr{R}_A+\mathscr{R}_I))+k_2k_3\varepsilon(1-(\mathscr{R}_A+\mathscr{R}'_L))+k_2k_4\varepsilon(1-(\mathscr{R}_I+\mathscr{R}''_L))+\mu(k_6+\tau)(k_2+k_3+k_4+k_5+\varepsilon)+k_1k_2k_5+k_1k_2\varepsilon+k_1k_3k_4+k_1k_3k_5+k_1k_3\varepsilon+k_1k_4k_5+k_1k_4\varepsilon+k_1k_5\varepsilon+k_2k_5k_6+k_2k_5\varepsilon+k_2k_6\varepsilon+k_3k_4k_5+k_3k_4k_6+k_3k_4\varepsilon+k_3k_5k_6+k_3k_5\varepsilon+k_3k_6\varepsilon+k_4k_5k_6+k_4k_5\varepsilon+k_4k_6\varepsilon+k_5k_6\varepsilon>0$, for $\mathscr{R}_e<1$ (i.e $\mathscr{R}_A<1$, $\mathscr{R}_I<1$, $\mathscr{R}'_L<1$, $\mathscr{R}''_L<1$),

$D_5=k_2k_3(1-\mathscr{R}_A)+k_2k_4(1-\mathscr{R}_I)+\mu(k_6+\tau)+k_1k_2+k_1k_3+k_1k_4+k_1k_5+k_1\varepsilon+k_2k_5+k_2k_6+k_2\varepsilon+k_3k_4+k_3k_5+k_3k_6+k_3\varepsilon+k_4k_5+k_4k_6+k_4\varepsilon+k_5k_6+k_5\varepsilon+k_6\varepsilon>0$, for $\mathscr{R}_e<1$ (i.e $\mathscr{R}_A<1$, $\mathscr{R}_I<1$),

$D_6=k_1+k_2+k_3+k_4+k_5+k_6+\varepsilon>0$,

Here, $D_0>0$, $D_1>0$, $D_2>0$, $D_3>0$, $D_4>0$, $D_5>0$ and $D_6>0$ for $\mathscr{R}_e<1$ (i.e $\mathscr{R}_A<1$, $\mathscr{R}_I<1$, and $\mathscr{R}_L<1$). Using Descartes (1937) rule of signs, we can conclude that the characteristic equation (A.20) has all roots of negative real part for $\mathscr{R}_e<1$. Hence this complete the proof of Theorem 4.2.2. □

APPENDIX B

PYTHON CODES

Below are Python scripts used for numerical simulations.

B.1 Odeint Scripts for stability analysis and parameter effects

```
import numpy as np
from scipy.integrate import odeint
from cycler import cycler
import matplotlib.pyplot as plt
#%matplotlib

def Lepto_model(x, y, Lamda,q,rho,K,betaA,betaI,betaL,alpha,nu
   ,delta,sigma,mu,muI,eps,omegaA,omegaI,gamma,eta,r,tau):
#Variables
S=x[0]
E=x[1]
A=x[2]
I=x[3]
R=x[4]
V=x[5]
L=x[6]
#Force of infection
lam=betaA*A+betaI*I+(betaL*L)/(K+L)
#Systems of equations
dSdt=(1-rho)*Lamda-b*q*I-lam*S+gamma*R+r*eta*V-tau*S-mu*S
dEdt=lam*(S+(1-r)*V)-alpha*E-mu*E
dAdt=(1-nu)*alpha*E-sigma*A-mu*A
dIdt=b*q*I+nu*alpha*E-delta*I-mu*I-muI*I
dRdt=sigma*A+delta*I-gamma*R-mu*R
dVdt=rho*Lamda-((1-r)*lam*V)+tau*S-r*eta*V-mu*V
dLdt=omegaA*A+omegaI*I-eps*L
return dSdt,dEdt,dAdt,dIdt,dRdt,dVdt,dLdt
```

```
#Parameter values
Lamda=0.15
q=0.2
rho=0.5
K=1000
betaA=0.0001
betaI=0.00005
betaL=0.005
alpha=0.1
nu=0.2
delta=0.00274
sigma=0.00137
mu=0.000685
muI=0.01
eps=0.0111
omegaA=0.014
omegaI=0.01
gamma=0.00185
eta=0.013
r=0.88
tau=0.05
b=0.000685
#
x0=[300,60,30,10,0,100,10] # [S(0), E(0), A(0), I(0), R(0), V
   (0), L(0)]
t=np.linspace(0, 365, 365)
x=odeint(Lepto_model,x0,t,args=(Lamda,q,rho,K,betaA,betaI,
   betaL,alpha,nu,delta,sigma,mu,muI,eps,omegaA,
omegaI,gamma,eta,r,tau))

sigma=[0.00137,0.00337,0.00537]

for j in sigma: # here j replace beta
x=odeint(Lepto_model,x0,t,args=(Lamda,q,rho,K,betaA,betaI,
   betaL,alpha,nu,delta,j,mu,muI,eps,omegaA,
omegaI,gamma,eta,r,tau))
```

```
S=x[:,0]
E=x[:,1]
A=x[:,2]
I=x[:,3]
R=x[:,4]
V=x[:,5]
L=x[:,6]

plt.plot(t,L,label=r'$\sigma$ = %s' % j, linewidth=2)
#plt.ticklabel_format(style='sci', axis='y', scilimits=(0,0),
   useMathText = True) #Format for y-value: m.0 x 10^n
plt.legend(fontsize=11)
plt.xlabel('Time (Days)', fontsize=13)
plt.ylabel('Leptospiral Load, $L(t)$', fontsize=13)

plt.xlim(left=0,right=365)
plt.ylim(bottom=0)
plt.tick_params(top=True, right=True, which='both')
plt.savefig('sigma_L.eps', format = 'eps')
```

B.2 Gekko script for optimal control simulation

```
import numpy as np
from gekko import GEKKO
import matplotlib.pyplot as plt

m = GEKKO(remote=False)
# constants
Lamda=0.15
q=0.2
rho=0.5
K=1000
betaA=0.0001
betaI=0.00005
betaL=0.005
```

```
alpha=0.1
nu=0.2
delta=0.0027
sigma=0.00137
mu=0.000685
muI=0.01
eps=0.0111
omegaA=0.014
omegaI=0.01
gamma=0.00185
eta=0.013
r=0.88
tau=0.05
b=0.000685

W1=2
W2=2
W3=1

c1=20
c2=1
c3=10

#define variables
S = m.Var(value=300)
E = m.Var(value=60)
A = m.Var(value=30)
I = m.Var(value=10)
R = m.Var(value=0)
V = m.Var(value=100)
L = m.Var(value=10)

#define control
u1 = m.MV(value=0,lb=0,ub=0)
u2 = m.MV(value=0,lb=0,ub=0.95)
u3 = m.MV(value=0,lb=0,ub=0.95)
```

```
# writing Equations
l=betaA*A+betaI*I+(betaL*L)/(K+L)
m.Equation(S.dt()==(1-rho)*Lamda-b*q*I-(1-u1)*l*S+gamma*R+eta*
   V-(0.1*u2)*S-mu*S)
m.Equation(E.dt()==(1-u1)*l*S-alpha*E-mu*E)
m.Equation(A.dt()==(1-nu)*alpha*E-(sigma+0.025*u3)*A-mu*A)
m.Equation(I.dt()==b*q*I+nu*alpha*E-(delta+0.05*u3)*I-mu*I-muI
   *I)
m.Equation(R.dt()==(sigma+0.025*u3)*A+(delta+0.05*u3)*I-gamma*
   R-mu*R)
m.Equation(V.dt()==rho*Lamda-(1-u1)*(1-r)*l*V+(0.1*u2)*S-eta*V
   -mu*V)
m.Equation(L.dt()==omegaA*A+omegaI*I-eps*L)

# time point
T=350
nt = 101; m.time = np.linspace(0,T,nt)
p = np.zeros(nt); p[-1] = 1.0
final = m.Param(value=p)
# initialize with simulation
m.options.IMODE=7
m.options.NODES=1
m.solve(disp=False)

# plot the prediction
plt.figure(figsize=(8,5))
#plt.plot(m.time, A.value, color='blue', lw=3,ls='--', label='
   without control')
# optimize
m.options.IMODE=6
#i.UPPER = 0.02
u1.STATUS = 1
u1.DCOST=0.00001
u2.STATUS = 1
u2.DCOST=0.00001
```

```
u3.STATUS = 1
u3.DCOST=0.00001
m.options.SOLVER = 3
m.options.TIME_SHIFT = 0
S.value = S.value.value
E.value = E.value.value
A.value = A.value.value
I.value = I.value.value
R.value = R.value.value
V.value = V.value.value
L.value = L.value.value
# J=m.Var(value=0)
# m.Equation(J.dt()==W1*Al +W2*Il +W3*It+W4*B + 0.5*c2*u2**2 +
    0.5*c1*u1**2)
# m.Obj(J*final)
#m.Minimize(u)

obj = m.integral(W1*A+W2*I+W3*L+0.5*c1*u1**2 + 0.5*c2*u2**2+
   0.5*c3*u3**2)
m.Minimize(final*obj)
m.solve(disp=False)
#plt.plot(m.time, A.value, color='red', lw=3, label='With
   Optimal Control')

#plt.plot(m.time, u1.value,lw=3, label='$u_1$ : prevention')
plt.plot(m.time, u2.value,lw=3, label='$u_2$ : vaccination')
plt.plot(m.time, u3.value,lw=3, label='$u_3$ : Treatment')

plt.tick_params(top=True, right=True, which='both')
plt.xlim(left=0,right=350)
plt.ylim(bottom=0)
plt.ylabel('Control Profile')
plt.legend()
plt.xlabel('Time (days)')
plt.savefig('u2u3_c_profile.eps', format = 'eps')
```

B.3 Script for Adams-Bashforth-Moulton PECE algorithm

```
import numpy as np
import matplotlib.pyplot as plt
from scipy.special import gamma

# Model RHS function
def f_all(t, Y, params):
SC, VC, IC, RC, SH, EH, IH, RH, L = Y
(LamdaC, LamdaH, rho, K, betaCC, betaCH, betaC, betaH, alphaH,
    delta,sigma, muC, muH, dC, dH, eps, omegaC, omegaH, gammaC
   , gammaH, eta, r, tau) = params

dSC = (1 - rho)*LamdaC - (betaCC*IC + (betaC*L)/(K + L))*SC +
   gammaC*RC + eta*VC - tau*SC - muC*SC
dVC = rho*LamdaC - (1 - r)*(betaCC*IC + (betaC*L)/(K + L))*VC
   - eta*VC + tau*SC - muC*VC
dIC = ((betaCC*IC + (betaC*L)/(K + L))*SC + (betaCC*IC + (
   betaC*L)/(K + L))*(1 - r)*VC
- sigma*IC - muC*IC - dC*IC)
dRC = sigma*IC - gammaC*RC - muC*RC
dSH = LamdaH - (betaCH*IC + (betaH*L)/(K + L))*SH + gammaH*RH
   - muH*SH
dEH = (betaCH*IC + (betaH*L)/(K + L))*SH - alphaH*EH - muH*EH
dIH = alphaH*EH - delta*IH - muH*IH - dH*IH
dRH = delta*IH - gammaH*RH - muH*RH
dL  = omegaC*IC + omegaH*IH - eps*L

return np.array([dSC, dVC, dIC, dRC, dSH, dEH, dIH, dRH, dL])
def pece_fde_solver(psi, h, T, Y0, params):
N = int(T / h)
t = np.linspace(0, T, N)
n_vars = len(Y0)

Y = np.zeros((N, n_vars))
Y[0] = Y0
```

```
F = np.zeros((N, n_vars))
F[0] = f_all(t[0], Y[0], params)

# Precompute weights
b = np.zeros((N, N))
a = np.zeros((N, N))

for n in range(1, N):
for j in range(n):
b[n, j] = (n - j + 1)**psi - (n - j)**psi
for j in range(n):
a[n, j] = (n - j + 1)**(psi + 1) - 2*(n - j)**(psi + 1) + (n -
    j - 1)**(psi + 1)

for n in range(1, N): # Predictor step
YP = np.zeros(n_vars)
for i in range(n_vars):
predictor_sum = np.sum(b[n, :n] * F[:n, i])
YP[i] = Y0[i] + (h**psi / gamma(psi + 1)) * predictor_sum

FP = f_all(t[n], YP, params)  # Evaluate at predicted YP

for i in range(n_vars): # Corrector step
corrector_sum = np.sum(a[n, :n] * F[:n, i])
Y[n, i] = Y0[i] + (h**psi / gamma(psi + 2)) * (FP[i] +
   corrector_sum)

F[n] = f_all(t[n], Y[n], params)  # Update function values
   with corrected Y

return t, Y

# Parameters
LamdaC = 0.15
LamdaH = 5
rho = 0.5
```

```
K = 1000
betaCC = 0.0001
betaCH = 0.0003
betaC = 0.0012
betaH = 0.005
alphaH = 0.092
delta = 0.072
sigma = 0.00274
muC = 0.000274
muH = 0.0009
dC = 0.01
dH = 0.0004
eps = 0.05
omegaC = 0.014
omegaH = 0.01
gammaC = 0.00185
gammaH = 0.089
eta = 0.013
r = 0.88
tau = 0.025

params = (LamdaC, LamdaH, rho, K, betaCC, betaCH, betaC, betaH
   , alphaH, delta,sigma, muC, muH, dC, dH, eps, omegaC,
   omegaH, gammaC, gammaH, eta, r, tau )

# Initial conditions
Y0 = np.array([500.0, 100.0, 20.0, 0.0, 100000.0, 1000.0,
   100.0, 0.0, 100.0])

# Time parameters
h = 0.1
T = 365

# Plot for different psi values
psi_values = [0.80, 0.85, 0.90, 0.95, 1.00]
#colors = ['b', 'r', 'g', 'purple', 'orange']
```

```
#plt.figure(figsize=(10, 6))

for i, psi in enumerate(psi_values):
t, Y = pece_fde_solver(psi, h, T, Y0, params)
L = Y[:, 8]  # Leptospira load
plt.plot(t, L, label=f"{\psi}")

plt.xlabel("Time (days)")
plt.ylabel("Leptospira Load $(L)$")
#plt.title("Fractional Model (PECE Method)")
plt.legend()
#plt.grid()
#plt.show()
plt.xlim(left=0,right=365)
plt.ylim(bottom=0)
#plt.ticklabel_format(style='sci', axis='y', scilimits=(0, 0))
plt.tick_params(top=True, right=True, which='both')
plt.savefig('L.eps', format = 'eps')
```